AN ABSTRACT OF THE DISSERTATION OF

J. Spencer Barrett for the degree of Doctor of Philosophy in Chemistry presented on August 27, 2015.

Title: Determination of Reaction Product Cross Sections in the ^{136}Xe + ^{208}Pb Multi-nucleon Transfer Reaction at E_{cm} = 450 MeV

Abstract approved: _____

Walter D. Loveland

The yields of 235 projectile-like and target-like fragments from the interaction of ^{136}Xe with a thick target of ^{208}Pb at a center-of-mass energy, E_{cm}, of 450 MeV were measured using γ-γ-γ coincidence data from Gammasphere and off-line γ-ray spectroscopy. The results give an expansive picture of the production cross sections from this reaction. Predictions from the GRAZING code were compared to the measured yields of projectile-like and target-like fragments, while the transfer model of Zagrebaev and Greiner, which emphasizes the role of shell effects in transfer reactions, were compared to only target-like fragment. There is good agreement between the measurements and the predictions of Zagrebaev and Greiner for nuclei near or below the target (Z = 74, 76, 78, 80, 82). However, the measured cross sections exceed the predicted values by up to an order of magnitude for neutron-rich trans-target nuclei (Z = 84, 86). The GRAZING model predictions are adequate for nuclei near the projectile and target (Z = 53-55; 81-83) but grossly underestimate the yields of all other reaction products.

Determination of Reaction Product Cross Sections in the $^{136}Xe + ^{208}Pb$ Multi-nucleon Transfer Reaction at $E_{cm} = 450$ MeV

by
J. Spencer Barrett

A DISSERTATION

submitted to

Oregon State University

in partial fulfillment of
the requirements for the
degree of

Doctor of Philosophy

Presented August 27, 2015
Commencement June 2016

Doctor of Philosophy dissertation of J. Spencer Barrett presented on August 27, 2015

APPROVED:

Major Professor, representing Chemistry

Chair of the Department of Chemistry

Dean of the Graduate School

I understand that my dissertation will become part of the permanent collection of Oregon State University libraries. My signature below authorizes release of my dissertation to any reader upon request.

J. Spencer Barrett, Author

ACKNOWLEDGEMENTS

A number of people were of great help to me as I worked through this experiment and analysis. You made my life easier in a very difficult time. You helped me in different ways, but in just the right way at the time.

This work was funded in part by the Roy G. Post Foundation scholarship, the Milton Harris Summer Research Fellowship, the Department of Energy, and the Department of Chemistry of Oregon State University. I appreciate these contributions so that my main focus could be my education, the science, and the research.

I express my gratitude and acknowledgement to my co-authors and collaborators from the different institutions that contributed to this experiment. From Argonne National Laboratory I thank Shaofei Zhu, John Greene, Robert Janssens, Mike Carpenter, Torben Lauritsen, and Akaa Ayangeakaa. From Brookhaven National Laboratory I am grateful to Libby McCutchan and Alejandro Sonzagni. Thanks also goes out to Chris Chiara, Jessica Harker, and William Walters from the University of Maryland.

I am grateful to our group postdoc, Dr. Ricardo Yanez. Many of our discussions allowed me to think and see things deeper than I would have otherwise. You questions challenged me to think differently and completely about whatever subject I approached you with. I appreciate the coaching you offered in working with experimental equipment, be it vacuum systems, detectors, electronic modules, or the DAQ.

Thank you to my group members. I appreciate your willingness to listen to me go on and on about the roadblocks I hit while analyzing the data. You took time out of your schedules, listened, offered up ideas, and were supportive when things got difficult.

A very large part of my success is due to my advisor, Dr. Walter Loveland. I appreciated the openness and willingness you have to teach. Whenever I had a question or concern, your door was always open (provided you were in town!) and it

allowed me to grow as a scientist. You value results and you let me go get them for myself, but didn't leave me out to dry when I got hung up. There's really nothing else I can say besides: Thank you.

I'm thankful for the support of my family. Swapping struggles with Aaron, laughing with Michelle, and relating to Chad and Kelly through sports and cooking allowed me a break just when I needed it. My parents, Lee and Judy, have always been supportive of my journey. Even when my endless explanations of my research caused your eyes to gloss over (or in many cases shut), you still were interested and gave me a mountain of support and advice to help me through.

Most of all, I'm thankful for my lovely wife, Ashley, and our children, Brendan, Korver, and Roxena. After a long day or a long trip I would come home to a house full of love. Nothing makes you feel better when things aren't going right than opening the door and having three adorable children at your feet waiting in line to give me hugs and kisses just because I'm home. Ashley, you have been my main support even before I came to Oregon State. You have stayed with me throughout and have shown an enormous amount of patience and love, even when I've been gone for a month. It is for all of you that I did this. I love you.

TABLE OF CONTENTS

TABLE OF CONTENTS (Continued)

Page

LIST OF FIGURES

LIST OF FIGURES (Continued)

Figure Page

LIST OF FIGURES (Continued)

LIST OF TABLES

1 INTRODUCTION

1.1 Nuclear Reactions in General

Recent efforts in nuclear science have utilized nuclear reactions in order to synthesize and study heavy nuclei at the limits of stability. An experiment to study a particular nuclear reaction usually involves a stationary target material that is bombarded by moving projectile, whether it be an uncharged neutron, a proton, or a heavy ion. This process can be used to produce a desired isotope, or the resulting reaction products can be detected and studied to further understand the reacting systems.

Many different outcomes may occur according to the nature of the chosen projectile and target. The bombarding projectiles may or may not physically interact with the target nuclei, depending on bombarding energy, trajectory, and repulsion (if the bombarding species is a charged particle). A given nuclear reaction can be split into three generic stages: initial, intermediate, and final. The diagram in Figure 1.1 shows possible outcomes of these different stages.

In the initial stage, the projectile is approaching the target nucleus. If the bombarding projectile is a neutron, no Coulomb repulsion exists and the neutron may interact with the target, depending on its trajectory. However, if the projectile is a charged particle, the Coulomb fields of both the projectile and the target will interact and may cause the incoming ion to change its trajectory, resulting in Rutherford or Coulomb scattering. Another interaction may also occur in this stage in which the two nuclei physically interact and the projectile changes trajectory but does not lose energy, resulting in shape inelastic scattering.

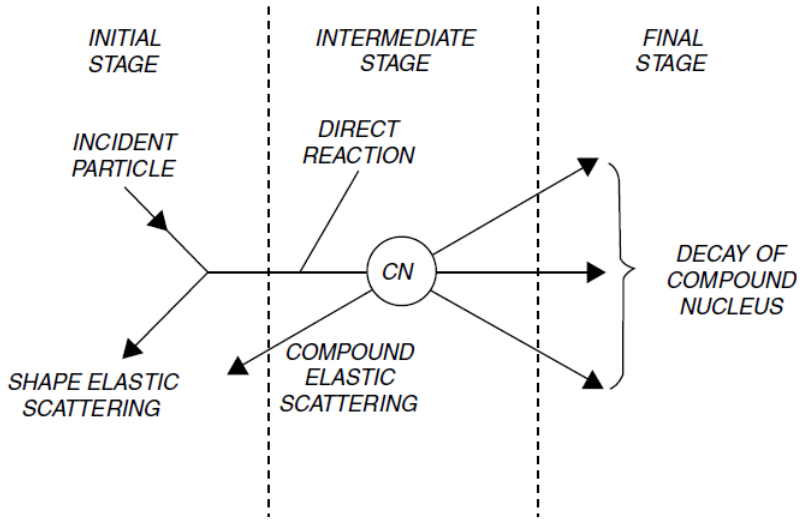

Figure 1.1: Schematic diagram showing three stages of nuclear reactions. Figure from [1].

The projectile may overcome the Coulomb potential, in which case projectile nucleons come into contact with nucleons of the target nucleus. When this occurs the system has moved on to the intermediate stage. Nuclear interactions in this stage depend on the trajectory of the incoming projectile and how much the projectile and target nuclei overlap. The projectile may come into contact with a single nucleon of the target, which may then populate a higher energy level. If this nucleon then is emitted from the target nucleus, a "direct reaction" is said to have occurred. If the collision was more head-on rather than offset, the projectile may continue to collide with other nucleons in the target, eventually distributing all of its kinetic energy and leading to the formation of a compound nucleus (CN) composed of both the projectile and target. This CN may undergo further particle emission itself. "Compound elastic scattering" occurs when the CN emits a particle that has the same structure and energy as the incident projectile.

Due to the complex interactions that take place in compound nucleus formation, once the CN is formed, it essentially "forgets" its mode of formation. This means that in the final stage, the mode of decay of the CN is independent of the incident projectile and mode of formation. Instead, the decay of the CN is determined by other factors, such as the resulting excitation energy of the CN, its angular momentum, and/or stability against radioactive decay. The CN may decay by releasing excess excitation energy by way of neutron evaporation, small particle emission, or, particularly in heavy systems, fission. If the CN is unstable, such as a heavy element or if it is neutron-rich or neutron-deficient, it may decay through alpha emission, beta emission, positron emission, or electron capture.

The rate at which nuclear reactions occur depends on the number of target nuclei (N), the number of incident projectile nuclei (Φ), and the cross section of the reaction, (σ). This rate is given by equation 1.1.

$$Rate = N\sigma\Phi \tag{1.1}$$

Here, the rate is given in reactions per second.

Figure 1.2 shows a standard reaction experiment scenario. A target of known thickness is exposed to a beam of incident particles with a given intensity (particles/second), which may be neutrons or other charged particles. A number of projectiles will pass through the target material (if the target is thin) without undergoing any interaction. Other incident ions will interact with target nuclei in some manner as described above. The fraction of the target area that blocks the beam can then be given by the product of the target thickness and the cross section: N (atoms/cm^2)*σ (cm^2/atom). In a general sense the cross section can be described as

the effective area subtended by one target atom. The cross section can also be used to describe the probability of a particular desired outcome, such as the probability of fusion (fusion cross section), the probability of absorbing an incident neutron (capture cross section), or the probability of producing a given nuclide (Z,A) as a reaction product (nuclidic cross section).

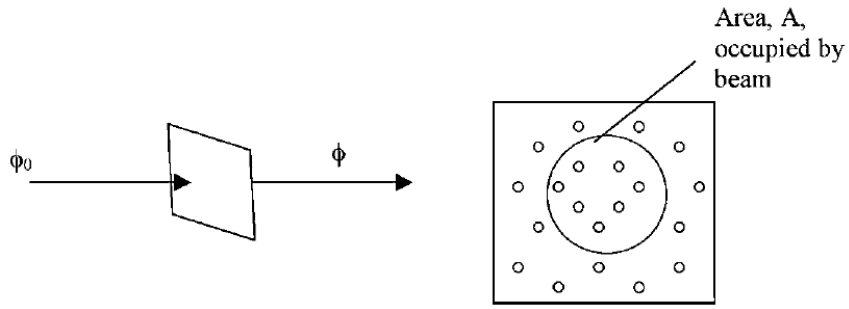

Figure 1.2: Schematic of a particle beam incident on a target foil. The beam is delivered with a known intensity in particles/second and the target is of known thickness, mg/cm^2. The effective area blocked by the target nuclei is described by the cross section (cm^2/atom). Figure from [1].

1.2 Coulomb vs Interaction Barrier

In the consideration of nuclear reactions discussed in the previous section, the repulsive Coulomb barrier was equated to the nuclear interaction barrier. This, however, is a simplified consideration. An in-depth discussion by Bass [2-4] explains the properties of the barriers involved in the different types of reactions.

Coulomb repulsion is due to positively charged protons in the two nuclei repelling each other as one comes closer to the other. The distance at which this force is felt extends past the matter radius of the nucleus. At this large distance, nucleons between the two colliding nuclei don't come into contact, and the only nucleus-nucleus interaction is Coulombic. The classic definition of the Coulomb barrier, V_c, is

the potential between two charged spheres, of charge $Z_p e$ for the projectile and $Z_t e$ for the target, at the distance of closest approach, R_C, without any physical nuclear reactions (equation 1.2).

$$V_C = \frac{Z_p Z_t e^2}{R_C} \tag{1.2}$$

In this equation e^2=1.44 fm·MeV and

$$R_C = r_{0C}\left(A_p^{\frac{1}{3}} + A_t^{\frac{1}{3}}\right) \tag{1.3}$$

The nuclear radius constant, r_{0C}, can vary between 1.2 fm – 1.4 fm depending on if one is considering the charge radius or the matter radius. A_p and A_t are the mass numbers of the projectile and target nuclei, respectively.

The projectile nucleons begin to interact with the target nucleons as the bombarding energy is increased. The bombarding energy necessary in the center-of-mass system for the two nuclei to interact at a distance, R_{int}, can be defined as the interaction barrier. Bass [2] defines the nuclear radius of the projectile and target as the radius at which the nuclear charge density has dropped to one half of its central value. Equation 1.4 is used to calculate this radius for a given nucleus.

$$R_i = 1.12A_i^{\frac{1}{3}} - 0.94A_i^{-\frac{1}{3}} \tag{1.4}$$

Bass [2] experimentally determined through the analysis of scattering data of several systems that R_{int} is ~3 fm larger than the sum of the half-density radii (equation 1.5).

$$R_{int} = R_P + R_t + 3\ fm \tag{1.5}$$

The interaction barrier, as defined by Bass, can now be given as

$$B_{int} = \frac{Z_p Z_t e^2}{R_p + R_t + 3.0\ fm} \quad (1.6)$$

Slightly different values may be obtained for the interaction barrier of a nuclear reaction [2-4] depending on the method used to determine either R_{int} or B_{int}. For example, the interaction barrier for the ^{136}Xe + ^{208}Pb reaction has been calculated to be 420 MeV in [5] and 434 MeV in [6]. For the purposes of this experiment, B_{int} for the ^{136}Xe + ^{208}Pb reaction is calculated using equations 1.4 – 1.6.

$$R_p = 1.12(136)^{\frac{1}{3}} - 0.94(136)^{-\frac{1}{3}} = 5.58\ fm \quad (1.7)$$

$$R_t = 1.12(208)^{\frac{1}{3}} - 0.94(208)^{-\frac{1}{3}} = 6.48\ fm \quad (1.8)$$

$$R_{int} = R_P + R_t + 3\ fm = 15.06\ fm \quad (1.9)$$

$$B_{int} = \frac{(54)(82)1.44\ fm \cdot MeV}{15.06\ fm} = 423\ MeV \quad (1.10)$$

1.3 Transfer Reaction Models

One of the main areas of investigation in nuclear physics is the synthesis of neutron rich heavy and super-heavy elements. Currently, the main method through which heavy and super-heavy elements have been produced has been complete fusion reactions using stable beams. In the heaviest systems, though, only neutron deficient heavy nuclei have been produced. It is desirable to synthesize neutron rich (n-rich) nuclei, which should have longer half-lives, in order to study their characteristics. Multi-nucleon transfer reactions have been suggested as a means by which these n-rich nuclei may be produced.

Transfers may occur through different reaction mechanisms, including quasi-elastic scattering, deep inelastic (DI) collisions, or quasifission. The type of

mechanism that occurs is dependent on the impact parameter of the collision. The impact parameter is the offset distance between the centers of the projectile and target nuclei. For example, in head-on collisions (with no offset) the impact parameter would be zero, and a peripheral collision would have a large impact parameter, approximately the sum of the two nuclear radii.

Quasi-elastic scattering reactions are those with large impact parameters. In these collisions there is little overlap of the two nuclei, minimal projectile energy loss occurs, and few nucleons are transferred. During DI collisions, those with moderate impact parameter values, there is a larger overlap region between the colliding nuclei, but the two nuclei do not merge. More energy from the projectile is lost and a larger number of nucleons may be transferred, compared to quasi-elastic collisions. Quasifission reactions are characterized by small impact parameters and very large projectile energy loss. In these collisions the two nuclei combine to form a di-nuclear system in which a neck is formed where large mass transfer may occur. However, the di-nuclear system never develops into a complete compound nucleus, instead resulting in a subsequent breakup into projectile and target-like fragments.

Efforts have been made to model multi-nucleon transfer reactions using a variety of approaches [6-21]. One model of multi-nucleon transfer reactions, developed by Aage Winther [12, 13], has been implemented in the computer code GRAZING [22, 23]. The model describes the projectile and target nuclei as collections of independent nucleons that vibrate around spherical shapes. The reactions considered by the model involve only those that occur in the grazing region.

Due to this restriction, quasifission reactions and reactions with smaller impact parameters that are not part of this region are not considered.

The boundary of the grazing region is defined by the nuclear potential, V, in a surface-to-surface interaction between a projectile, p, and a target, t. The model [13] uses the formalism in equation 1.11 to calculate this potential.

$$V(r) = -16\pi\gamma a \frac{R_p R_t}{R_p + R_t}\left[\frac{1}{1+e^{(r-R_p-R_t)/a}}\right] \tag{1.11}$$

The nuclear radii, R_p and R_t, are given by

$$R_i = \left(1.20A_i^{\frac{1}{3}} - 0.09\right) fm \tag{1.12}$$

and the inverse of the nuclear diffuseness, 1/a, in the exponential is

$$\frac{1}{a} = 1.17\left(1 + 0.53\left(A_p^{\frac{1}{3}} + A_t^{\frac{1}{3}}\right)\right) fm^{-1} \tag{1.13}$$

The surface tension, γ, from 1.11 is given by

$$\gamma = -0.95\left[1 - 1.8\frac{(N_p - Z_p)(N_t - Z_t)}{A_p A_t}\right] MeV\ fm^{-2} \tag{1.14}$$

Equation 1.11 has been developed such that the distance between the nuclei, r, gives a maximum value as this distance decreases.

$$\frac{\partial V}{\partial r} = 4\pi\gamma \frac{R_p R_t}{R_p + R_t} cosh^{-2}\left(\frac{r - R_p - R_t}{2a}\right) \tag{1.15}$$

For the ^{136}Xe + ^{208}Pb reaction, Figure 1.3 shows the results of equation 1.15. The maximum corresponds to r=13.1 fm, which is the sum of the projectile and target radii, when calculated using equation 1.12. Reactions that occur where r<13.1 fm are assumed to merge and are not considered in this model.

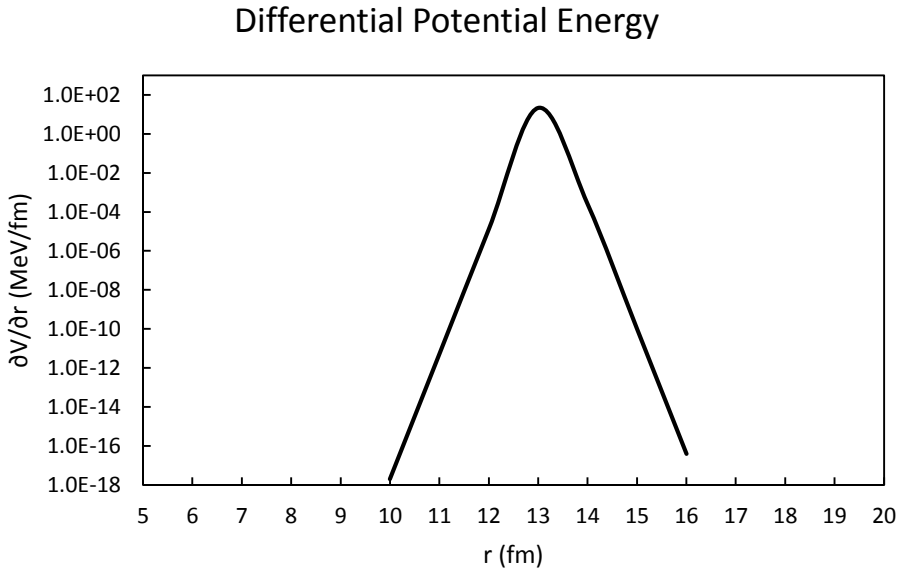

Figure 1.3: Differential potential energy as the distance between two nuclei changes. The maximum denotes the boundary of the grazing region. For distances below the maximum, the nuclei are assumed to fuse.

The GRAZING code [22] is used to implement this model and calculate formation cross sections depending on the chosen projectile and target nuclei, as well as the reaction energy. The user may alter several parameters of the program used in the calculation of predicted cross sections. Some of these parameters include the effective Q values of the reaction, the ion-ion potential, the level density parameter, and the nuclear radius parameter, which is used in the calculation of form factors for transfers.

Form factors are functions used to describe properties of complex phenomena based on experimental observations. In this code, the form factors are used to describe the behavior of single particle transfer between the colliding nuclei [12]. Parameters used in the calculation of proton and neutron form factors are not altered directly. Instead, a correction factor may be introduced by the user in order to change

their normalizations. Correction factors may be applied to neutron and/or proton form factors. Figure 1.4 shows the effect of applying an increased correction factor for the proton form factors in the $^{40}Ca + {}^{96}Zr$ reaction at E_{lab}=152 MeV.

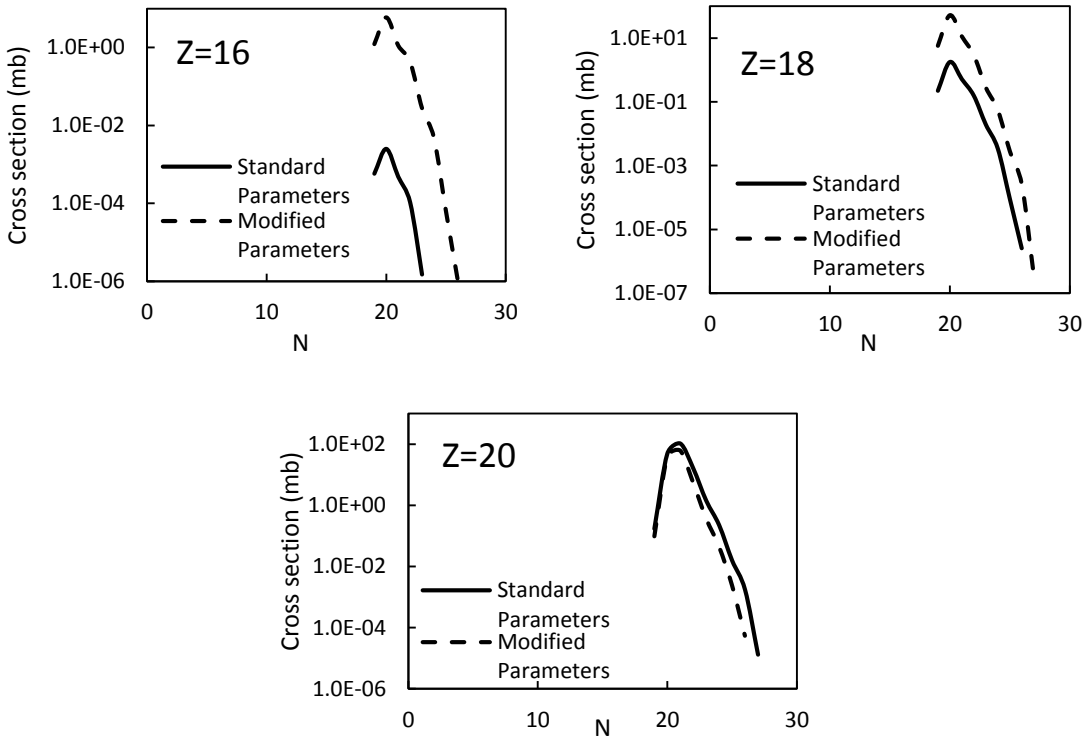

Figure 1.4: GRAZING simulations using standard and modified parameters. The modified parameter was obtained by applying a correction factor of 10 to the proton form factor while keeping the neutron form factor constant. This increases the magnitude of the predicted transfer cross section by up to nearly three orders of magnitude for ΔZ=-4 (Z=16).

It is worth noting that between the two scenarios the location of the distribution peaks remain at the same neutron number, showing that this adjustment affects mainly the transfer of protons, not neutrons. If the neutron form factor is adjusted and no adjustment is made to the proton form factor, the result is a change in the width of the distribution. For example, the standard parameters in GRAZING [22] for the reaction above produce cross sections for isotopes between N=19 and N=27

for the Z=18 reaction product. When a factor of 5 is applied to the neutron parameter, this distribution broadens to products between N=16 and N=29. Conversely, if the correction factor applied is reduced, the result is a smaller neutron distribution range. For the purposes of the ^{136}Xe + ^{208}Pb reaction, the standard parameters were used for all predicted cross sections.

GRAZING [22] can output results such as angular distributions, excitation functions, total reaction cross section, or isotopic distributions for either pre or post-neutron emission reaction products. One de-excitation channel that is not included in the standard GRAZING code is fission, which becomes more dominant with heavier systems. In an effort to include fission as an exit channel, a recent modification was done to this code, called GRAZING-F [24], and nuclidic yield predictions were calculated for several heavy systems.

An example calculation of GRAZING-F for the ^{238}U + ^{238}U reaction at a center-of-mass energy, E_{cm}=1000 MeV [24] is shown in Figure 1.5. The dotted line shows the primary fragment distribution. If neutron evaporation is the dominant decay mechanism present, then one would expect the peak of the distribution of the secondary fragments (solid line) to be shifted to lower A values. However, the lower magnitude of the secondary fragment distribution shows that fission as a de-excitation mode decreases the production cross sections. For the ^{136}Xe + ^{208}Pb reaction at E_{cm}=450 MeV, both GRAZING [23] and GRAZING-F [24] produced the same results, showing that fission is not an dominant de-excitation channel in this reaction.

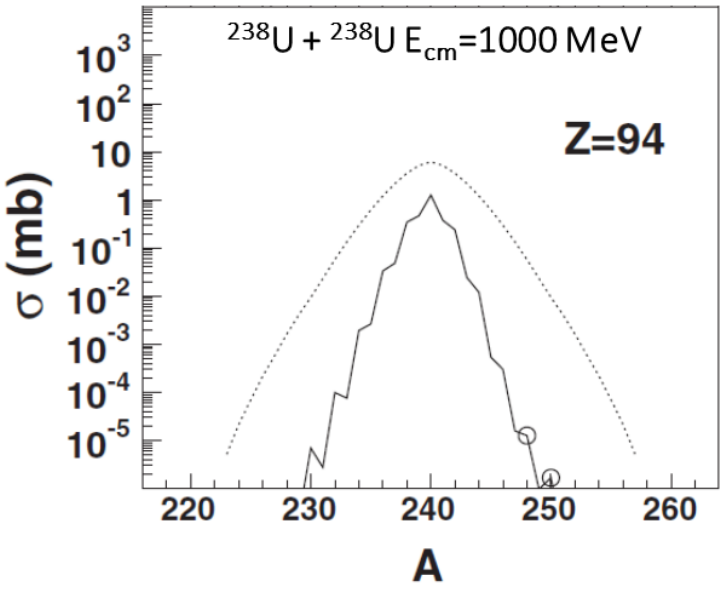

Figure 1.5: Primary and secondary Z=94 fragment distributions calculated using GRAZING-F. This calculation was performed for the reaction of ^{238}U + ^{238}U at E_{cm}=1000 MeV. The dotted line shows the primary fragment distribution, and the solid line shows the secondary fragment distribution. The open circles represent unknown isotopes of Pu. Figure from [24] (title added).

Transfer reactions have also been described within the framework of time-dependent Hartree-Fock (TDHF) calculations [11]. These calculations were performed in an attempt to obtain a fully microscopic description of transfer reactions. In this effort, the colliding nuclei are considered to be spherical in shape and are composite systems of individual neutrons and protons. The neutrons and protons are described in the calculations as single-particle orbitals, based on spatial and spin coordinates. The reaction space is divided into two regions representing the projectile-like fragments (PLFs), V_p, and target-like fragments (TLFs), V_t. During the interaction of the two nuclei, the single-particle orbitals can extend to both regions, and the probability of the number of protons and neutrons in each region after the collision is calculated.

The probability of a transfer reaction, $P_{Z,N}$, is given as the product of the probabilities that Z protons and N neutrons will exist in either V_p or V_t. For example, the probability of forming a given PLF at an impact parameter, b, is

$$P_{Z,N}(b) = P_Z(b)P_N(b) \tag{1.16}$$

Primary fragment cross sections are then determined by integrating over b.

$$\sigma(Z,N) = 2\pi \int_{b_{min}}^{\infty} bP_{Z,N}(b)db \tag{1.17}$$

Here, b_{min} represents the minimum impact parameter before complete fusion of the two nuclei occurs. De-excitation modes of the primary fragments are not taken into account in this formalism.

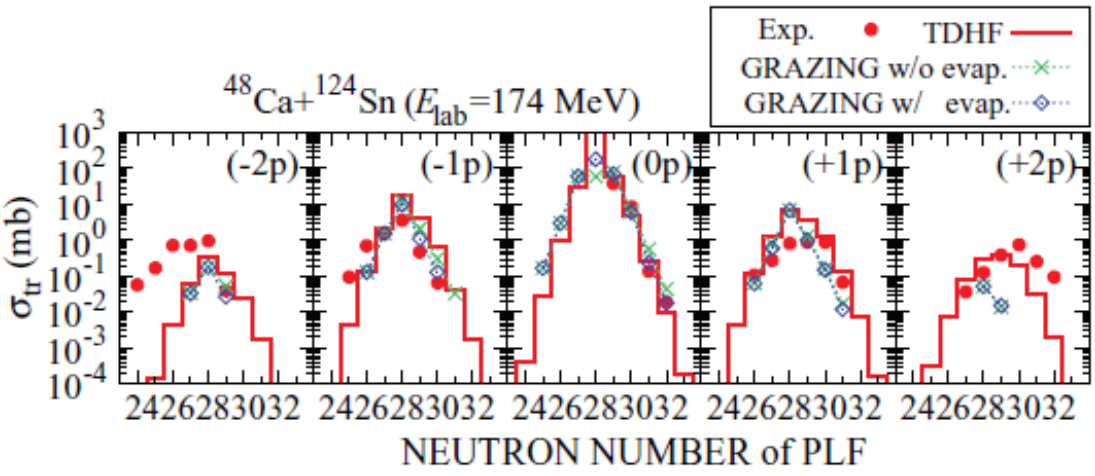

Figure 1.6: Comparison of cross section predictions from TDHF calculations and the GRAZING code. The GRAZING predictions include pre (dotted line with open diamonds) and post (dotted line with x's) neutron evaporation fragments. Both the GRAZING and TDHF predictions (solid lines) are compared to experimental results (filled circles). Figure from [11].

Figure 1.6 shows a comparison of the predicted cross sections for primary fragments using TDHF calculations to those from the GRAZING code for both pre- and post-neutron emission fragments [11]. The reaction is ^{48}Ca + ^{124}Sn at a lab energy

of E_{lab}=174 MeV. Predicted cross sections from both sources agree with experimental results in the case of only neutron transfer (ΔZ=0) and that of ΔZ=±1. However, as ΔZ increases, predicted cross sections from both the TDHF calculations and GRAZING shift to higher (for ΔZ = -2) or lower (for ΔZ = +2) neutron numbers compared to the experimental data.

The agreement between the TDHF and GRAZING calculations is encouraging for the use of GRAZING as a model of transfer reactions. However, the disagreement between the predicted and experimental cross sections for large proton transfers is discouraging, and the reason for this disagreement is not well understood at this time.

In another model of multi-nucleon transfer reactions, Zagrebaev and Greiner [6, 14-21] have emphasized the role of neutron and proton shell effects in determining formation cross sections. Their model attempts to simultaneously describe quasi-elastic, deep inelastic, and quasifission collisions. Potential energy valleys, influenced by closed shell stabilization, are given as the driving force for the formation of projectile-like fragments and target-like fragments. The potential is dependent on the distance between the colliding nuclei, their deformation (resulting in differences in the elongation of the di-nuclear system), and the mass asymmetry, η, between the projectile and target, given by

$$\eta = \frac{A_t - A_p}{A_t + A_p} \tag{1.18}$$

As the reaction proceeds, nucleon transfers occur such that the resulting fragments populate these minimized potential energy regions.

An example of this driving force is shown in Figure 1.7 for the $^{136}Xe + ^{209}Bi$ reaction at E_{cm}=569 MeV [14]. This shows the potential energy as a function of the neck elongation and mass asymmetry of the colliding system. The point of contact between the two nuclei, shown in the figure, corresponds to an elongation of approximately 13 fm, which is the sum of the nuclear radii, and a mass asymmetry of 0.21. The paths in the figure show the most likely trajectories of the resulting fragments toward the lower potential energy regions, meaning that this system should produce PLFs and TLFs that are very similar to the projectile and target with mass asymmetries of ±0.2.

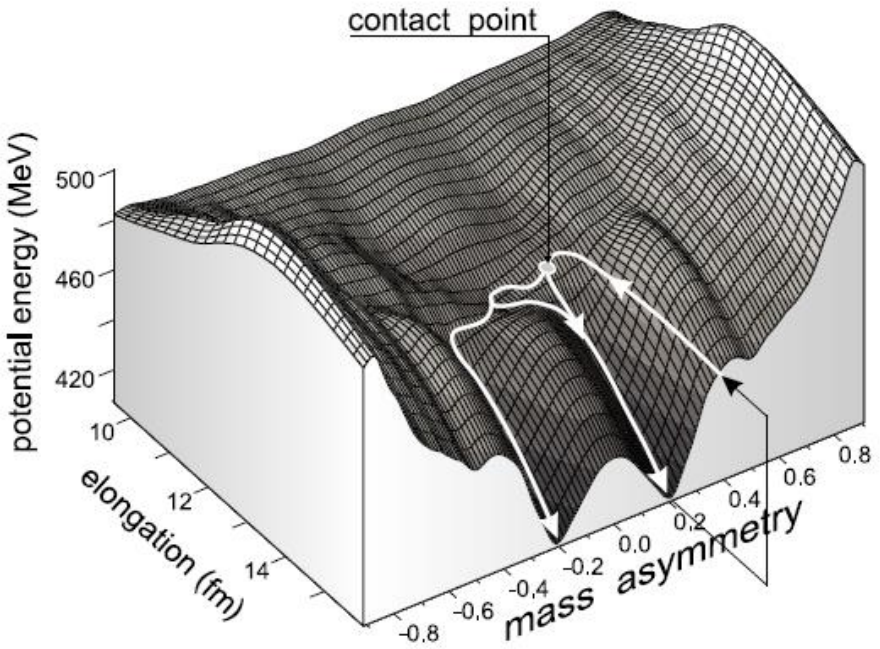

Figure 1.7: Potential energy surface diagram calculated through the model of Zagrebaev and Greiner. This diagram was calculated for the $^{136}Xe + ^{209}Bi$ reaction at E_{cm}=569 MeV. The elongation and mass asymmetry of the reacting system at the contact point is shown, and the paths/arrows along the surface show schematically the most probable trajectories for fragment formation. From [14].

This model uses Langevin-type equations [6, 15, 25] to describe the transfer of nucleons between the colliding nuclei. The equations for protons, Z, and neutrons, N, have the form

$$\frac{d\eta_Z}{dt} = \frac{2}{Z_{CN}} D_Z^1 + \frac{2}{Z_{CN}} \sqrt{D_Z^2}\Gamma(t) \tag{1.19}$$

$$\frac{d\eta_N}{dt} = \frac{2}{N_{CN}} D_N^1 + \frac{2}{N_{CN}} \sqrt{D_N^2}\Gamma(t) \tag{1.20}$$

In these equations, Z_{CN} and N_{CN} are the proton and neutron numbers of the compound nucleus, D^1 and D^2 are the transport coefficients, and η_Z and η_N are the proton and neutron mass asymmetries, respectively. The proton asymmetry is defined as

$$\eta_Z = \frac{2Z - Z_{CN}}{Z_{CN}} \tag{1.21}$$

where Z is the proton number for one fragment. The neutron asymmetry is also calculated using equation 1.21, substituting in N and N_{CN} for Z and Z_{CN}, respectively.

The assumption is made that sequential single nucleon transfers in a fragment with mass A (i.e. A → A'; A'=A±1) are the main component involved in the mass rearrangement of the system. With this assumption, the transport coefficients are given by equations 1.22 and 1.23.

$$D_{Z,N}^1 = \lambda_{Z,N}^{(+)}(A \rightarrow A+1) - \lambda_{Z,N}^{(-)}(A \rightarrow A-1) \tag{1.22}$$

$$D_{Z,N}^2 = \frac{1}{2}\left[\lambda_{Z,N}^{(+)}(A \rightarrow A+1) + \lambda_{Z,N}^{(-)}(A \rightarrow A-1)\right] \tag{1.23}$$

The transition probabilities, $\lambda_{Z,N}^{(\pm)}$, for A→A±1 are given by the nuclear level densities.

$$\lambda_{Z,N}^{(\pm)} = \lambda_0 \sqrt{\frac{\rho(A\pm1)}{\rho(A)}} \tag{1.24}$$

Here, the nucleon transfer rate, λ_0, is given as approximately 0.5×10^{-22} s^{-1} [25]. The level densities, ρ, are given by $\rho \sim \exp(2\sqrt{aE^*})$, where E* is the excitation energy and (a) is the level density parameter.

Cross sections, as well as energy and angular distributions, are calculated [6] using

$$\frac{d^2\sigma_{Z,N}}{d\Omega dE}(E,\theta) = \int_0^\infty bdb \frac{\Delta N_{Z,N}(b,E,\theta)}{N_{tot}(b)} \frac{1}{\sin(\theta)\Delta\theta\Delta E} \quad (1.25)$$

In this equation $\Delta N_{Z,N}(b, E, \theta)$ is the number of events in which a nucleus with Z protons and N neutrons is formed at a given impact parameter, b, with a kinetic energy between E and E+ΔE at a center-of-mass angle in the region of θ and θ+dθ. $N_{tot}(b)$ is the total number of events at the given impact parameter. The results of equation 1.25 give primary product distributions. The mode of de-excitation of the primary fragments is then determined within a statistical model that takes into account the survival probability against fission of the resulting fragments as well as neutron evaporation and γ-emission competition.

Predicted cross sections from this model have also been compared to TDHF calculations for the reaction of ^{58}Ni + ^{208}Pb at E_{lab}=328.4 MeV [11]. The comparison is shown in Figure 1.8 and also includes predictions from Complex WKB (CWKB) model, which is also based on direct reactions, similar to GRAZING. The figure shows the predicted and experimentally measured cross sections for reaction products that involve either pure proton stripping without neutron transfer or pure neutron pickup without proton transfer.

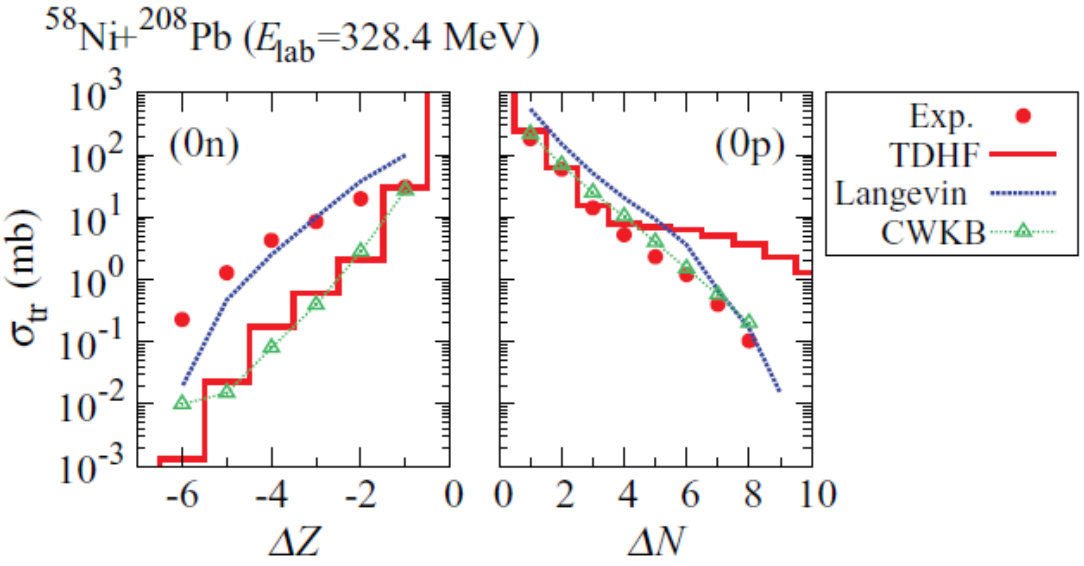

Figure 1.8: Comparison of model predictions for pure proton and neutron transfers in the reaction of ^{58}Ni + ^{208}Pb at E_{lab}=328.4 MeV. The pure proton transfers are shown on the left and the pure neutron transfers are shown on the right. The points are experimentally measure cross sections, the histogram comes from TDHF calculations, the triangles are predictions from the CWKB model, and the dotted lines are predictions from the model of Zagrebaev and Greiner. From [11].

The Zagrebaev and Greiner model predictions are slightly higher than other model predictions and measured cross sections for the pure neutron transfers. However, in the pure proton transfers, the TDHF calculations as well as the other model predictions, underestimate the production cross sections by greater amounts (near an order of magnitude) as more protons are stripped from the projectile. The predictions of Zagrebaev and Greiner are in much closer agreement to the measured cross sections. The one exception is in the case of one proton transfer, where the Zagrebaev and Greiner predictions overestimate the production cross section.

Using this model, Zagrebaev and Greiner have described two possible scenarios [20] of transfer reactions depending on the projectile and target chosen (shown graphically in Figure 1.9). In one scenario, a small projectile (^{48}Ca) and a

large target (^{248}Cm), which have a large mass difference, are chosen for the reacting system. In this type of reaction the nucleons would preferentially transfer from the heavier ^{248}Cm nucleus to the lighter ^{48}Ca until the ^{248}Cm has the structure of ^{208}Pb. This transfer process is labeled as "symmetrizing" or normal quasifission since the mass asymmetry decreases as the reaction proceeds.

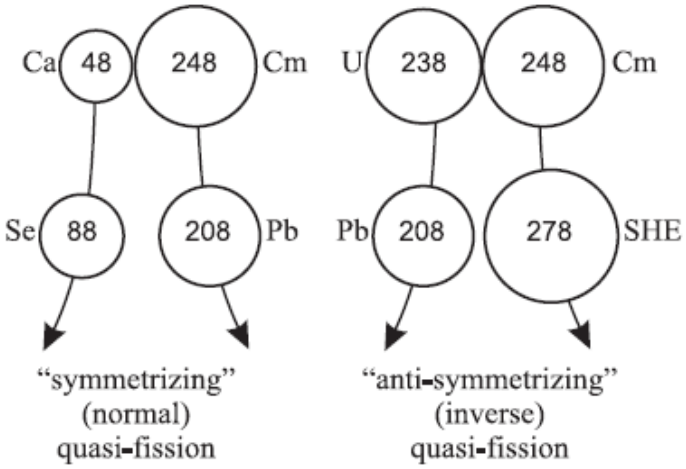

Figure 1.9: Diagram of normal and inverse quasifission. In normal quasifission nucleons are transferred from the heavy target to the lighter projectile. During inverse quasifission nucleons are transferred from the lighter projectile to the heavier target, transferring as many as 30 nucleons and resulting in a neutron rich, super heavy target-like fragment. From [20].

The other scenario is that of reacting nuclei that have similar masses, such as a ^{248}Cm target being bombarded by a ^{238}U projectile. In this "anti-symmetrizing" quasifission reaction the nucleons would transfer from the lighter ^{238}U nucleus to the ^{248}Cm. This process would be driven by the ^{238}U nucleus being closer to the potential energy valley caused by Z=82 and N=126. Zagrebaev and Greiner predict that this reaction could result in a potential transfer of 30 nucleons to the ^{248}Cm, leaving a neutron rich super-heavy target-like fragment.

Very recently, the production of heavy n-rich nuclei has also been predicted within the di-nuclear system (DNS) model [26]. In this model, the transfer of nucleons is considered a diffusion process along the proton and neutron degrees of freedom. Individual probabilities of single particle transfers from one fragment to the other are summed to give the total distribution of fragments. One unique aspect of the DNS model is the treatment of quasifission events [26]. The quasifission rate, $\Lambda(\Theta(t))$ s^{-1}, used in the model is given by equation 1.26.

$$\Lambda\big(\Theta(t)\big) = \frac{\omega}{2\pi\omega^{B_{qf}}}\left[\sqrt{\left(\frac{\Gamma}{2\hbar}\right)^2 + (\omega^{B_{qf}})^2} - \frac{\Gamma}{2\hbar}\right]\exp\left[-\frac{B_{qf}(Z_1,N_1)}{\Theta(t)}\right] \qquad (1.26)$$

The quantity B_{qf} (Z_1,N_1) is the quasifission barrier and $\Theta(t)$ is the temperature. This value is calculated using the expression

$$\Theta = \sqrt{\frac{E_1}{a}} \qquad (1.27)$$

where E_1 is excitation energy of the fragment and (a) is the level-density parameter, given by a = A/12 MeV^{-1}. The symbol ω^{Bqf} is the frequency of the inverted harmonic oscillator, which approximates the potential, V(r), at the top of the quasifission barrier, while ω is the frequency of the harmonic oscillator that approximates V(r) at the bottom of the potential pocket when the two nuclei are in contact. The friction coefficient is represented by Γ. The latter values are set in the model [26] at Γ=2.8 MeV, $\hbar\omega^{Bqf}$ =2.0 MeV, and ħω=3.0 MeV.

The primary fragments are assumed to share the excitation energy proportionally according to their masses. The code GEMINI [26] is then used to determine the number of subsequent neutron evaporations from the excited primary

fragments. Competition between small particle emission (such as neutron, proton and alpha particles), γ-decay and fission is considered in the de-excitation process to determine surviving secondary reaction products.

These models are the beginning efforts to understand these complicated reaction systems. They must be tested in order to experimentally confirm the included physics of the colliding nuclei, or identify and correct possible deficiencies for a wide range of reaction systems. By doing so, predictions for the formation of neutron rich heavy and super-heavy elements will increase in accuracy and the "northeast" part of the chart of nuclide may begin to be further populated.

2 PREVIOUS EXPERIMENTS

2.1 Early Experiments

Experiments investigating multi-nucleon transfer reactions were performed as early as the 1970s and 1980s. During these efforts, multiple characteristics of these reactions were observed such as angular distributions [27, 28], charge and mass distributions [29-36], excitation functions [37, 38], and production cross sections for actinide nuclei [39-43]. Some of the observations that were made during those experiments will be discussed here.

In an experiment performed by Lee et al in 1982 [44], ^{248}Cm was bombarded by two isotopes of oxygen, ^{16,18}O, and two isotopes of neon, ^{20,22}Ne, at low energies. The bombarding energies for the oxygen ions were E_{lab}=97 and 98 MeV for ^{16}O and ^{18}O, respectively. The energies for the neon ions were E_{lab}= 115 and 116 for ^{20}Ne and ^{22}Ne, respectively. Radiochemical techniques were used to separate and determine the formation cross sections for isotopes of Bk through No. The outcome of the reaction of ^{16,18}O + ^{248}Cm is shown in Figure 2.1. The isotopic distributions for various trans-target nuclei are plotted for both ^{16}O and ^{18}O. In each case, the peak of the distribution from the ^{18}O atoms is two neutrons richer than that from the ^{16}O atoms. This trend was the same for the ^{20}Ne and ^{22}Ne atoms, showing that n-rich projectiles produce n-rich reaction products. This effect was also observed in a later experiment reacting different Xe projectiles with ^{248}Cm [45]. This shows that projectiles chosen to synthesize new heavy elements should be as n-rich as possible.

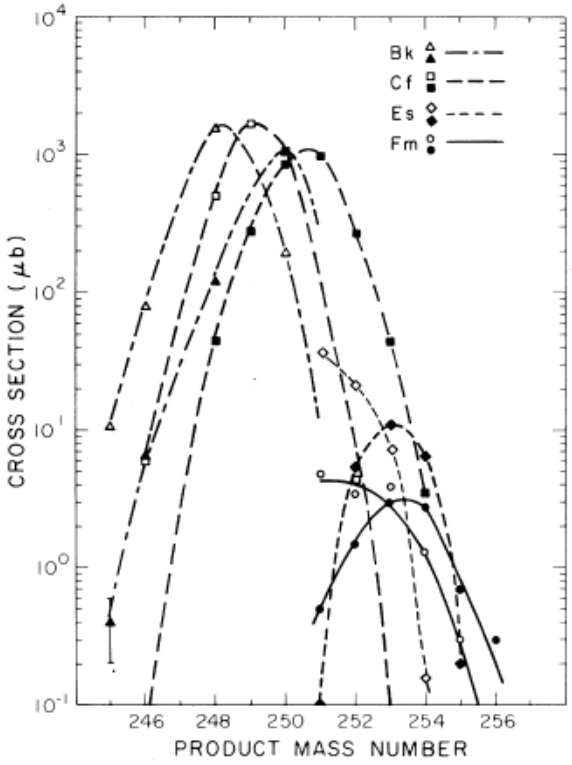

Figure 2.1: Isotopic distributions for trans-target nuclei in the reaction $^{16,18}O$ + ^{248}Cm. Open symbols are cross sections produced from ^{16}O, closed symbols are cross sections produced from ^{18}O. The more neutron rich projectiles produced reaction products that were two neutrons richer than those produced with the lighter ions. From [44].

Another experiment was that of Hoffman et al. in 1985 [37]. In this experiment ^{248}Cm was bombarded by $^{40,48}Ca$ ions at various energies to determine excitation functions for the resulting nuclides. Reaction products of Bk, Cf, Es, and Fm isotopes were isolated through radiochemical techniques and analyzed using radioactive decay activities. The excitation functions for various isotopes of Cf are shown in Figure 2.2. The data are plotted at the midpoints of the measured energy ranges, which are 223-239 MeV, 247-263 MeV, 272-288 MeV, and 304-318 MeV.

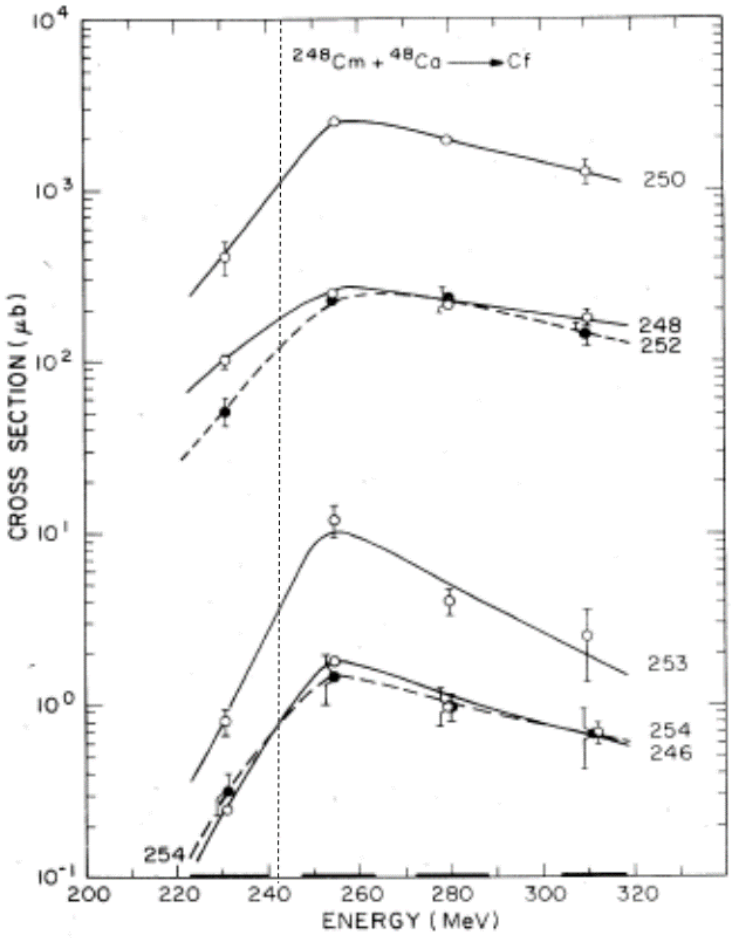

Figure 2.2: Excitation functions for isotopes of Cf in the $^{48}Ca + ^{248}Cm$ reaction. Using the formalism described in section 1.2, the interaction barrier is at E_{lab}=242 MeV (shown by the dotted line). The excitation functions increase to a peak approximately 5% above barrier, followed by decreasing cross sections as incident energy increases. From [37].

These isotopes of Cf were formed during the reaction with ^{48}Ca. There is an increase in production cross section for each isotope until a maximum is reached. According to the formalism used in section 1.2, the interaction barrier would be at E_{lab}=242 MeV. The peaks of all of the excitation functions occur at approximately 255 MeV, which is only 5% above the interaction barrier. The shape of the excitation functions show the effects of increasing cross sections at low energies as excitation

energy, E*, increases. Also shown is the decrease in cross sections at higher energies, due to decreasing survival probability as the highly excited fragment becomes more likely to fission.

Two experiments involving very heavy nuclei were performed by Schädel et al [42, 43]. One experiment bombarded a ^{238}U target with a ^{238}U projectile, and the other used the same projectile with a ^{248}Cm target. In the ^{238}U + ^{248}Cm reaction the projectile was reduced in energy to 1761 MeV in the lab frame, which is ~18% above the barrier, V_B=1495 MeV. The resulting fragments were isolated radiochemically, and the cross sections were determined through radioactive decay analysis. The reported cross sections are a mix of cumulative (cross sections of nuclei produced in the reaction and through precursor beta decay) and independent (cross sections corrected for beta decay production) yields. Some of the results comparing the two experiments are shown in Figure 2.3.

These experiments with heavy projectiles and targets showed limited success in producing heavy, trans-target nuclei. Production cross sections in the ^{238}U + ^{248}Cm reaction were several orders of magnitude higher than those from the ^{238}U + ^{238}U reaction for isotopes of Cf through Fm. It is worth noting that Fm isotopes were produced with cross sections near 1 μb, peaked around ^{254}Fm. This corresponds to a transfer of ΔZ=4 and ΔN=2 above the Cm target. However, larger transfers [40-43] showed a large drop off in production cross section. Overall, it was observed that fission of the resulting fragments increased with higher excitation energies, which limited the production of heavy, n-rich nuclei.

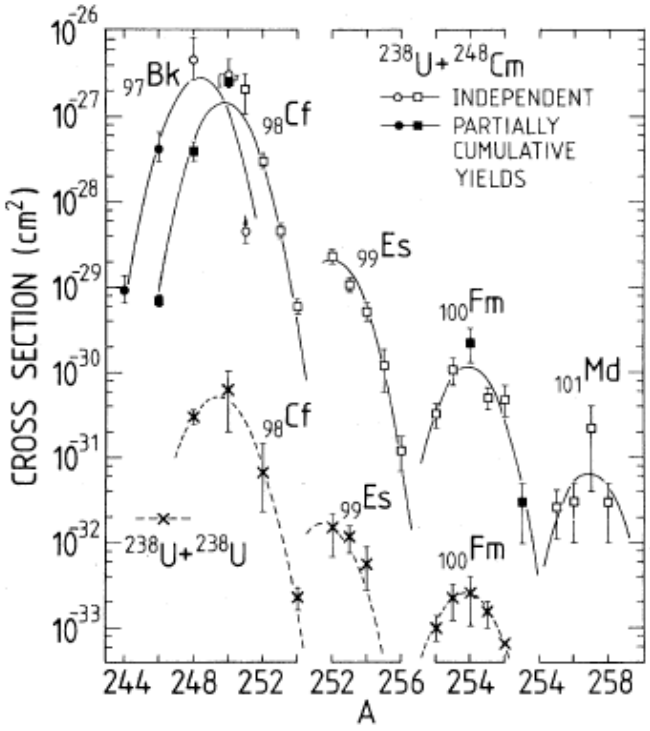

Figure 2.3: Production cross sections of heavy nuclei from the reaction of $^{238}U + ^{238}U$ and $^{238}U + ^{248}Cm$. The latter reaction resulted in higher cross sections for heavy nuclei, up to 1 μb for Fm isotopes. From [42].

2.2 Modern Experiments

In recent years, multi-nucleon transfer experiments have been performed using a variety of projectiles and targets, and the results compared to the predictions from the GRAZING code [22, 23], those from the model of Zagrebaev and Greiner [12-20], and the DNS model. The following is a discussion of some of the encouraging results.

2.2.1 Experiments Testing the GRAZING Code

Szilner et al. performed an experiment bombarding a thin ^{96}Zr target with ^{40}Ca ions at a lab energy of 152 MeV [46]. The projectile-like fragments were identified using the PRISMA magnetic spectrometer, which consisted of a time-of-flight (TOF)

spectrometer and a ΔE-E ionization chamber. The cross sections determined for the neutron transfer channels and the one proton, multi-neutron transfer channels for PLFs were compared to those from the GRAZING code and are shown in Figure 2.4. Both the data points and predictions from GRAZING include neutron evaporation.

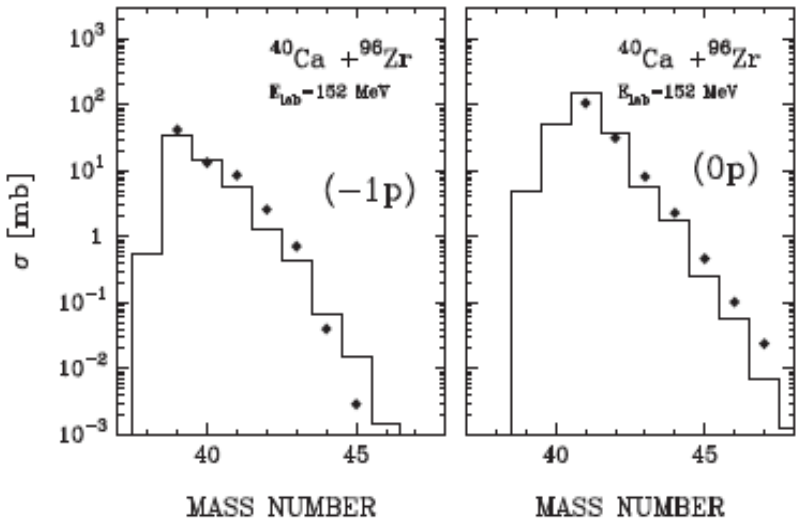

Figure 2.4: Isotopic distributions for the ΔZ=0, -1 projectile-like fragments. The left plot shows K (Z=19) isotopes, and the right plot shows Ca (Z=20) isotopes. The points are experimental cross sections and the histograms are the predictions from the program GRAZING. From [46].

The comparisons with the GRAZING code were only performed for the neutron transfer channels to the projectile nuclei and the -1 proton nuclei. The measured cross sections are very similar to those predicted for nuclei with neutron numbers close to that of the projectile, with discrepancies appearing near the edges of the distributions. However, overall there is good agreement between experiment and theory for these types of transfers.

An experiment by Corradi et al. [47] used ^{64}Ni projectiles incident on ^{238}U at a E_{lab}=390 MeV. The ^{238}U target was 200 μg/cm^2. The detection apparatus was a TOF

magnetic spectrometer, also with a ΔE-E type ionization chamber. The cross sections for PLFs were obtained by integrating over the angular distribution and Q values. These cross sections are shown in Figure 2.5.

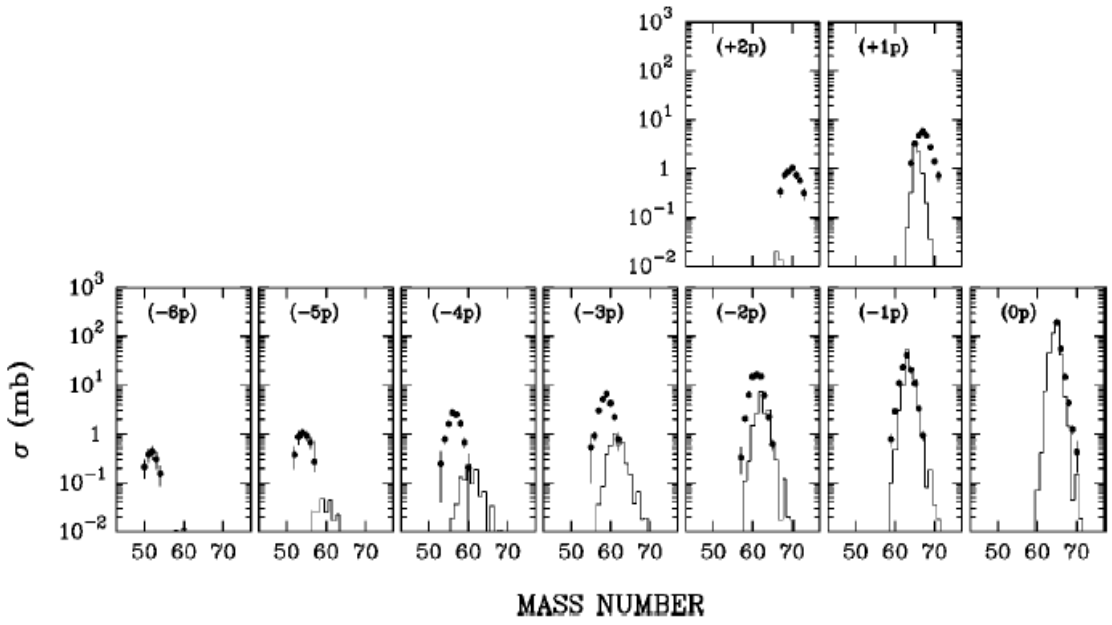

Figure 2.5: GRAZING predictions compared to experimental cross sections in the ^{64}Ni + ^{238}U reaction at E_{lab}=390 MeV. The labels in each plot refer to the change in proton number (ΔZ) relative to the projectile, Ni (Z=28). The points are the experimental cross sections and the histograms are the predictions from GRAZING. From [47].

The authors did not state whether the GRAZING predictions included neutron evaporation. Therefore, it is assumed that the GRAZING calculations reflect pre-neutron emission fragments. For the neutron transfer channels in the projectile isotopes, GRAZING predicts a large drop in cross section for each neutron that is picked up. The experimental data follows those predictions. However, as the number of transferred protons changes, whether protons are stripped or picked up, the disagreement between experiment and theory increases. Not only are the magnitudes

of the cross sections from theory lower, but also the peaks of the distributions tend to be more neutron rich than what is observed experimentally for the proton stripping channels.

A more recent experiment by Watanabe et al. was an investigation of the $^{136}Xe + ^{198}Pt$ reaction at E_{lab}=1,088 MeV [48]. Projectile-like fragments were detected using a combination of VAMOS++, a large acceptance magnetic spectrometer, and EXOGAM, a large array of Ge detectors. Figure 2.6 shows the cross section results of this experiment compared to the predicted post-neutron evaporation cross sections from GRAZING. The authors [48] attribute the discontinuity (dip) in the calculated cross sections to potential shell effects during the evaporation process. The dip shifts to higher A values with increasing Z values and is not present in the pre-neutron emission calculations [48]. However, the A and Z values in the figure would correspond to a neutron value of N~70, where no shell closure exists.

The results for the proton stripping channel agree well with the GRAZING predictions for this system. However, when comparing the proton pickup channels, very large discrepancies are observed as $+\Delta Z$ increases. In the worst case, the predictions from GRAZING for Ce isotopes (ΔZ=+4) are approximately two orders of magnitude lower than those observed experimentally.

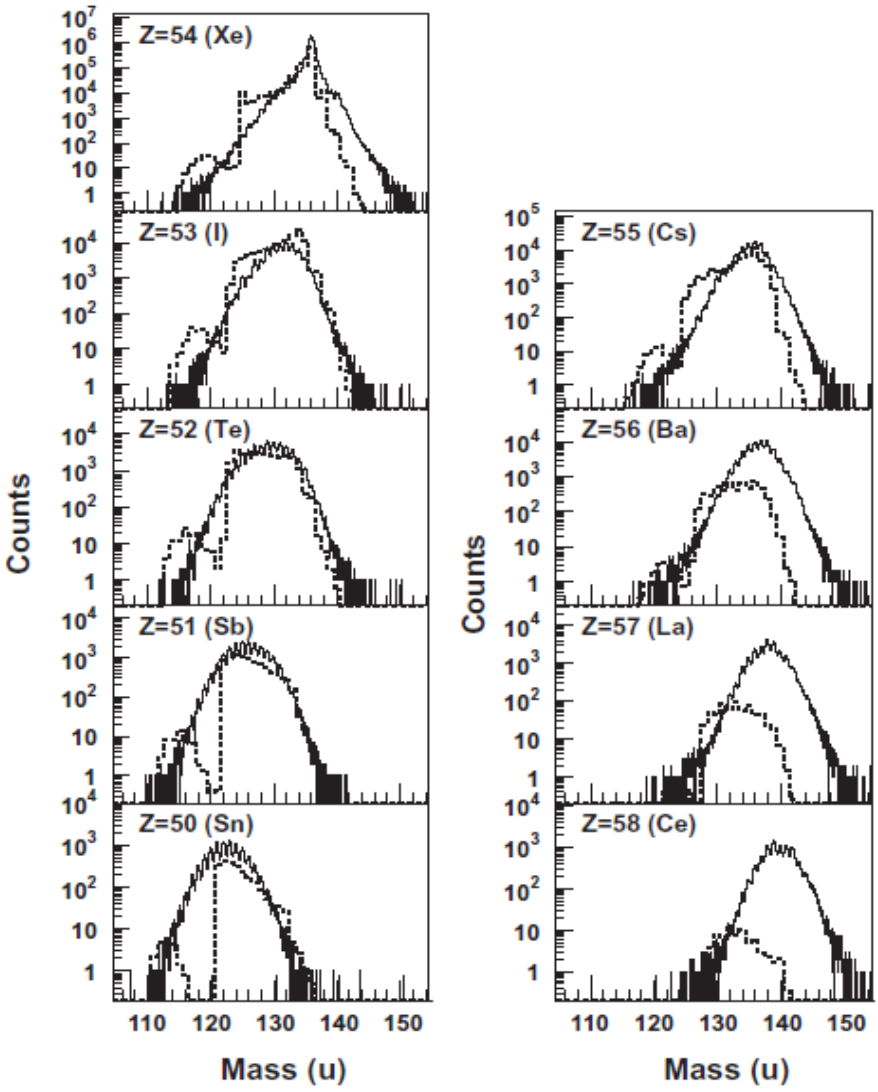

Figure 2.6: Projectile-like isotopic distributions for the ^{136}Xe + ^{198}Pt reaction compared to GRAZING. The energy for this experiment was E_{lab}=1088 MeV. The GRAZING predictions are the dashed lines and the measured cross sections are the histograms. From [48].

2.2.2 Previous Experiments Testing the Zagrebaev and Greiner Model

In their model, Zagrebaev and Greiner predict production cross sections for a number of systems that involve heavy projectiles and/or targets [12]. However, performing these experiments are difficult because of the low cross sections of the reactions, low intensities of heavy ion beams, fission of reaction recoils, and

difficulty in detecting low yield, heavy reaction products in the sea of elastically scattered and otherwise produced products. Therefore, they applied their model to a number of surrogate reactions [13-20] involving lighter nuclei to serve as a stepping stone to ensure that their model accurately predicts formation cross sections. In the event that there are discrepancies, the data from the lighter systems could be used to refine their model.

One of the first surrogate reactions tested was the "anti-symmetrizing" reaction of ^{160}Gd + ^{186}W [49]. This experiment was performed using the ATSCAT facility at Argonne National Lab. The center of target energy was E_{cm}=462 MeV, and the recoiling products from the reaction were collected using Mylar and aluminum catcher foils. These foils were divided according to their angles relative to the beam axis and were analyzed using γ-ray radioactive decay analysis. Figure 2.7 shows a section of the resulting mass distribution. Due to the nature of the analysis, stable and short-lived nuclei were not determined in this experiment.

Figure 2.7 shows only a selected area of the results from this experiment [20, 49]. The red histogram in this figure is the mass distribution for this system as calculated by the liquid drop model only. Zagrebaev and Greiner then included shell effects into their calculation and the result is the black histogram. The interesting result is that the cross sections for trans-target nuclei are "enhanced" relative to the predictions of Zagrebaev and Greiner. In some cases the enhancement is close to an order of magnitude.

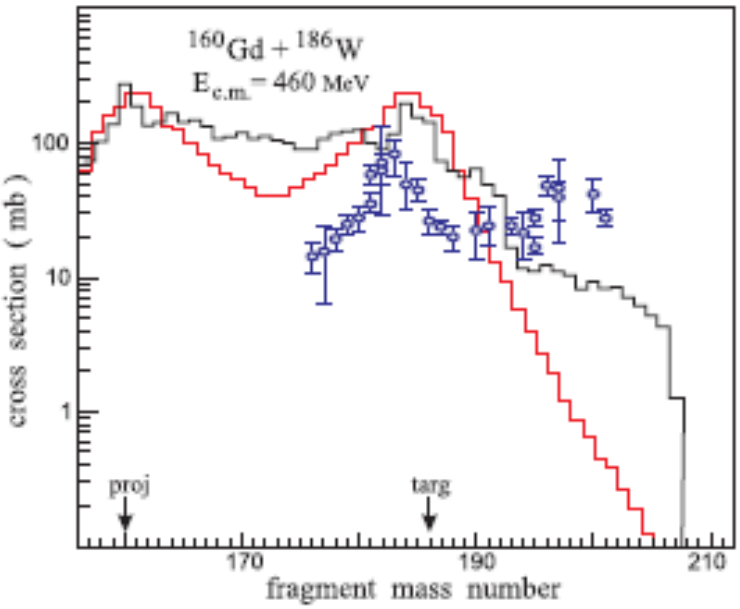

Figure 2.7: Comparison of theoretical and experimental mass distributions in the ^{160}Gd + ^{186}W reaction at E_{cm}=460 MeV. The red histogram is the mass distribution calculated using only the liquid drop model, the black histogram includes shell effects, and the dots are the experimental data points. Figure from [20].

Another experiment used the SHIP velocity filter at GSI investigated the ^{64}Ni + ^{207}Pb reaction [50-52]. This experiment was done at several near barrier energies ranging from E_{cm}=234.7 – 289.4 MeV, which allowed excitation functions to be determined. The target was 380 μg/cm^2 ^{207}PbS that had been evaporated onto 40 μg/cm^2 carbon foils with a carbon cover layer that was 10 μg/cm^2 thick. The acceptance window for the velocity filter only allowed fragments that were emitted within ±2° from the beam axis.

Results for Rn isotopes from this experiment were compared to results from a previous experiment of the reaction ^{64}Ni + ^{208}Pb at E_{cm}=268 MeV using a large array of γ-ray detectors [53]. Isotopic distributions for the reaction products from SHIP were determined for E_{cm}=244.4 MeV. This comparison is shown in Figure 2.8.

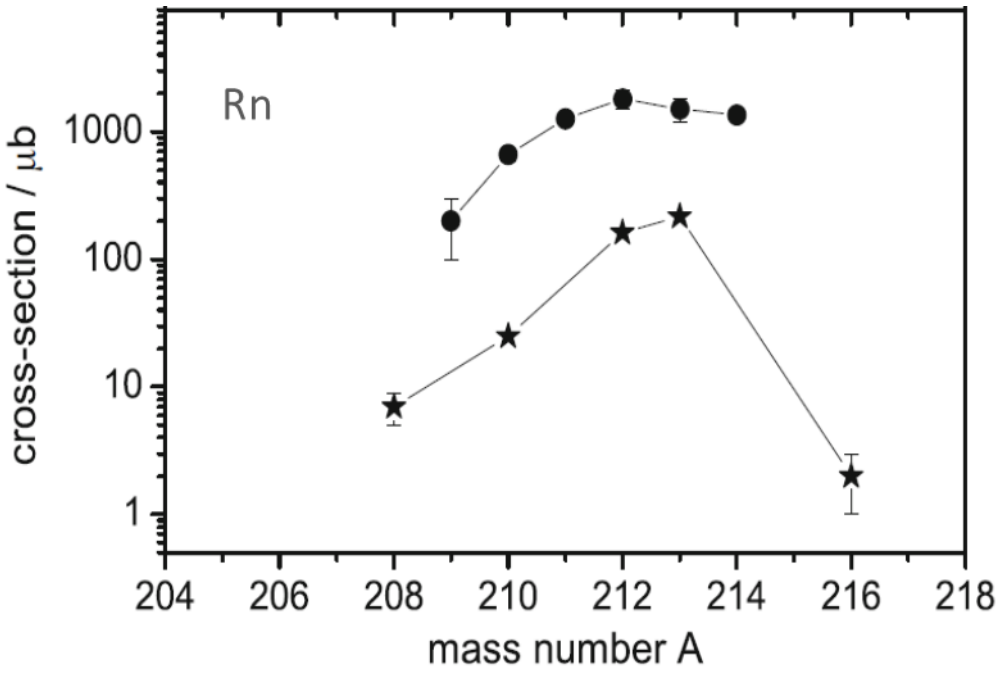

Figure 2.8: Isotopic distribution comparison for Rn isotopes from previous experiments. The circles represent the cross sections determined in the ^{64}Ni + ^{208}Pb reaction at E_{cm}=268 MeV using an array of HPGe detectors. The stars represent data from the ^{64}Ni + ^{208}Pb reaction at E_{cm}=244.4 MeV at SHIP.

The results from the experiment using the array of γ-ray detectors are approximately an order of magnitude larger than the cross sections measured at SHIP. Acknowledging that these experiments were performed at different energies and used different targets (SHIP used ^{207}Pb, [53] used ^{208}Pb), the magnitude of the disagreement between the two experiments is unexpected. It remains to be seen if this disagreement is caused by the detection methods, choice of targets, energies, or some other cause.

The results from the SHIP [50] experiment were also compared to theoretical predictions by Zagrebaev and Greiner. Measured and predicted cross sections for Rn and Fr isotopes are shown in Figure 2.9.

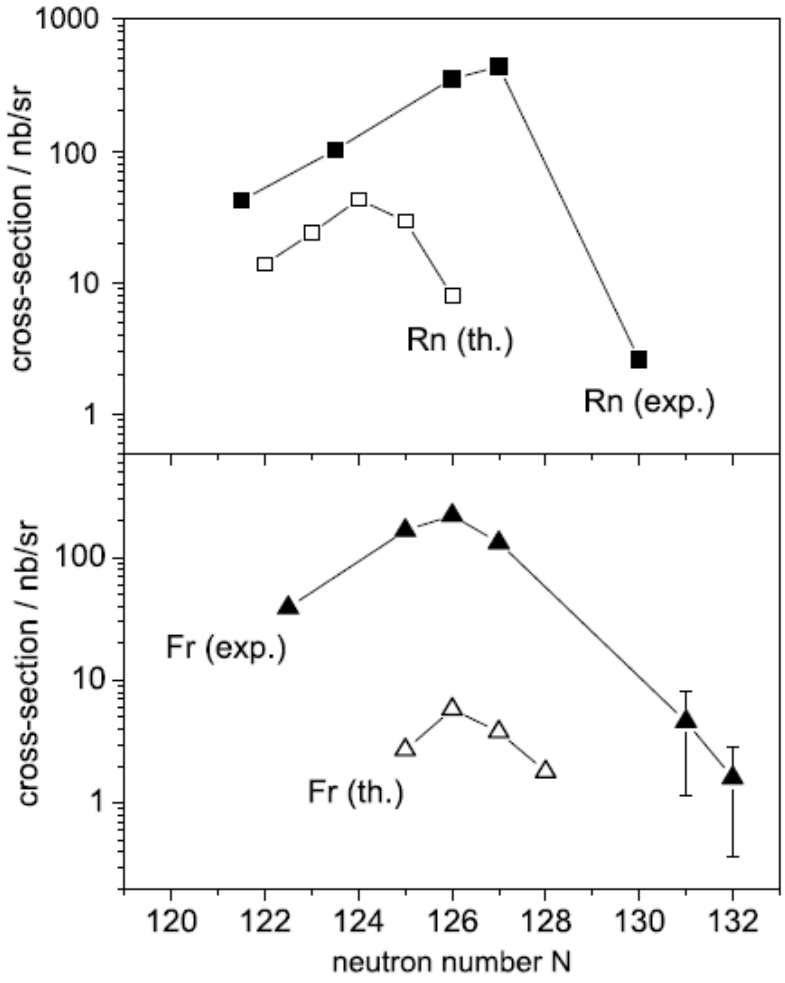

Figure 2.9: Isotopic distributions of Rn and Fr from the reaction of ^{64}Ni + ^{207}Pb at E_{cm}=244.4 MeV. The solid points are the experimental results, and the open point are the calculated theoretical cross sections. From [50].

Once again, for these trans-target nuclei there is an enhancement of measured cross section relative to theory. In some cases this enhancement is larger than an order of magnitude. These results are encouraging for the prospect of producing heavy and super-heavy trans-target nuclei.

Zagrebaev and Greiner's model calculations focus on the region around ^{208}Pb due to the potential energy valley caused by this doubly magic nucleus. They have proposed a surrogate reaction involving a semi-magic projectile, ^{136}Xe, incident upon

a ^{208}Pb target in an effort to use the stabilizing shell effects to preferentially create nuclei along the closed neutron shell, N=126.

An experiment has been carried out by Kozulin et al. [5] to investigate this system as a possible candidate to produce N=126 nuclei at various energies around the Coulomb barrier (E_{cm}=423, 526, and 617 MeV). The experiment was performed using the two-arm TOF spectrometer, CORSET. The target was 200 μg/cm^2 ^{208}Pb deposited onto a 50 μg/cm^2 carbon backing. Measurements of this reaction include total kinetic energy (TKE), kinetic energy loss (TKEL), and the mass distribution, which is shown in Figure 2.10. The experimental cross sections are compared to the calculated mass distribution of Zagrebaev and Greiner. Only events that had a TKEL greater than 40 MeV were included, meaning that quasi-elastic scattering events were omitted.

When comparing the experimentally determined mass distribution to that calculated by the model of Zagrebaev and Greiner, one again notices enhanced cross sections relative to theory for trans-target nuclei. These are the nuclei with approximately A>220 amu in Figure 2.9. During this reaction the authors state that nuclei up to A=238 were observed in this reaction with cross sections on the order of 0.1 mb at E_{cm}=526 MeV. This corresponds to a transfer of 20 nucleons from the ^{136}Xe projectile to the ^{208}Pb target.

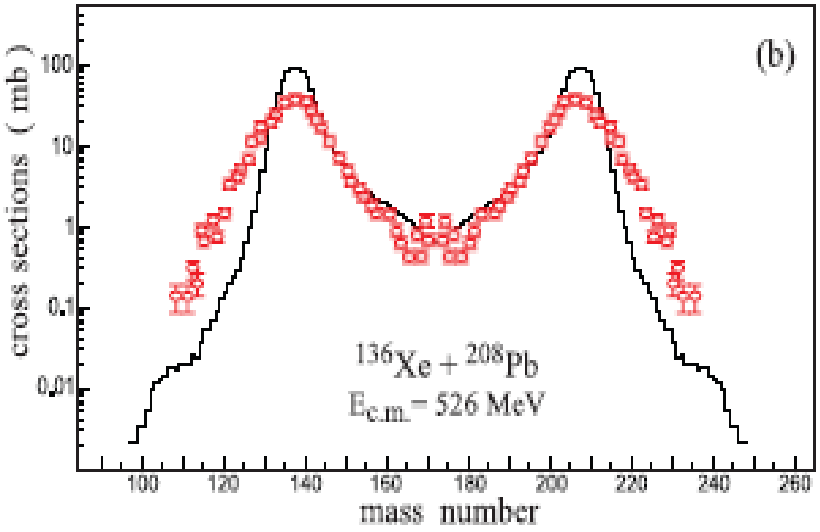

Figure 2.10: Mass distribution of the ^{136}Xe + ^{208}Pb reaction at E_{cm}=526 MeV. Only events with TKEL>40 MeV were included, excluding quasi-elastic events. The measured results show enhanced cross sections relative to theory for trans-target nuclei. The black histogram is the calculated mass distribution. The red points are the measured cross sections from [5]. Figure from [20].

In an effort to confirm the production of target-like fragment nuclei with A>210 amu a second experiment was performed [5]. The same reaction system was used at an energy of E_{cm}=514 MeV, and Al catcher foils at angles of 45° and 55°, with respect to the beam, were used to collect the recoiling reaction products. Then, α-decay spectroscopy was performed to determine cross sections. Through this analysis, cross sections for ^{210}Po, ^{222}Rn, and ^{224}Ra were determined and are shown in Figure 2.11.

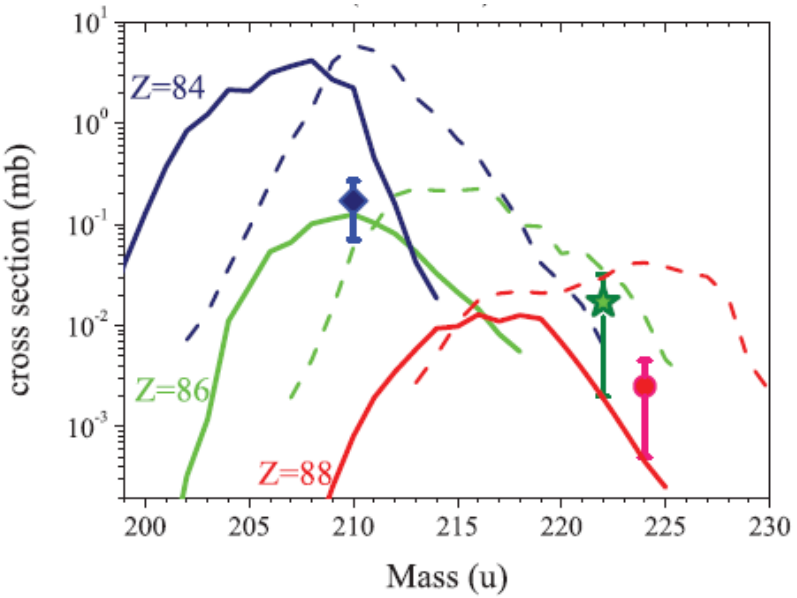

Figure 2.11: Cross sections of ^{210}Po, ^{222}Rn, and ^{224}Ra from the ^{136}Xe + ^{208}Pb reaction at E_{cm}=514 MeV. The ^{210}Po data is blue, ^{222}Rn data is green, and ^{224}Ra data is red. The dashed lines are the calculated primary fragment distributions and the solid lines are the calculated secondary fragment distributions. From [5].

The calculated secondary fragment distribution was overestimated for ^{210}Po by almost an order of magnitude, while the calculated distributions for Rn and Ra were underestimated by approximately an order of magnitude. No information about N=126 nuclei specifically is available from this experiment.

The results from this experiment were also compared to the recent model developed using DNS systematics [26]. Figure 2.12 shows the results of this comparison. Contrary to the predictions of Zagrebaev and Greiner, this model underestimates the secondary yield of ^{210}Po by close to an order of magnitude. The yield for ^{222}Rn is also severely underestimated compared to the measured cross section. However, there is good agreement between the predictions in [26] and ^{224}Ra.

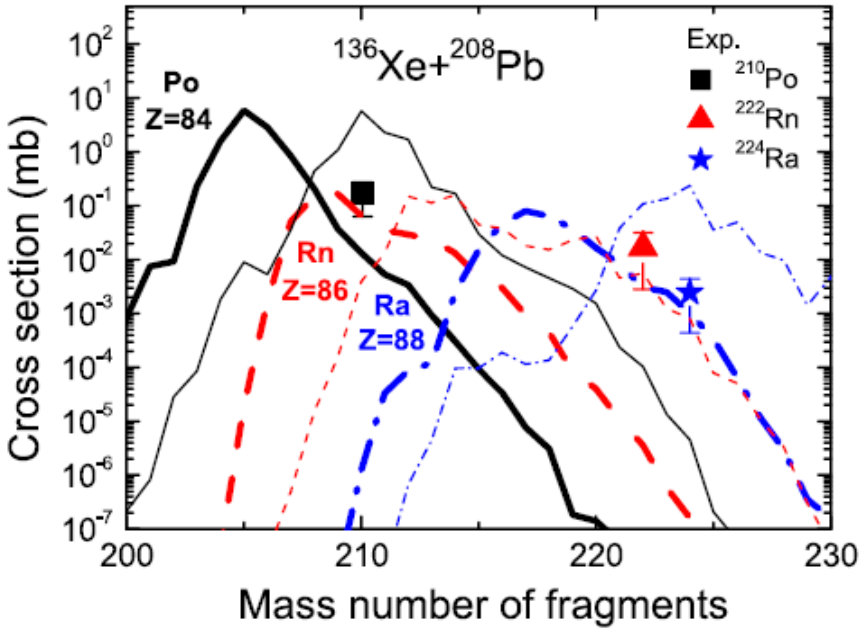

Figure 2.12: Comparison of predicted and measured cross sections from the ^{136}Xe + ^{208}Pb reaction using the DNS model. E_{cm}=514 MeV. The black lines represent the predicted yields of primary (thin) and secondary (thick) Po isotopes. The red dashed lines represent the predicted yields of primary (thin) and secondary (thick) Rn isotopes. The blue dashed/dotted lines represent predicted yields of the primary (thin) and secondary (thick) Ra isotopes. Experimental points are from [5] and the figure is from [26].

Comparing Figures 2.11 and 2.12 one will notice differences between the predictions of the DNS model and the model of Zagrebaev and Greiner. The model of Zagrebaev and Greiner predicts the peak of the secondary cross sections for Po isotopes to be at A=208, while the DNS model predicts it to be at A=205. The peak magnitudes of the secondary distributions between the two models are roughly equal, except for Ra isotopes where the DNS model predicts the peak cross section to be almost an order of magnitude higher than that of Zagrebaev and Greiner. The shapes of the secondary distributions are slightly different as well, with those of Zagrebaev and Greiner appearing more Gaussian-like. The specific origin of these differences is

not entirely clear. They are the result of the different characteristics and parameters of these two complicated models, such as the role of shell effects or how the interaction potentials during the collision are determined [14, 26].

In all of the experiments discussed so far there has been an "enhancement" of cross sections for nuclei that are heavier than the target. Having this experimental data available greatly helps theorists to refine their models in order to improve accuracy. However, when considering the vast amounts of reaction products that are formed in multi-nucleon transfer reactions, the experimental cross section results are only available for a relatively small number of nuclei. Zagrebaev and Greiner have stated that more experimental data is necessary in order to continue to improve their model [20].

Thick target experiments using γ-γ coincidence data from large arrays of high purity Ge (HPGe) detectors have been used to as a tool for nuclear spectroscopy [54-59] and to determine relative and absolute yields of the nuclei produced [53, 60, 61]. These experiments have produced data for a large number of reaction products, including stable nuclei and those with short half-lives. One such experiment, performed by Królas et al. [53], was the investigation of ^{64}Ni + ^{208}Pb at E_{cm}=350 MeV. This experiment utilized the OSIRIS γ-spectrometer, which is an array containing 11 Compton-suppressed HPGe detectors.

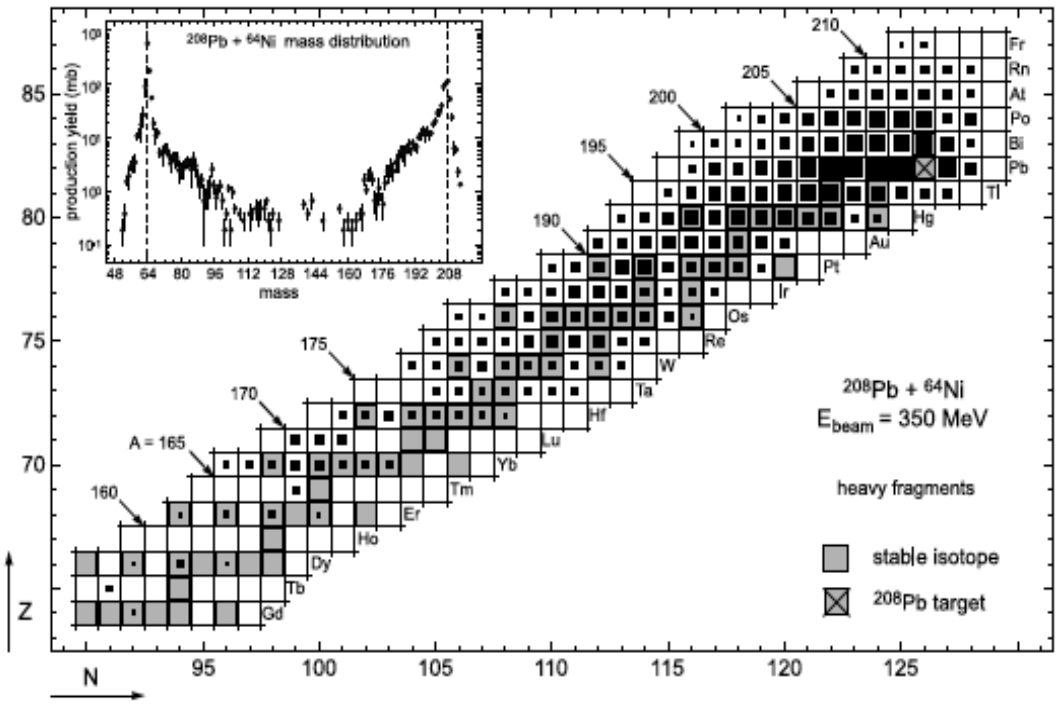

Figure 2.13: Nuclidic cross section map of target-like fragments in the ^{64}Ni + ^{208}Pb reaction at E_{cm}=350 MeV. Cross sections were determined for over 200 reaction products through a combination of in-beam and radioactive decay analysis. From [53].

The nuclides produced were identified through a combination of an analysis of γ-γ coincidence events during the irradiation and radioactive decay analysis after irradiation was completed. Cross sections for long lived nuclei were obtained through the radioactive decay analysis, and cross sections for stable and short-lived nuclei were determined through an analysis utilizing relative yields from γ-rays both during and between beam bursts. As a result, nuclidic yields for over 200 nuclei were determined from this single experiment. Figure 2.13 shows a cross section "map" of the observed nuclei according to neutron number, N, and proton number, Z.

As mentioned earlier, there is interest in the use of shell stabilized projectiles and targets in multi-nucleon transfer reactions for the synthesis of neutron rich heavy elements. Unfortunately, the experimental results from these types of reactions are thus far limited and fragmentary [20]. More experimental data is needed to further understand these mechanisms, and for theory to improve their predicted cross section calculations.

The goal of the present experiment is to utilize a method similar to that of Królas et al. This experiment utilizes Gammasphere, a large array of HPGe detectors, to obtain independent production cross sections for a large number projectile and target-like fragments. Through this work, a semi-magic projectile (^{136}Xe) and doubly magic target (^{208}Pb) will be used to test the multi-nucleon transfer models of GRAZING [22, 23] and Zagrebaev and Greiner [6, 20] at E_{cm}=450 MeV. Production cross sections for N=126 nuclei will be investigated, and the large number of independent yields should help theory to refine their models in order to provide more accurate predictions for the future.

3 EXPERIMENTAL PROCEDURE

3.1 Experimental Overview

This experiment took place at the ATLAS facility of Argonne National Laboratory in collaboration with scientists from Brookhaven National Laboratory and University of Maryland. Cross section results from this experiment have already been published in Physical Review C [62].

The data acquisition for this experiment was performed in two parts. First, a ^{208}Pb target was bombarded by ^{136}Xe projectiles inside of Gammasphere, a large array of HPGe detectors. This in-beam data was later used to identify and determine cross sections of stable and short-lived reaction products.

After target irradiation had completed, involved the collection of radioactive decay data. This data was first collected in Gammasphere, followed by multiple decay measurements using a single, well-calibrated HPGe detector. These measurements were used to calculate cross sections through standard radioactive decay analysis.

3.2 Measurements During Irradiation

3.2.1 Gammasphere

Gammasphere is a large HPGe detector array that has been instrumental in a number of physics studies [63]. When completely functional there are 110 Compton-suppressed HPGe detectors arranged in a honeycomb pattern that cover nearly 4π geometry. The detectors are Compton-suppressed through the use of 6 BGO elements that surround each detector, as well as a 4 cm thick BGO back plug (see Figure 3.1). The detectors are covered by a Hevimet (a tungsten alloy) collimator and absorbers, which are used to reduce the number of incoming low energy photons [64].

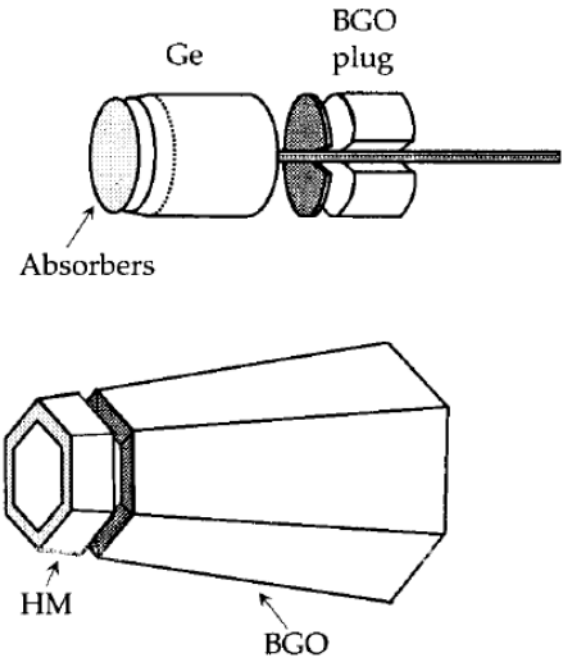

Figure 3.1: Schematic diagram of a single HPGe detector from Gammasphere. Each detector is surrounded by 6 BGO elements, as well as a 4 cm thick BGO back plug. The front of the detectors are covered with Hevimet collimators and absorbers to reduce the number of incoming x-rays and low energy γ-rays. Figure from [64].

The Ge crystals are 7.1 cm in diameter and are 8 cm long, giving an active volume of 317 cm^3. The detectors have a full energy efficiency of 75% and an energy resolution of 2.5 keV for 1.33 MeV γ-rays. The time resolution, through the use of leading edge discrimination, is FWHM=8.5 ns using a ^{60}Co γ-ray source [65, 66]. For this experiment 90 detectors were operational.

Figure 3.2 shows the interior of Gammasphere, and Figure 3.3 shows Gammasphere in the closed position. The quality of the HPGe detectors should ensure uniform efficiency throughout the array. The exception to this may be near the beam entrance and exit. Compton suppression may not be as effective since the beam pipe occupies detector spots in these regions, which will affect the efficiency.

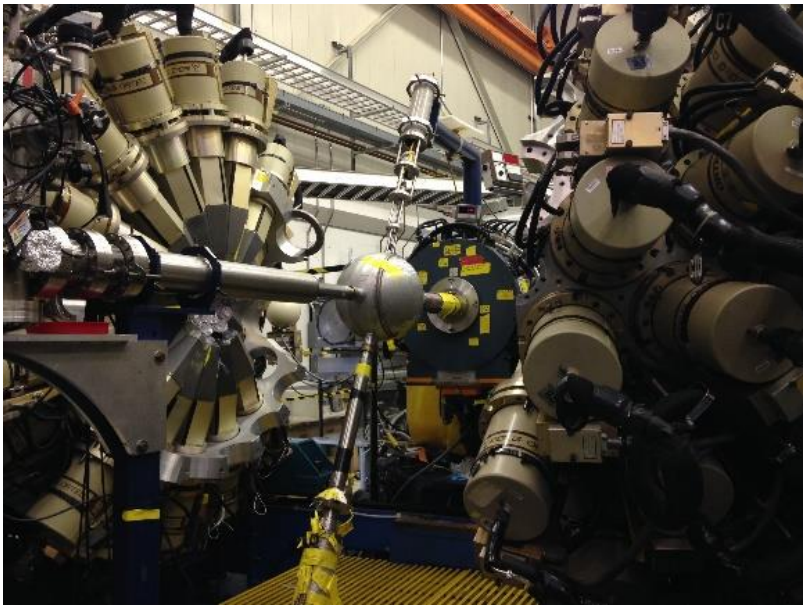

Figure 3.2: Gammasphere in the open position. The metal sphere chamber in the center contains the target ladder as well as the beam pipe. Each detector was covered with 0.010” Cu and 0.002” Ta discs. These discs are X-ray absorbers to lower the background during irradiation.

Figure 3.3: Gammasphere in the closed position. The black tubes are used to periodically fill the dewers with liquid nitrogen to ensure proper operation of the HPGe detectors.

The interior chamber, shown in Figure 3.2, is connected to the beam line and contains the target ladder. In this experiment, the target ladder was occupied by the tuning target, an open frame, and the ^{208}Pb target according to the diagram in Figure 3.4.

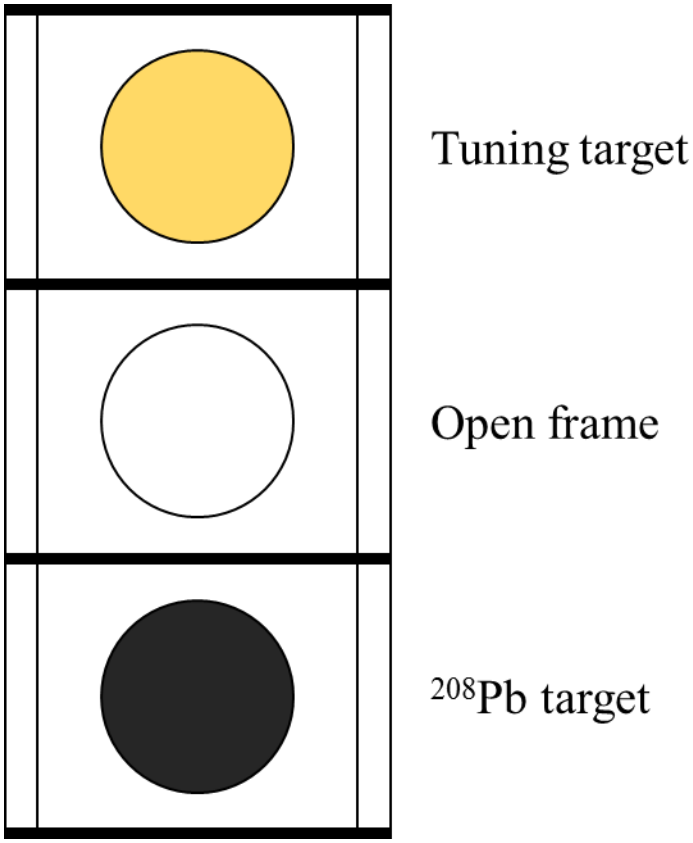

Figure 3.4: Schematic of the target ladder used in Gammasphere. The top slot contained the tuning target. The middle slot was open, and the bottom slot contained the 49 mg/cm^2 (99% enriched) ^{208}Pb target.

The tuning target, used to tune the ^{136}Xe beam, consists of a central region and a collimator. The beam current in the different regions gives a beam profile and ensures that the projectile beam is striking the target in the proper position. The open frame position was not used in this experiment.

The absorbers used in this experiment were 0.010 inch Cu and 0.002 inch Ta plates. These plates were placed on the detectors to reduce the number of low energy X-rays and γ-rays that were produced during the irradiation. This allowed for a cleaner spectrum of γ-rays, but also affected the efficiency of Gammasphere. Since low energy photons are absorbed, the peak of the efficiency curve shifts to a higher energy (~290 keV) than is normally observed in HPGe detectors. Without the use of absorbers, an HPGe detector will usually have a peak efficiency around 100 keV. Figure 3.5 shows an efficiency curve for Gammasphere [67] that was previously measured showing this effect.

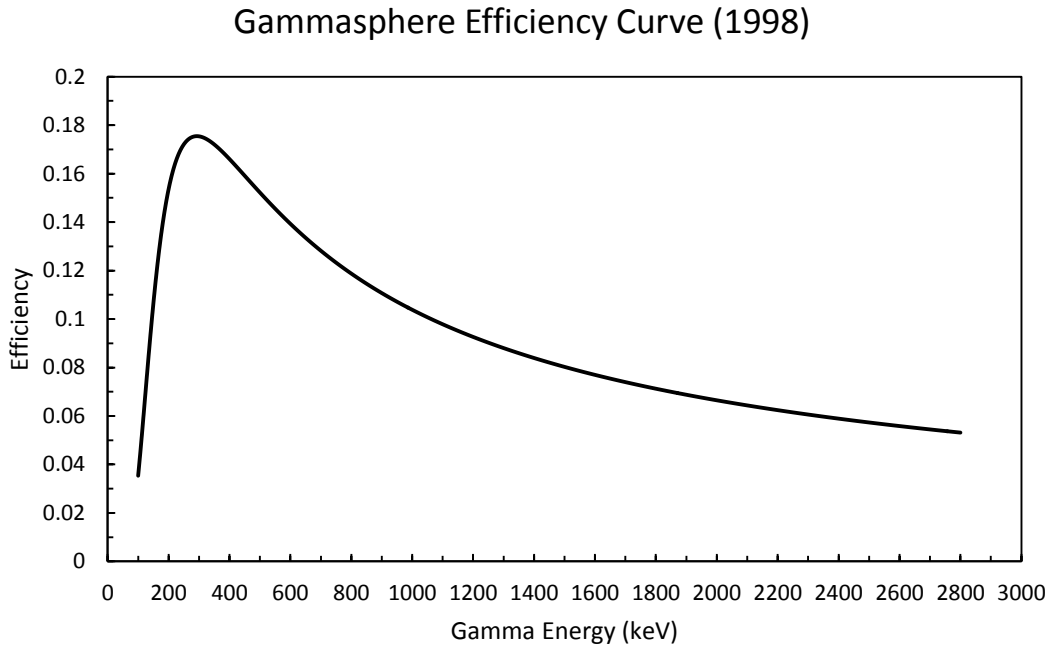

Figure 3.5: Previously measured efficiency curve for Gammasphere. This measurement was taken in April 1998 using ~100 operational detectors and the plot was recreated from the data present in [67].

3.2.2 Energy Calibration

The energy calibration was performed using four different sources: ^{152}Eu, ^{243}Am, ^{56}Co, and ^{182}Ta. Table 3.1 lists the energy ranges of the emitted γ-rays used in the calibration and the number of γ-rays observed from each source. The program ECAL, from the RadWare [68] software suite, determined the energy calibration using a linear fit, given by

$$E_\gamma = 0.3334x - 0.249 \quad (3.1)$$

Here, E_γ is the γ-ray energy and x is the channel number of the detector.

Table 3.1: Nuclides used in the energy calibration of Gammasphere. The number of peaks used is listed as well as the energy ranges of the γ-rays. The ^{152}Eu source was useful for a broad energy range (especially energies between 350-1000 keV), ^{243}Am was useful for low energy γ-rays, ^{56}Co was useful for high energies, and ^{182}Ta was useful to determine the turnover region of the efficiency curve with greater detail.

Nuclide	No. of γ-rays	Eγ Range (keV)
^{152}Eu	16	122 - 1408
^{243}Am	9	75 - 334
^{56}Co	14	847 - 3451
^{182}Ta	18	66 - 264/1121 - 1231

3.2.3 Beam and Thick Target Considerations

Thick target experiments that stop the beam and reaction products in the target material have previously been performed [53-56, 60]. These experiments then detect the γ-rays emitted from the products for spectroscopic studies or to determine production cross section. When using this technique for cross section determination, one must understand that the reaction energy is no longer simply the beam energy.

Instead, the measured cross sections are the result of an integration of beam energy from the entrance energy down to the interaction barrier.

The beam produced at ATLAS was a $^{136}Xe^{30+}$ pulsed beam that was bunched every 82.4 ns. A sweeper knocks out 9 of every 10 bursts, giving the time between bursts on the target to be 824 ns. The entrance beam energy was E_{lab}=785 MeV, or

$$E_{cm} = E_{lab}\frac{A_t}{A_p+A_t} = 785\ MeV\left(\frac{208}{136+208}\right) = 475\ MeV \tag{3.2}$$

An integration of the reaction cross section can be used to find the average energy through the target until the interaction barrier is reached. The reaction cross section is given by

$$\sigma_R = \pi R^2\left(1-\frac{V_{int}}{E}\right) \tag{3.3}$$

In this equation, R is the sum of the nuclear radii, V_{int} is the interaction barrier energy, and E is the projectile energy. Since the main concern is the energy dependence of this equation and the other terms are constant, only the term inside the parenthesis of equation 3.3 will be considered. Equation 3.4 is used to find the average amount of beam energy lost, X_{ave}, from the entrance energy, E_0, to the interaction barrier.

$$X_{ave} = \frac{\int_{B_{int}}^{E_0}\left(1-\frac{V_{int}}{E}\right)dE}{E_0-B_{int}} \tag{3.4}$$

Evaluating this integral produces

$$X_{ave} = \frac{(E_0-B_{int})-\left(V_{int}\ln\left(\frac{E_0}{B_{int}}\right)\right)}{E_0-B_{int}} \tag{3.5}$$

Using the center-of-mass energy values (E_0=475 MeV, V_{int}=B_{int}=423 MeV), it is determined that an average of 27 MeV (5%) of the beam energy is lost between

entering the target and reaching the interaction barrier. This corresponds to an average beam energy of E_{cm}=448 MeV.

A simplified version of this calculation is given by

$$E_{ave} \sim B_{int} + \frac{(E_0 - B_{int})}{2} \tag{3.6}$$

Entering in the values for E_0 and B_{int}, the average reaction energy is

$$423\ MeV + \frac{475\ MeV - 423\ MeV}{2} = 449\ MeV \tag{3.7}$$

The ^{208}Pb target (99% enriched) was prepared by John Greene at Argonne National Laboratory. The target thickness was 49 mg/cm^2, which was thick enough to completely stop the beam in the target. The "effective" thickness is the thickness of the target needed for the beam to degrade from its entrance energy of E_{cm} = 475 MeV to the interaction barrier energy, E_{cm} = 423 MeV. This is the point at which no more nuclear interactions occur, and therefore don't contribute to the reaction product cross sections. The programs SRIM [69] and RANGE [70] were used to model the beam traversing the target, giving an "effective" thickness of 3.1 mg/cm^2 to reach the interaction barrier.

3.2.4 The ^{136}Xe + ^{208}Pb Run

After tuning and calibration were complete, data collection began. The data acquisition system (DAQ) was separated into three different computer stations. One station was used as the main DAQ controller and monitor. At this station, runs were started, stopped, and monitored for beam loss or any other system malfunctions that may have occurred. The second computer was used as the main storage center. Data

from this computer was copied to the third station, which was used for initial off-line analysis and data transfer to a mobile drive.

In-beam data collection lasted 3.8 days. The DAQ was set to trigger on triple coincidence events in order to limit saturation of the detectors during the beam on periods, as well as minimize dead time. Compton suppression was constantly enabled during irradiation. When the beam was lost during the run, the system was set to trigger on single events to record radioactive decay data until the beam returned. The trigger was again set to triple events when the beam returned.

Figure 3.6 is an example of the count rate changes observed when the beam was lost during the experiment. The higher rates (~8000-9000 cnts/sec) represent periods when the beam was on, with the trigger set to triples. The areas where the rate drops (~3000-4000 cnts/sec) are times when the beam was lost and the trigger was set to singles. The areas where no count rate is observed occur when no beam is on target and the trigger is left on triples. One can see the stark difference in count rates between beam on and off periods as a qualitative representation of the amount of data that was collected during this experiment. It should be noted that this figure is not representative of the overall experiment. Over the entire 3.8 day bombardment, the beam was on target for 86% of the total irradiation time with an average beam intensity of 27.6 ± 4.1 electrical nA. The total fraction of beam off time was 14%.

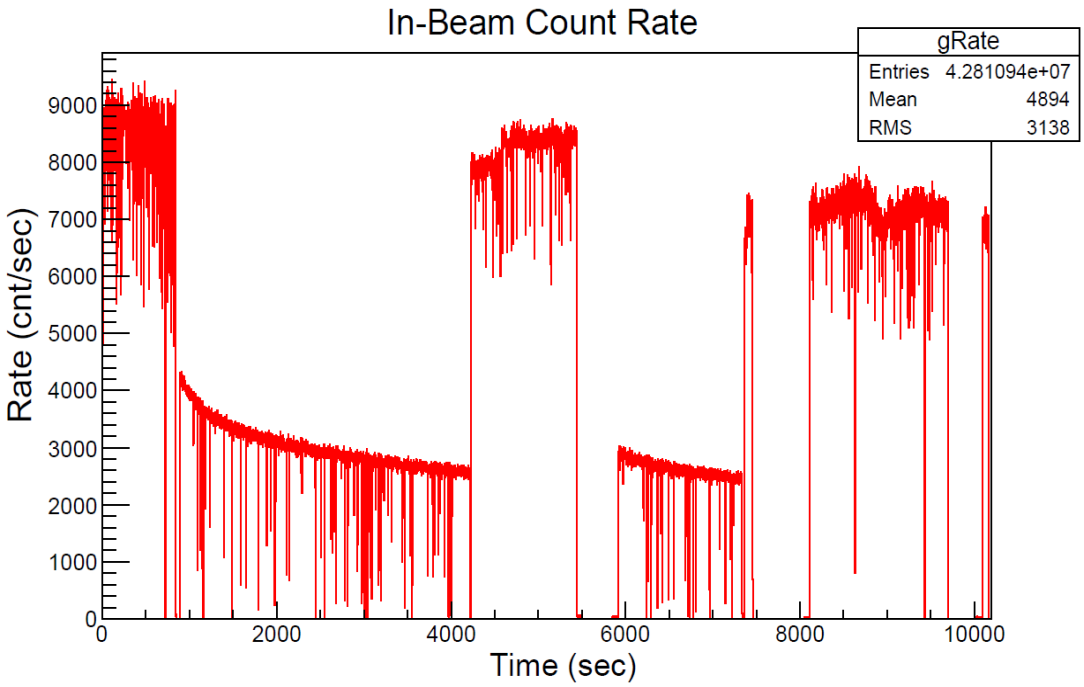

Figure 3.6: Example plot of the count rates observed during the experimental run due to beam-on-target or beam loss conditions. The higher rates reflect beam-on-target periods with the DAQ set to trigger on triple events. The lower rates reflect beam off periods when the DAQ was set to trigger on single events. The periods during beam loss when no count rates were is observed is due to the DAQ being set to trigger on triple events. The beam was "on target" for 86% of the 3.8 day irradiation.

Periodically during the run a suppressed Faraday cup was inserted into the beam line just ahead of the target. This allowed the beam current to be measured, which was later used in calculations to determine cross sections. To determine the beam current for beam on periods between the direct measurements, the currents measured before and after these periods were averaged. Table 3.2 contains a complete beam irradiation history showing the beam on and off periods as well as their respective electrical beam currents in electrical nanoamps.

Table 3.2: Complete beam history during in-beam irradiation. The times listed are relative to the start of irradiation in minutes. Also included are duration of each beam on/beam off period (ΔT), the beam status (on/off), and the estimated beam current for each period in electrical nanoamps.

Time Start (min)	Time Stop (min)	ΔT (min)	Beam Status	Beam Current (enA)
0	308	308	on	14
308	329	21	off	-
329	708	379	on	13.5
708	852	144	off	-
852	868	16	on	29.5
868	919	51	off	-
919	920	1	on	29.5
920	965	45	off	-
965	994	29	on	29.5
994	1003	9	off	-
1003	1009	6	on	29.5
1009	1013	4	off	-
1013	1060	47	on	30
1060	1066	6	off	-
1066	1236	170	on	30
1236	1240	4	off	-
1240	1259	19	on	30
1259	1268	9	off	-
1268	1309	41	on	30
1309	1316	7	off	-
1316	1373	57	on	30
1373	1379	6	off	-
1379	1761	382	on	30
1761	1779	18	off	-
1779	1806	27	on	30
1806	1821	15	off	-
1821	1824	3	on	30
1824	1873	49	off	-
1873	1880	7	on	28
1880	1968	88	off	-
1968	2419	451	on	28

Continued on next page

Continued from previous page

2419	2476	57	off	-
2476	2496	20	on	28
2496	2527	31	off	-
2527	2566	39	on	28
2566	2573	7	off	-
2573	2580	7	on	28
2580	2635	55	off	-
2635	2645	10	on	27
2645	2650	5	off	-
2650	2671	21	on	28
2671	2675	4	off	-
2675	3524	849	on	29
3524	3598	74	off	-
3598	4095	497	on	28
4095	4104	9	off	-
4104	5179	1075	on	28
5179	5203	24	off	-
5203	5232	29	on	28
5232	5243	11	off	-
5243	5255	12	on	28
5255	5261	6	off	-
5261	5511	250	on	24
5511	5517	6	off	-
5517	5526	9	on	28

The electrical current is converted into the beam flux, which is the number of particles incident on the target per second, Φ, by equation 3.8.

$$\Phi = \frac{I}{q * 1.602x10^{-19}\frac{Coulomb}{ion}} \tag{3.8}$$

Here, I is the beam current in amps and q is the charge of the projectile ion (+30). The projectile charge was measured before reaching the target area based on the mass-to-charge ratio of the particle beam, and was provided by the operations staff at ATLAS.

3.3 Radioactive Decay Measurements

3.3.1 Gammasphere

At the end of bombardment (EOB) Gammasphere was switched to trigger on single events and the sample was left for 39 hours to collect radioactive decay data. Figure 3.7 shows the count rate during the first 8 hours after EOB.

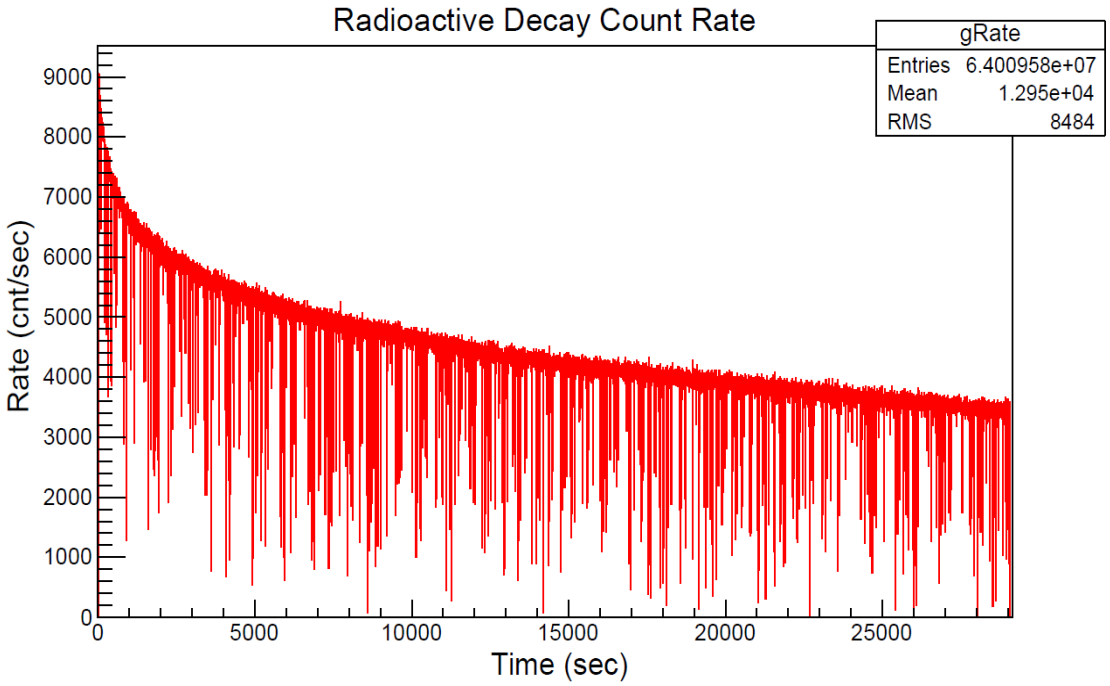

Figure 3.7: The count rate during the first 8 hours of measuring radioactive decay in Gammasphere. Gammasphere was set to singles mode, acting like one large 4π detector. The expected shape of a first order exponential decay curve can be observed.

This data generated three raw data files. These files were cut into 5 time periods so that a total of 15 activity measurements could be obtained and plotted as decay curves (see chapter 4). The first file contained the data from the first 484 minutes, and each time cut had a Δt of 96 minutes. The second file contained decay data for the next 835 minutes, with each cut having a Δt of 160 minutes. Finally, the

last file contained the data for the last 1138 minutes, and each cut had a Δt of 226 minutes.

3.3.2 Single HPGe Detector

After the Gammasphere measurements were complete, the sample was placed on a target card (Figure 3.8) and radioactive decay measurements were recorded using a single HPGe detector. The beam spot is visible in the figure and has an oblong shape. This is different than a point source because the γ-rays entering the detector may be generated from different locations, causing slightly different geometries. In addition, the beam spot was mounted slightly offset from the center of the counting card by approximately 2 mm, also affecting the detection geometry. The combined effect of these two considerations will affect the efficiency of the detector. The magnitude of these effects adds an uncertainty of 1.1% to the calculated cross sections.

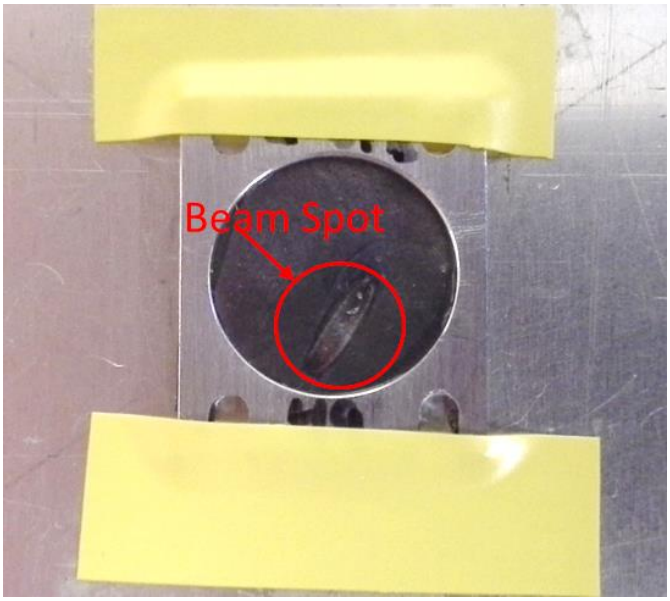

Figure 3.8: The ^{208}Pb target mounted to the target card. The beam spot is visible as a stripe on the bottom half of the target and was mounted ~2 mm offset from center.

A target card holder was placed over the HPGe detector and contained five slots of varying distance from the face of the detector. The holder was placed as close to the face as possible and the card containing the target was placed in the closest slot to the detector. The distance between the target and the face of the detector was approximately 1 cm, and the distance from the detector face to the Ge crystal is 3 mm. The calibration source and target distances were held constant during both calibration of the detector and the decay runs so that only one detector efficiency curve was needed.

Before the sample target was installed, a background measurement and detector calibration were performed. The background was measured with the card holder and mounting apparatus present to ensure that the background from all of the material present in the actual runs was accounted for. The measurement lasted for 24 hours with an overall dead time of 0.01%. The resulting background activities were subtracted during the analysis of the target γ-ray spectra. For comparison, the background activity in the range of 510 - 513 keV was 0.0237 counts/second. The activity for this same energy range in the last decay measurement was 0.869 counts/second. Thus the magnitude of the background subtraction was 3% of the total activity.

Detector calibration was performed using a standard, calibrated multi-radionuclide source. The activity for each nuclide in the source was determined on a specific reference date, allowing for the activity at the time of detector calibration to be determined using equation 3.9.

$$A_t = A_0 e^{-\lambda t} \tag{3.9}$$

The nuclides, γ-ray energies, half-lives, reference activities, and current activities used in the calibration are listed in Table 3.3.

Table 3.3: The nuclides used in the energy and efficiency calibration of the single HPGe detector. Data from a multi-nuclide source includes the γ-ray energies, half-lives, initial activities, and current activities on at the time of calibration.

Nuclide	Eγ (keV)	Half-Life (Days)	A_0 (γps)	A_{expt} (γps)
^{241}Am	59.5	1.580E+05	2.239E+03	2.232E+03
^{109}Cd	88.0	4.626E+02	3.084E+03	1.006E+03
^{57}Co	122.1	2.718E+02	1.643E+03	2.440E+02
^{139}Ce	165.9	1.376E+02	2.296E+03	5.308E+01
^{113}Sn	391.7	1.151E+02	3.228E+03	3.573E+01
^{137}Cs	661.7	1.098E+04	2.065E+03	1.970E+03
^{60}Co	1173.2	1.925E+03	3.863E+03	2.951E+03
^{60}Co	1332.5	1.925E+03	3.864E+03	2.952E+03
^{88}Y	1836.1	1.066E+02	8.156E+03	6.304E+01

Since the current activity for each nuclide was known, the detector's absolute efficiency could be determined according to equation 3.10.

$$\varepsilon_{abs} = \frac{N_{\gamma-obs}}{N_{\gamma-tot}} \tag{3.10}$$

Both the energy and efficiency calibrations were performed using the FitzPeaks [71] γ-ray analysis software. The energy calibration equation determined by FitzPeaks for the single HPGe detector is shown in equation 3.11, where x is the channel number.

$$Energy = 1.7702 + 0.41972 * x - 1.277 * 10^{-7} * x^2 \tag{3.11}$$

The detector efficiency, ε, is given by

$$\varepsilon = CE_{\gamma}^{-A} \tag{3.12}$$

In this equation, ε is the detector efficiency, E_γ is the γ-ray energy, A is the order of the equation, and C is a constant determined and stored by the fitting algorithm. In FitzPeaks, the order was set to A=4 and the percent difference between the measured and fitted efficiencies were 0.107, 1.062, 2.719, 0.353, 0.314, 0.346 and 8.662% for γ-ray energies of 59.5, 88.0, 122.1, 661.7, 1173.2, 1332.5, and 1836.1 keV, respectively.

Radioactive decay measurements were taken over 5.3 days, during which 15 individual decay samples were taken. The maximum dead time observed was 1.09%, allowing the closest geometry to the detector face to be utilized without saturating the detector. Table 3.4 shows a run history of the radioactive decay measurements, including the run number, live times, real times, and percent dead time observed.

Table 3.4: Sample history from the single HPGe detector measurements using the ATLAS hot laboratory.

Sample	Δt_{live} (sec)	Δt_{real} (sec)	Dead time (%)
1	26624.3	26917.4	1.09
2	20264.0	20464.4	0.98
3	37189.9	37520.4	0.88
4	30024.4	30264.4	0.79
5	17983.9	18118.6	0.74
6	40366.3	40648.4	0.69
7	25746.7	25914.1	0.65
8	20074.8	20199.4	0.62
9	40982.7	41223.0	0.58
10	23423.9	23553.6	0.55
11	22160.7	22278.9	0.53
12	38459.5	38655.0	0.51
13	31087.1	31236.8	0.48
14	53772.6	54016.3	0.45
15	27673.3	27791.8	0.43

4 DATA ANALYSIS

4.1 Radioactive Decay

4.1.1 Single HPGe Detector

The procedure to determine absolute nuclidic cross sections from radioactive decay data can be broken up into three main parts. First, the measured activities during the various runs are corrected for background and the efficiency of the detector. Second, these data are then used to construct decay curves for the different nuclides. Using these decay curves, the activity at the end of bombardment is determined. Finally, using this EOB activity, the cumulative absolute cross sections are calculated and corrected for precursor beta decay in order to obtain independent absolute cross sections.

The program FitzPeaks [71] was used to analyze the γ-ray spectra obtained from the single HPGe detector (Figure 4.1). The calibration was performed using a multi-nuclide source containing ^{241}Am, ^{109}Cd, ^{57}Co, ^{139}Ce, ^{113}Sn, ^{137}Cs, ^{60}Co, and ^{88}Y (Table 3.3), taking into account decay from the date of reference. The efficiency of the detector was also determined using this program and was automatically applied to the measured peak areas. The peak areas were determined using the automated peak search and fit algorithms of the program. The peak detection sensitivity parameter was set to 3, which allowed the program to find all of the peaks of interest in the spectrum. As part of the search, if a single Gaussian distribution didn't fit a particular peak, or a small bump was present in the peak front or tail, the program would prompt the user to add another peak to improve the fit. The new peak was also included in the peak fit analysis.

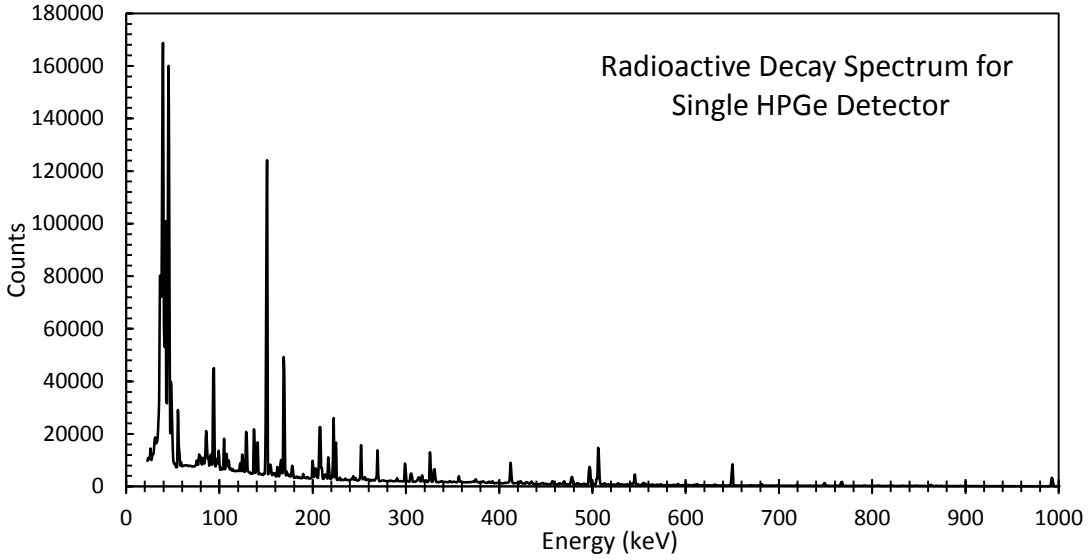

Figure 4.1: Spectrum from single HPGe detector measurements. FitzPeaks [71] was used to determine peak activities for the radioactive decay measurements from the single HPGe detector.

The output of the FitzPeaks [71] program included the peak energies, areas, activities in counts per second (γps), and the activity uncertainty. The time of measurement relative to the EOB (EOB being time zero) was assigned to the data sets from each decay run. The energies of each peak from the various runs were combined and averaged to give the mean peak energy. This data was then used to construct an input file that would later be used for decay curve analysis. The first column of the input file contained the mean peak energies, the second column listed the number of data points for the given energy and the activities at each time point. The third column contained the uncertainty in the activities, and the fourth column was the time point of each measurement. An example of the input file format is presented in Table 4.1.

Table 4.1: Example of Radioactive Decay Input File. The file is organized by mean energy, measured activity, uncertainty, and time of measurement relative to EOB. The first row in the activity column for each new peak energy lists the number of data points present for that particular energy.

Energy (keV)	A (γps)	Error	Time (days)
241.8286	6		
241.8286	0.9790	0.2878	2.1781
241.8286	0.8112	0.1777	2.5142
241.8286	0.7665	0.2729	2.9076
241.8286	0.5165	0.3130	3.1882
241.8286	0.4639	0.1693	3.5292
241.8286	0.2806	0.1434	4.5399
250.4308	13		
250.4308	174.0700	6.0925	1.9017
250.4308	113.4800	4.0853	2.1781
250.4308	66.4330	2.5245	2.5142
250.4308	32.4130	1.6855	2.9076
250.4308	19.5120	0.8585	3.1882
250.4308	10.5370	0.4531	3.5292
250.4308	5.3132	0.3985	3.9167
250.4308	3.2596	0.3194	4.1840
250.4308	1.6516	0.2263	4.5399
250.4308	0.8584	0.1545	4.9163
250.4308	0.4985	0.1984	5.1823
250.4308	0.4922	0.1255	5.5361
250.4308	0.2467	0.0927	6.4438

This input file was used by the FORTRAN program analysis-rev-oo.for (see Appendix), which constructed decay curves, allowed the user to determine the identity of the nuclides, and determined EOB activities. The program used this file to plot the data points on a semi-logarithmic plot with the time of measurements on the x-axis and the natural log of the activities on the y-axis.

The resulting decay curves may have various forms. If the decay curve is composed of only one decaying nuclide, then the plot will simply be a straight line like the ones shown in Figure 4.2.

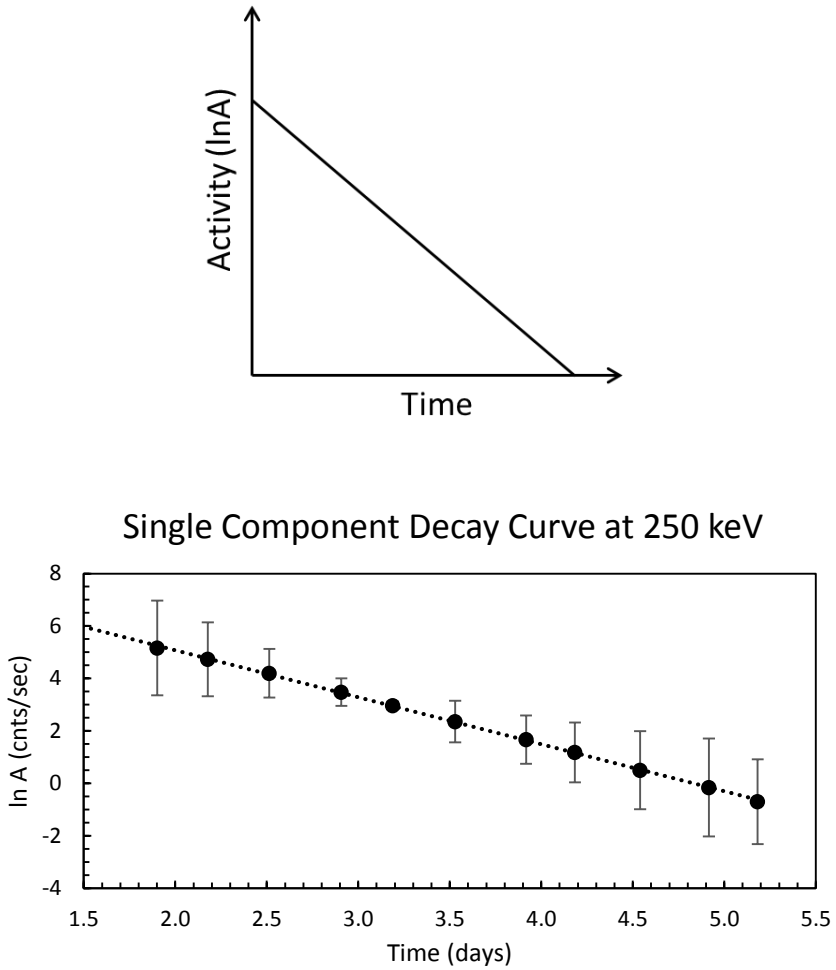

Figure 4.2: Single component radioactive decay curves. The upper plot shows an idealized version of a single component decay curve. The x-axis is the measurement time and the y-axis is the natural log of the activity measurement. The bottom plot shows the decay curve for the measured γ-ray activity at 250 keV. The dotted line is the fit to the data with χ^2=0.002.

The equation of this line is given by equation 4.1.

$$lnA = -\lambda t + lnA_0 \tag{4.1}$$

In this equation, A is the activity of the individual data point, t is the time point, A_0 is the activity at EOB, and λ is the decay constant. The decay constant is related to the half-life ($t_{1/2}$) of the nuclide by equation 4.2

$$t_{1/2} = \frac{ln2}{\lambda} \tag{4.2}$$

The nuclide is then identified by both its half-life and the γ-ray energy (or energies if more than one γ-ray is observed). A_0 is used later in the cross section calculation.

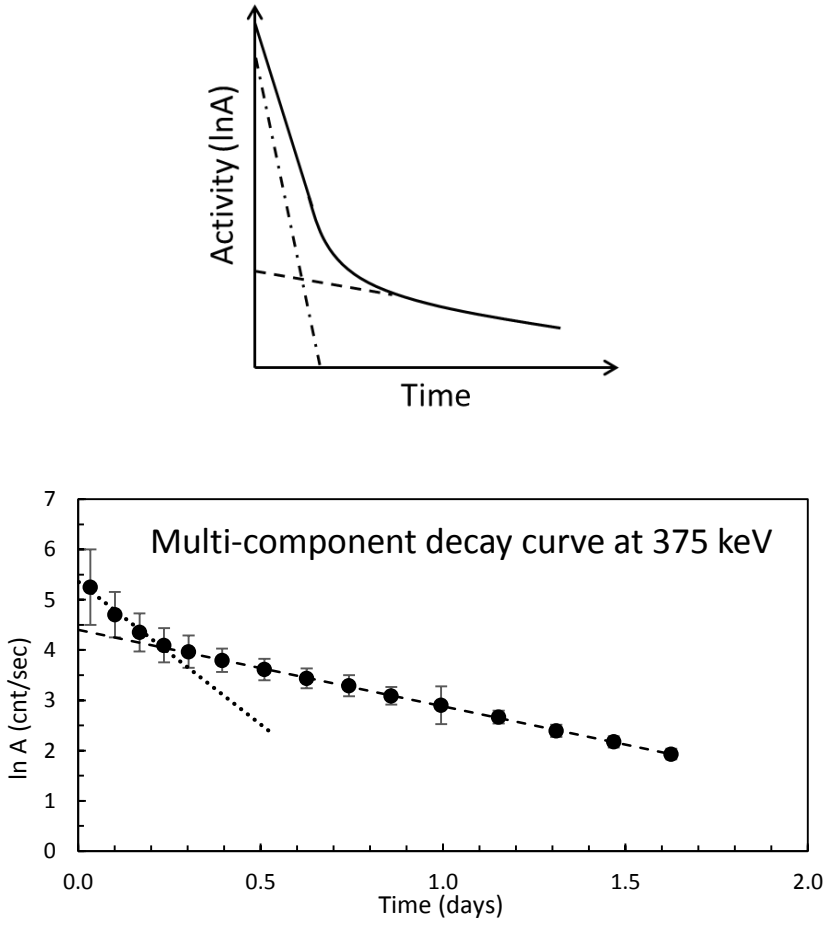

Figure 4.3: Plots of two-component decay curves. In the upper plot, the dashed-dotted line represents a nuclide with a short half-life. The dashed line represents a longer lived nuclide. The observed curve (solid line) is a combination of the two components. The lower plot shows a two-component decay curve at 375 keV. The dotted line shows the fit to the faster decaying component with χ^2=0.005, and the dashed line is the fit for the longer lived nuclide with χ^2=0.0007.

More than one nuclide may decay at a particular, or very similar, energy. The decay plot for a combination of two decaying nuclides may result in a curved shape. If the two nuclides have sufficiently different half-lives, the decay curve may be broken up into its linear components, as shown in Figure 4.3. Equations 4.1 and 4.2 are then used on each linear component to identify each nuclide and determine A_0. A similar procedure is used for decay curves with 3 components.

Using the data, the program determines the most likely half-life associated with a given curve. The user can use this half-life value as a guide to identify the nuclide or nuclides that are decaying. To identify the decaying product(s), the program utilizes a library to show the user nuclides with similar peak energies along with their respective half-lives. The user then chooses a single nuclide, or a combination of multiple nuclides if necessary. The program fits the data points using the chosen nuclides and calculates the reduced χ^2 of the resulting fit. The fitting process is repeated at each peak energy for all possible single nuclides and/or combination of nuclides that generate the lowest possible value of reduced χ^2. The program determines the A_0 value for each component, accounting for the branching ratios of each γ-ray according to the modified γ-ray tables of Reus and Westmeier [72, 73]. The data is then saved to a text file that is used in the calculation of absolute cross section.

The data in the text file is reorganized by nuclide and isomeric or ground state by another FORTRAN program, desort.for (see Appendix). The beam history is added to the beginning of this file, which includes the durations of the beam on/off

periods and the total number of beam particles incident on the target during those times. The result is used as the input file for the FORTRAN program cross.for (see Appendix). This program calculates and stores the flux (Φ) in particles per second, the irradiation time (TIM), the total time of bombardment (TOB), and the time after irradiation until EOB (TIAB) for the ith beam on/off period.

$$TIAB_i = TOB - TOTTIM_i \tag{4.3}$$

The total elapsed time after the ith beam period (TOTTIM), for n beam on/off periods, is given by:

$$TOTTIM_i = \sum_{i=1}^{n} TOTTIM_{i-1} + TIM_i \tag{4.4}$$

Equation 4.5 shows the equation for nuclidic activity at time t after irradiation of a target.

$$A_t = N\sigma\Phi(1 - e^{-\lambda t_1})e^{-\lambda t_2} \tag{4.5}$$

In this equation, A_t is the activity at the time of measurement, t_1 is the irradiation time, t_2 is the time elapsed after irradiation (decay time), N is the number of target nuclei, and σ is the cross section. When there are multiple beam on and beam off periods, substituting in the variables from equations 4.3 and 4.4 into equation 4.5, the cross section for a given nuclide can be calculated using equations 4.6 and 4.7.

$$\sum FLUX = \sum_{i=1}^{n} \Phi_i\left(1 - e^{-\lambda TIM_i}\right)e^{-\lambda TIAB_i} \tag{4.6}$$

$$\sigma = \frac{A_{EOB}}{N\sigma \sum FLUX} \tag{4.7}$$

This cross section, or yield, represents the cumulative nuclidic cross section. This includes the yield of nuclei produced directly in the reaction of ^{136}Xe + ^{208}Pb and the yield from precursor beta decay of a parent and grandparent nucleus. The

correction for precursor beta decay and the determination of independent yields will be discussed in further detail in section 4.1.3.

There may be cases when a nuclide is misidentified in the decay curve analysis. Two criteria were used to ensure that the correct nuclides were identified when reported in the final results. First, the number of γ-rays observed from a particular decaying nuclide were considered. If a nuclide emits multiple γ-rays during decay, yet only one γ-ray from that nuclide was observed, this identification of the nuclide was considered to be incorrect, and the cross section was not calculated.

The second criteria was to ensure that the observations were consistent with the branching ratio intensities found in the modified Reus and Westmeier tables [72, 73] as well as from the National Nuclear Data Center [74]. For example, if a 350 keV γ-ray with a 2% branching ratio was observed but a 500 keV γ-ray with a 20% branching ratio from the same nuclide was not observed, this nuclide was determined to be misidentified. Since only the less intense γ-ray was observed and the larger intensity γ-ray wasn't, the cross section was not calculated for this nuclide.

4.1.2 Gammasphere

As was discussed in section 3.3.1, the radioactive decay measurement from Gammasphere was divided into 15 time segments for which the activity during each segment was determined. This division was performed as part of the data sorting script, GSSort [75]. The resulting spectra were analyzed, and peak fits were performed using the program gf3 from the RadWare software [68]. The program output the peak energies, number of counts, and error. Using the real time that elapsed during each decay measurement, the activities were determined. The analysis

procedure for this data set was then the same as that for the single HPGe detector (section 4.1.1), starting with the determination of mean γ-ray energies for the input file used in the program analysis-rev-00.for.

The absolute efficiency of Gammasphere was not measured; therefore, it was necessary to first deduce an absolute efficiency curve before final results could be obtained. To do this, the data analysis was performed on the non-efficiency corrected data from Gammasphere. Identification of the nuclides was still possible because the slopes of the decay curves are dependent on nuclide half-life, not activity. The slopes of the curves are the same for efficiency corrected and non-efficiency corrected data. However, the latter plot would be shifted down on the activity axis, as is shown in Figure 4.4.

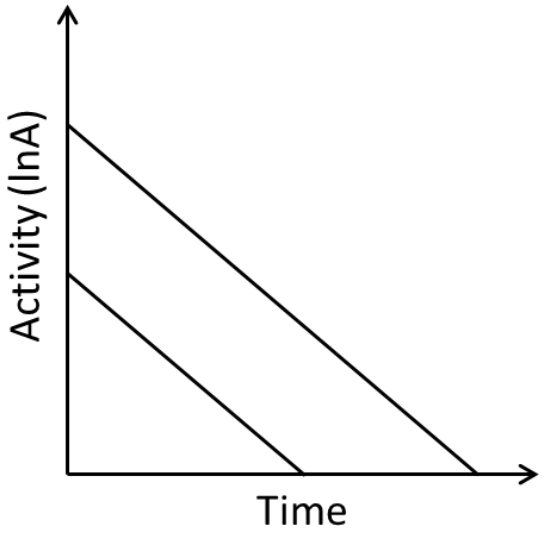

Figure 4.4: Diagram of efficiency corrected and non-efficiency corrected single-component decay curve. The lower line represents the non-efficiency corrected curve, while the upper line represents the efficiency corrected curve. The slopes of the curves are identical since they are produced by the same nuclide.

Once the decay curves and the EOB activities were obtained, a ratio of the activities of the non-efficiency corrected data to the efficiency corrected data was taken for common nuclei in the single HPGe and Gammasphere data sets. By plotting these ratios against the most intensely observed γ-ray energies of the nuclides, an absolute efficiency curve for Gammasphere was determined, shown in Figure 4.5. This curve is comparable to that previously obtained by [67].

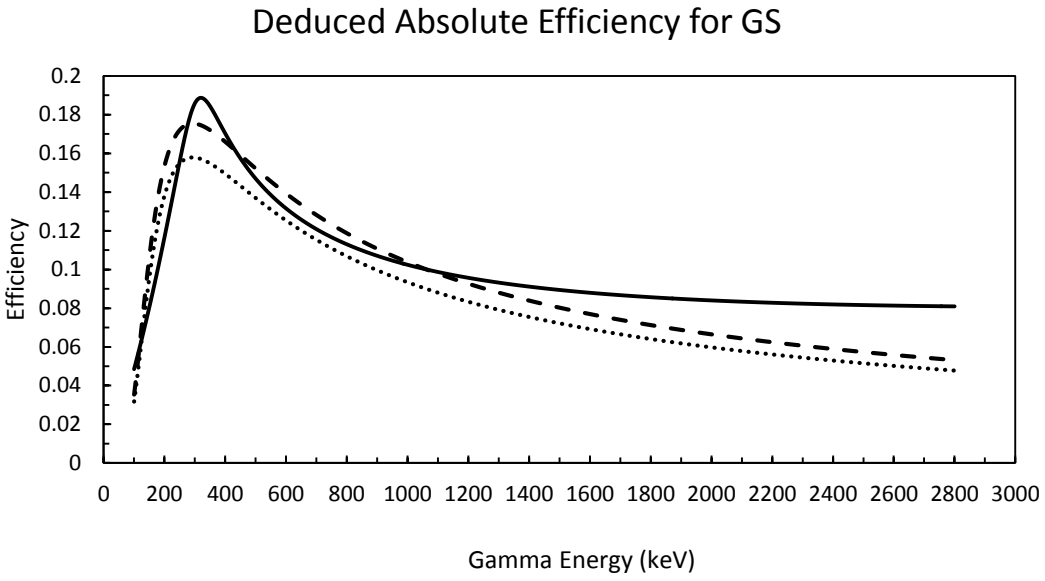

Figure 4.5: Deduced absolute efficiency curve for Gammasphere. This curve is comparable to that in [67] (dashed line) with ~100 operational detectors. The dotted line is the efficiency curve of [67] scaled to 90 operational detectors. For the deduced curve (solid line) EOB activities from a non-efficiency corrected analysis were compared to efficiency corrected EOB activities for common nuclides in the single HPGe detector data set and plotted against the principal γ-rays from each nuclide.

Using the efficiency curve in Figure 4.5, the Gammasphere decay data was corrected for efficiency and re-analyzed. The results were comparable to those found in the single detector analysis, showing that the Gammasphere decay analysis, including dividing the runs and obtaining the efficiency curve, was correct. Figure 4.6

shows the ratio of cross sections obtained from the single HPGe detector analysis and from Gammasphere for 19 different nuclides. The mean ratio between the two data sets is 0.96 ± 0.11. The cross sections are in agreement within a systematic error of 20%.

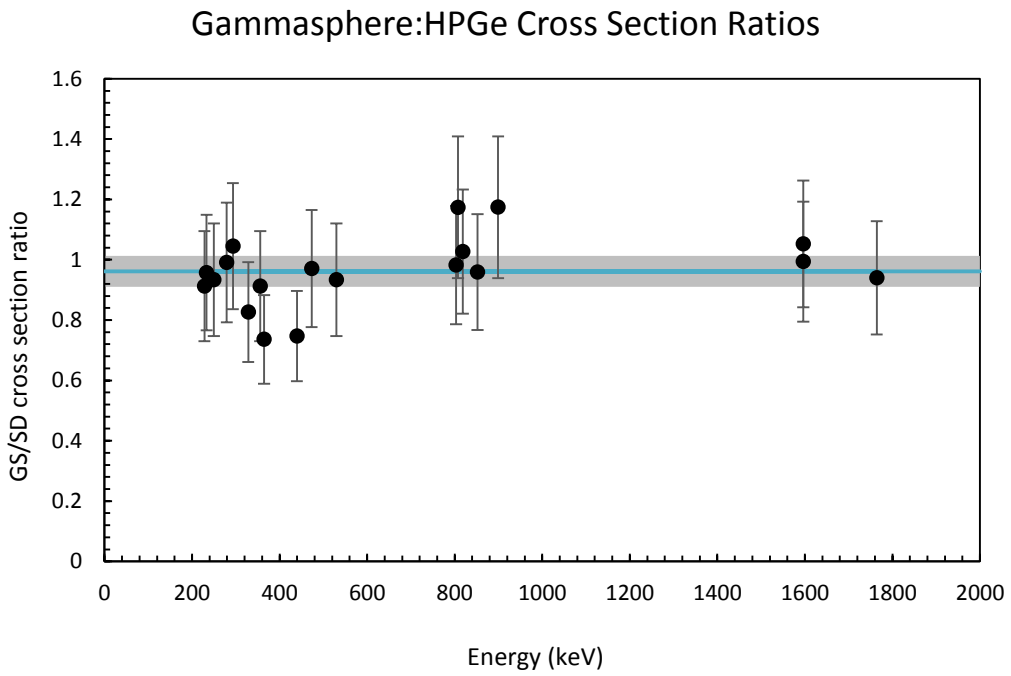

Figure 4.6: Ratios of cross sections determined from radioactive decay analysis of Gammasphere and single HPGe detector data. The blue line represents the mean ratio of the cross sections, and the 95% confidence interval (shaded region) is also shown. Results shown are for 19 nuclei that are present in both data sets.

The single HPGe detector yielded cross section results for over 30 nuclei, while the Gammasphere radioactive decay analysis contributed over 60 nuclidic cross sections. Approximately 20 nuclei were observed in both analyses. Therefore, nearly 70 independent cross sections of the final cross section results were obtained from the post-irradiation counting analysis. In the cases where common nuclides were observed in both data sets, the yields were averaged to get the final cumulative cross

sections. Decays originating from the ground state or from an isomeric state of the different nuclides were also accounted for.

4.1.3 Independent Yield Cross Sections

As mentioned earlier in this chapter, the nuclides observed may have been a direct reaction product or formed through beta decay of a parent, and possibly a grandparent, nucleus. A correction for this beta decay "feeding" must be performed to convert the cumulative, measured yields into independent yields. The general approach to this correction [76] is to assume that the independent cross sections for a given nucleus, σ(Z,A), can be expressed as a histogram that lies along a Gaussian curve, according to equation 4.8.

$$\sigma(Z,A) = \sigma(A)[2\pi C_Z^2(A)]^{-1/2} \exp\left[\frac{-(Z-Z_{mp})^2}{2C_Z^2(A)}\right] \quad (4.8)$$

In this equation, $C_Z(A)$ is the width parameter of the Gaussian for mass number A, Z_{mp} is the most probable Z value, and σ(A) is the isobaric cross section for that given A. Sheppard's correction [1], which was not used in this analysis, may be applied to $C_Z(A)$ to distinguish between a smooth, continuous charge distribution obtained through this equation and the histogram charge distributions one obtains in reality. Using the further assumption that the value of σ(A) varies smoothly and slowly as a function of A, one can combine adjacent isobars of A to determine C_Z and Z_{mp} for a given A range and use the laws of radioactive decay [77] to iteratively correct for the precursor decay.

This procedure was carried out using the FORTRAN program MASSY.for (see Appendix). The program performs the corrections for nuclides produced via

direct reaction and precursor beta decay from a parent and grandparent nucleus. To start the analysis the user provides starting values of C_Z and Z_{mp}. Independent fractional yields (cross sections) are output after the corrections are applied. The data are then plotted on a Gaussian curve and the parameters C_Z and Z_{mp} are iterated to obtain the best fit. Along with the independent cross sections, the program also outputs an estimate for σ(A) for each nuclide. These σ(A) values are used to obtain a mass distribution for the reaction.

4.2 In-Beam Analysis

4.2.1 Identification of Radionuclides

The first task in analyzing the in-beam data is to identify nuclides that were produced using γ-γ-γ coincidences. The restriction of using a triple coincidence requirement was implemented to reduce the chances of mis-identification of the nuclides. The observation of only one γ-ray does not allow for the identification of the decaying nucleus since many other nuclides may emit γ-rays with the same, or similar, energy. Observing a γ-γ coincidence during a decay increases the probability that a nuclide in question is being identified correctly. However, there is still a chance that the coincidence is due to a random γ-ray with the proper energy from a different decaying nucleus entering the detector within the coincidence resolving time. Requiring a γ-γ-γ coincidence greatly reduces the chances of misidentifying the nucleus in question. In this analysis, only triple coincidence events were considered and used to calculate cross sections.

The in-beam data was analyzed primarily using the RadWare [68] suite of programs. The γ-ray spectra from the irradiation were plotted on three axes by the

program LEVIT8R [78] to produce three-dimensional histograms of the data, called cubes. For this analysis, two cubes were created. One was constructed using events that occurred during the beam burst, and is labeled as IB (for in-beam). The coincidence time window for this cube was 82 ns. The other cube was constructed using events that were collected out of the beam burst and is labeled as OB (for out-of-beam) with a coincidence window of 820 ns. The program then projects the cubes onto a single axis (x-axis), which allows the user to gate on either one or two γ-ray transitions and observe the resulting γ-rays that occurred in coincidence. Figure 4.7 shows the ungated OB cube projected onto the x-axis.

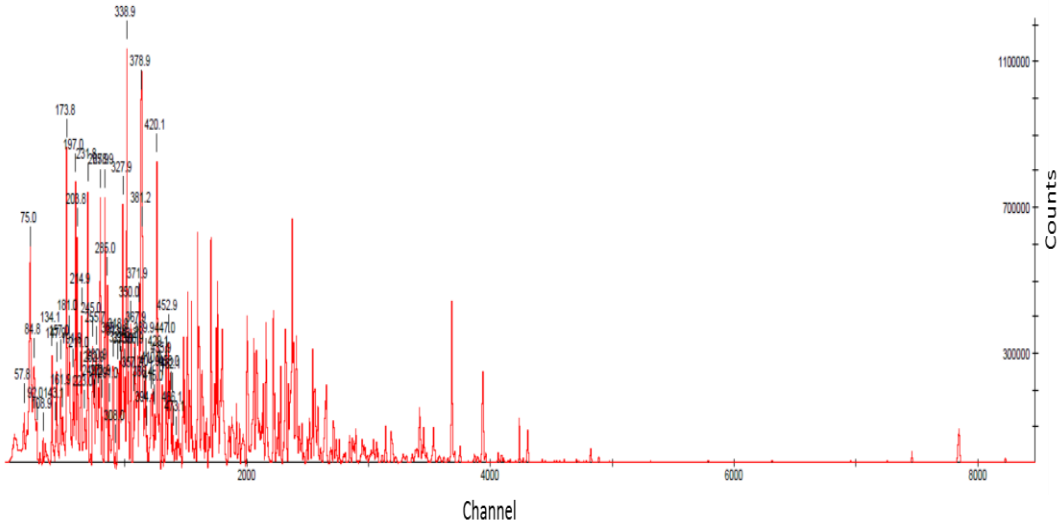

Figure 4.7: Ungated spectrum from the OB cube projected onto a single axis. Channel numbers are given on the x-axis, and the γ-ray energies are given above the peaks (in keV). Counts are given on the y-axis. This shows the number of events recorded as well as the variety of gamma energies that were observed. Using the program LEVIT8R [78], gates were applied to find γ-γ-γ events.

The identification process for the nuclei observed during irradiation was different than that for the radioactive decay data. In radioactive beta decay, a nucleus

emits a beta particle (or undergoes electron capture) and the resulting daughter nucleus can be left in an excited state. The release of this excitation energy occurs in the form of either γ-ray emission or internal conversion (section 4.2.2).

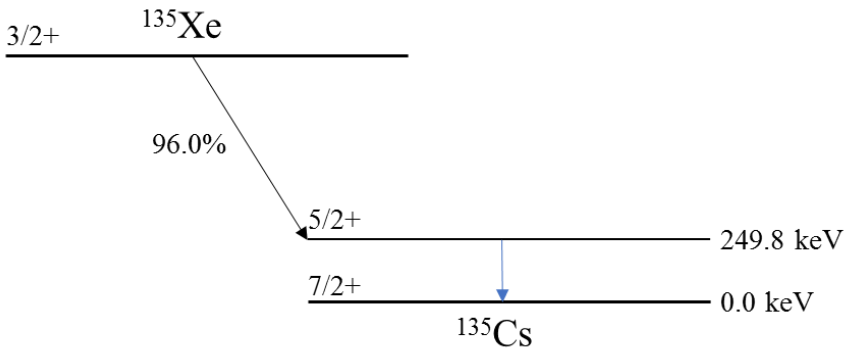

Figure 4.8: Simplified decay scheme for the beta decay of ^{135}Xe to ^{135}Cs. The beta decay from the ground state of the ^{135}Xe to the 5/2+ excited state at 249.8 keV of ^{135}Cs (black line) occurs with a 96% branching ratio. As the excited ^{135}Cs nucleus de-excites to the ground state, the 249.8 keV of energy is given of as a γ-ray (blue line). These γ-rays are used to identify and calculate the cross section of the Xe parent.

The γ-ray emission process is shown in Figure 4.8, which is a simplified decay scheme for the decay of ^{135}Xe to ^{135}Cs. The 249.8 keV γ-ray that is emitted when the ^{135}Cs nucleus de-excites to the ground state is used to identify the ^{135}Xe nucleus, and the activity of this emission is used to calculate the cross section of ^{135}Xe. Thus, the γ-ray transitions of the daughter were used to identify and calculate the cross section of the parent nucleus.

For the in-beam data, nuclei were identified, and cross sections calculated, using the γ-rays that were emitted from excited energy states to the ground state of the nucleus being considered. The identification procedure is described using the ^{212}Rn nuclide as an example. Figure 4.9 shows an abbreviated γ-ray level scheme for ^{212}Rn. The three lowest γ-decays leading to the ground state will emit γ-rays of 138.3

keV, 227.7 keV, and 1273.8 keV for the transitions going from the 6+ → 4+, 4+ → 2+, and 2+ → 0+ levels, respectively. It is these transitions that were used to identify this nucleus. The two lowest transitions (2+ → 0+ and 4+ → 2+) were used as gates, showing all other γ-rays that were recorded in coincidence. The γ-ray peak for the next lowest transition (6+ → 4+) was used in subsequent cross section calculations.

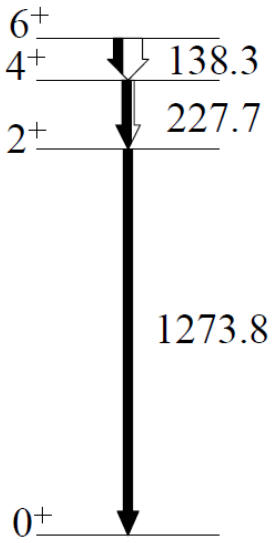

Figure 4.9: Abbreviated level scheme for ^{212}Rn. This shows the three lowest γ transitions leading to the ground state in keV. These γ-rays were used in the identification and cross section calculation for this nucleus.

This same procedure was performed for all possible isotopes between Z=48 and Z=86, which were the lowest and highest Z values for which reaction products were observed. For some nuclides, more than one path that lead to the ground state of the nucleus was observed. When this occurred, the different paths were integrated using the procedure described above, and the results were summed together after the corrections described in section 4.2.2 were applied.

4.2.2 Corrections and Determination of Cross Sections

Once the peaks were integrated, corrections were applied in order to calculate the total number of γ-rays emitted. The necessary corrections include detector efficiency (for a given γ-ray), triple coincidence detection efficiency, and internal conversion (IC). The IC correction was the smallest in magnitude, affecting the calculated cross section by less than 0.01%. The detector efficiency was the largest correction since the peak detection efficiency is only ~19% for lower energy γ-rays. Another 40-50% correction came from the triple coincidence efficiency. After these corrections the total number of γ-rays was calculated then used to calculate the cross section for a given nuclide.

The absolute efficiency curve for Gammasphere obtained for the radioactive decay analysis (Figure 4.4) was also used for the efficiency correction of the in-beam data set. The efficiency was applied for each γ-ray used in the analysis, i.e. both of the gating γ-rays and the γ-ray that was used for integration. The correction applied was then the product of the three efficiencies.

The triple coincidence efficiency was determined using the method outlined by Cocks et al. [58, 59]. In this method, gates are set on two higher lying transitions in the yrast rotational band, which is the minimum energy band for a given angular momentum. Making the assumption that no γ-ray intensity feeds out of the band, then the relative triple coincidence efficiency is proportional to the lower lying γ-ray intensities in that band.

The number of γ-decays, N_γ, is determined by applying these corrections according to equation 4.9.

$$N_\gamma = \frac{PA}{\varepsilon_1 \varepsilon_2 \varepsilon_3 \varepsilon_{tc}} \tag{4.9}$$

The peak area is given by PA, $\varepsilon_{1\text{-}3}$ are the absolute detector efficiencies for each of the three γ-rays used in the analysis, and ε_{tc} is the triple coincidence efficiency.

Next, the correction for internal conversion is applied. When a nucleus is in an excited state, the method of decay may not be through the release of a γ-ray. Instead, the excited nucleus interacts electromagnetically with an inner shell electron, which is then emitted. This process is called internal conversion and is done radiationlessly, which is to say, without the emission of a photon during energy transfer. A higher energy electron then fills the vacancy, emitting a characteristic X-ray. Since the inner-most shell, K shell, electrons spend more time in the nucleus than others, they interact more readily with the excited nucleus and are more likely to be the electrons ejected. It is for these conversion electrons for which the correction will be applied. The ratio of the number of K shell internal conversion decays, N_{IC}, to the number of γ-ray decays, N_γ, is given by the internal conversion coefficient, α_K, which can be found in [74].

$$\alpha_K = \frac{N_{IC}}{N_\gamma} \tag{4.10}$$

After rearranging equation 4.10, the total number of decays, N_{tot}, can be determined using the total number of γ-rays from equation 4.9 and equation 4.11.

$$N_{tot} = N_\gamma + (N_\gamma * \alpha_K) \tag{4.11}$$

Taking into account the beam flux during the different beam on/off periods, the cross sections are then calculated.

$$\sigma = \frac{N_{tot}}{N \sum_{i=1}^{n} \Phi_i \Delta t_i} \quad (4.12)$$

In equation 4.12, N is the number of target nuclei, Φ and Δt are the flux and irradiation times of the ith beam interval through n beam on/off periods.

The results of this calculation represent cumulative cross sections of the nuclides produced. As in the radioactive decay analysis, corrections for nuclei produced directly from the reaction, as well as those produced through precursor beta decay, were performed. Independent cross sections were determined according to the procedure discussed in section 4.1.3.

Throughout the Gammasphere analysis, as in the radioactive decay analysis, whether the ground state or isomeric state was populated was taken into consideration. When final independent cross sections from both analyses were determined, the ground state and isomeric state cross sections for the same nuclide were summed. Nuclides for which only isomeric cross sections were determined were not included in the final results.

Estimating the cross section uncertainties from the Gammasphere in-beam analysis is difficult since the absolute efficiency of Gammasphere was not measured in this experiment. Also, the triple coincidence requirement added complexity to the uncertainty estimation. To better understand what uncertainties may be present, cross sections of common nuclides from the in-beam and radioactive decay analyses were compared. A ratio was taken between these in-beam Gammasphere and radioactive decay cross sections, with the assumption is that the radioactive decay analysis more accurately reflects the absolute values. The results are shown in Figure 4.10.

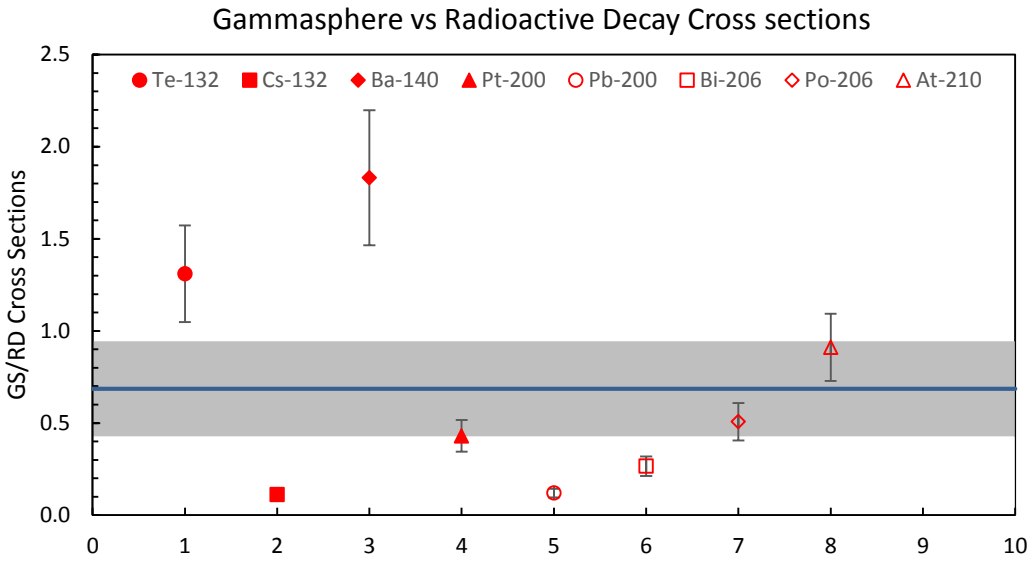

Figure 4.10: Ratios of Gammasphere to radioactive decay cross sections. The solid line shows the average ratio, and the shaded region is the 95% confidence interval.

A combination of eight PLF and TLF nuclei were used for this comparison. The average ratio was 0.69 ± 0.62. The majority of the cross sections from Gammasphere were lower than their radioactive decay counter parts. This plot shows that there are obviously systematic errors associated with Gammasphere that are not well understood. With continued use of Gammasphere to make absolute cross section measurements, better efficiency measurements need to be made. As this occurs, these errors will decrease, and the agreement between these two analysis methods will increase.

5 RESULTS AND CONCLUSION

5.1 Summary of Results

A total of 235 independent nuclidic cross sections were determined in this experiment, including 118 projectile-like fragments and 117 target-like fragments. The PLFs range from Z=48 (Cd) to Z=69 (Tm) while the TLFs range from Z=70 (Yb) to Z=88 (Ra). The minimum and maximum cross sections observed were 0.0016 mb and 64.3 mb for the PLFs and 0.0036 mb and 20.6 mb for the TLFs.

A number of nuclides with shell stabilized neutron numbers, N=82 and N=126, were produced in the reaction. For the N=82 nuclei, nuclides from Z=52 (Te) to Z=61 (Pm) were observed. Cross sections for this isotone ranged from 0.261 mb to 0.0153 mb, with a maximum, not including the projectile, of 6.04 mb (^{138}Ba). Nuclides from Z=80 (Hg) to Z=88 (Ra) were observed for the TLFs, with cross sections ranging from 0.0093 mb to 0.0033 mb. The maximum non-target cross section observed in this group was 1.19 mb (^{210}Po). It should be noted that ^{205}Au was observed in the data through γ-γ coincidences. However, since the γ-γ-γ criteria was not satisfied, the production cross section was not determined in this analysis.

As a check on the quality of the data, the mass distribution determined in this experiment is compared to those from the previous experiment of Kozulin et al. [5]. A 5 point Savitzky-Golay filter [79] was applied to the data, and the result is shown in Figure 5.1. The mass resolution of this experiment was 1 u, and the detector used in [5], which was a two-arm time-of-fight spectrometer named CORSET, has a mass resolution of 7 u. It should be noted that the energies studied during that experiment were E_{cm}=423 MeV and E_{cm}=526 MeV, while the center-of-mass energy in the

present experiment was 450 MeV. Also, quasi-elastic events were excluded from the mass distributions of [5]. Given these qualifications, the agreement between the mass distribution of this experiment and those of [5] seem acceptable.

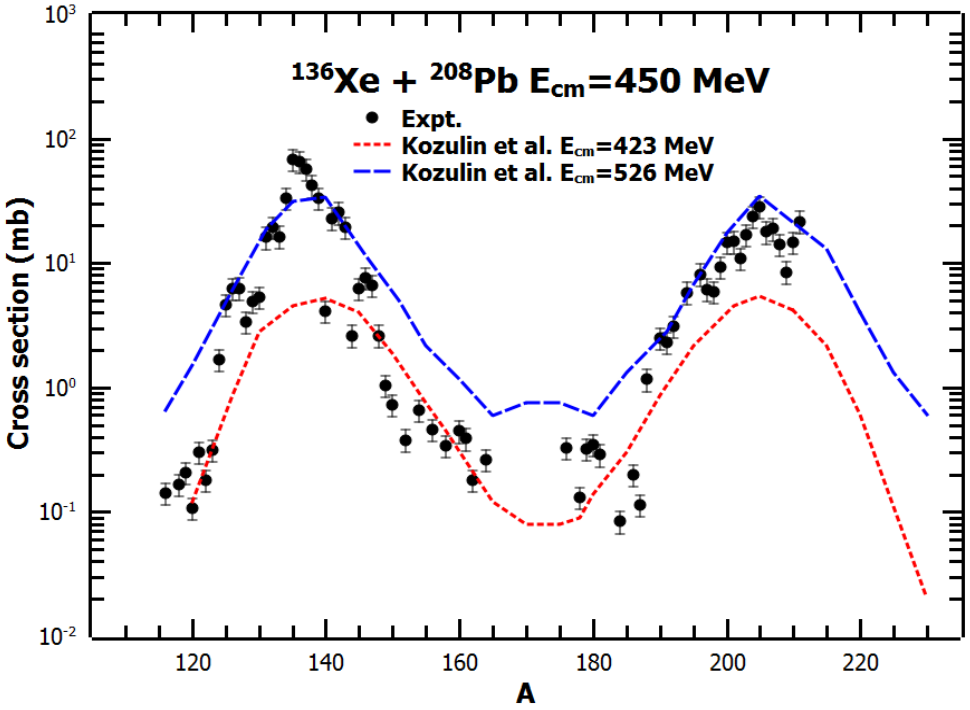

Figure 5.1: Mass distribution comparison between Gammasphere and CORSET. The measurements made in [5] did not include quasi-elastic events and had a mass resolution of 7 u, while the mass resolution of this experiment was 1 u. The center-of-mass energies in [5] were 423 MeV and 526 MeV. E_{cm} for the present experiment was 450 MeV.

Another check was the comparison of the measured reaction cross section, σ_R, to calculated values. The measured value of σ_R for this experiment was 359 ± 90 mb, which was determined by averaging the integration of the PLF (413 ± 103 mb) and TLF (305 ± 76 mb) peaks in the mass distribution. The value for σ_R from the Bass model [2] is 567 mb, and σ_R based on the formalism from [80] is 496 mb at E_{cm}=452 MeV. The discrepancies in these values indicate the presence of systematic uncertainties in this data.

Figure 5.2 shows a landscape of the observed PLFs. Most of the 118 observed PLFs were produced "north" and "northeast" of the projectile, though some nuclides "southwest" of the projectile were also populated. The observed nuclides ranged from Cd (Z=48) to Tm (Z=69).

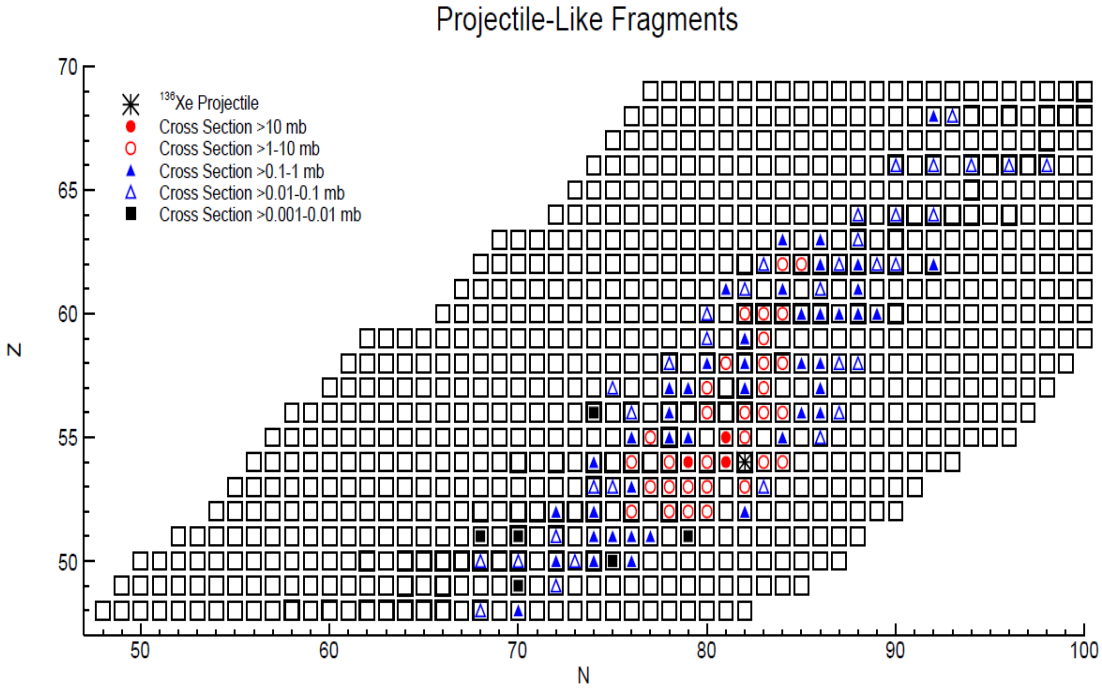

Figure 5.2: Landscape of PLFs determined in the reaction of ^{136}Xe + ^{208}Pb at E_{cm}=450 MeV. There were 118 PLFs observed, ranging from Z=48 to Z=69. Stable nuclides are those with dark outlines and observed nuclides are given by the symbols in the squares, based on the order of magnitude of the cross section.

The landscape of the TLFs is given in Figure 5.3. The 117 observed TLFs range from Yb (Z=70) to Ra (Z=88). Most of the nuclides produced are "southwest" of the target, with a limited number of nuclides "north" of the target being produced. When evaluating these cross section "maps," they follow the trend predicted by Zagrebaev and Greiner [18]. This shows that this is a "symmetrizing" reaction, with

the majority of the TLFs formed "southwest" of the ^{208}Pb target and the majority of the PLFs formed "northwest" of the ^{136}Xe projectile.

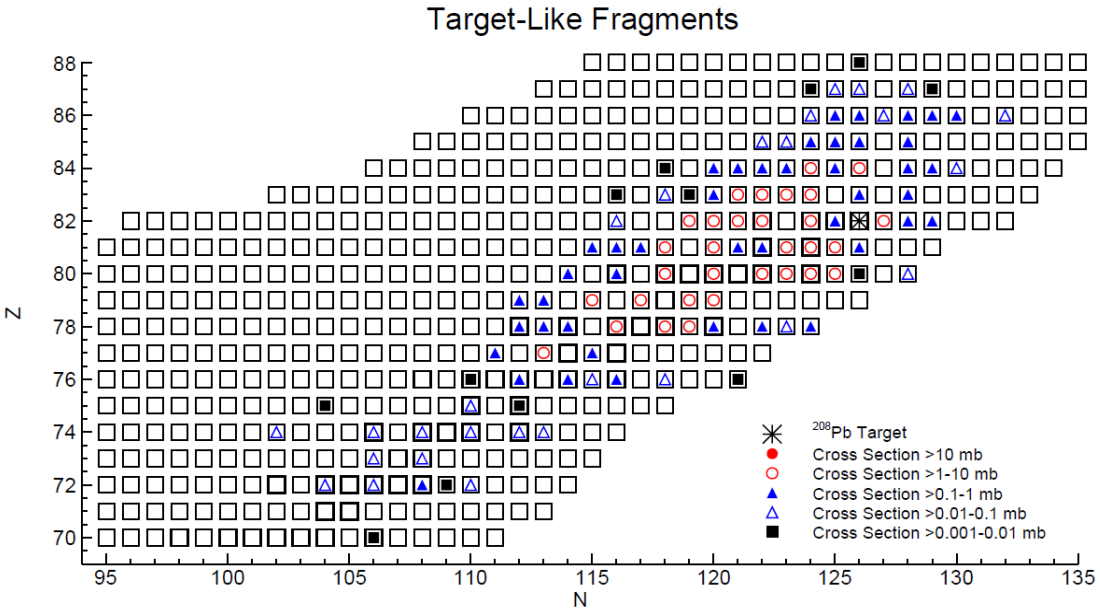

Figure 5.3: Landscape of TLFs determined in the reaction of ^{136}Xe + ^{208}Pb at E_{cm}=450 MeV. There were 117 TLFs observed, ranging from Z=70 to Z=88. Stable nuclides are those with dark outlines and observed nuclides are given by the symbols in the squares, based on the order of magnitude of the cross section.

The cumulative and independent nuclidic cross sections for all nuclides determined in this experiment are given in Table 5.1. The data used in the determination of each cross section is given by the symbols OB, IB and RD. The symbols OB and IB mean that the nuclides with these labels were observed in these respective cubes and quantified using the in-beam analysis (section 4.2). RD means that the nuclide was determined in the radioactive decay analysis (section 4.1). No differentiation is given for whether the nuclide was observed in the Gammasphere decay or single HPGe decay measurements. The estimated uncertainties include statistical and systematic error, such as the beam intensity measurements. The

average beam current differs by as much as 15% over the course of the irradiation (27.6 ± 4.1 enA), and the overall error is estimated to be 20%.

Table 5.1: Cumulative and independent nuclidic cross sections. The symbols in the furthest right column denote what data sets contributed to determining the final result. The symbols OB and IB denote nuclides that were observed in these respective cubes from the in-beam analysis, and RD denotes nuclides determined through the radioactive decay analysis. No distinction is given for cross sections determined from the Gammasphere for single HPGe detector decay measurements.

Nuclide	σ_{CY} (mb)			σ_{IY} (mb)			OB/IB/RD
^{116}Cd	0.108	±	0.022	0.0636	±	0.013	OB,IB
^{118}Cd	0.156	±	0.031	0.133	±	0.027	IB
^{119}In	0.0080	±	0.0016	0.0055	±	0.0011	OB
^{121}In	0.0181	±	0.0036	0.0168	±	0.0034	OB
^{118}Sn	0.0134	±	0.0027	0.0132	±	0.0026	OB
^{120}Sn	0.237	±	0.047	0.0982	±	0.020	OB,IB
^{122}Sn	0.443	±	0.089	0.347	±	0.069	OB,IB
^{123}Sn	0.0170	±	0.0034	0.0153	±	0.0031	OB,IB
^{124}Sn	0.383	±	0.077	0.367	±	0.073	OB
^{125}Sn	0.0083	±	0.0017	0.0083	±	0.0017	OB
^{126}Sn	0.318	±	0.064	0.316	±	0.063	OB,IB
^{119}Sb	0.0016	±	0.0003	0.0016	±	0.0003	OB
^{121}Sb	0.0071	±	0.0014	0.0017	±	0.0003	OB
^{123}Sb	0.111	±	0.022	0.0583	±	0.012	OB
^{125}Sb	0.189	±	0.038	0.165	±	0.033	OB,IB
^{126}Sb	0.655	±	0.13	0.655	±	0.13	RD
^{127}Sb	0.548	±	0.11	0.513	±	0.10	OB,IB,RD
^{128}Sb	0.418	±	0.084	0.396	±	0.079	RD
^{130}Sb	0.0026	±	0.0005	0.0026	±	0.0005	OB
^{124}Te	0.195	±	0.039	0.192	±	0.038	OB,IB
^{126}Te	1.22	±	0.24	0.744	±	0.15	OB,IB
^{128}Te	1.15	±	0.23	1.05	±	0.21	OB,IB
^{130}Te	1.88	±	0.38	1.83	±	0.37	OB,IB
^{131}Te	2.28	±	0.46	1.79	±	0.36	OB,RD

Continued on next page

Continued from previous page

^{132}Te	2.43	±	0.49	2.28	±	0.46	OB,IB,RD
^{134}Te	0.261	±	0.052	0.261	±	0.052	OB
^{127}I	0.0463	±	0.0093	0.0223	±	0.0045	IB
^{128}I	0.0849	±	0.017	0.0849	±	0.017	IB
^{129}I	0.934	±	0.19	0.668	±	0.13	IB
^{130}I	3.10	±	0.62	3.10	±	0.62	RD
^{131}I	4.58	±	0.92	3.61	±	0.72	OB,IB,RD
^{132}I	5.40	±	1.1	5.34	±	1.1	RD
^{133}I	4.34	±	0.87	3.46	±	0.69	OB,IB,RD
^{135}I	2.05	±	0.41	2.04	±	0.41	IB,RD
^{136}I	0.0201	±	0.0040	0.0200	±	0.0040	IB
^{128}Xe	0.190	±	0.038	0.188	±	0.038	OB,IB
^{130}Xe	5.72	±	1.1	5.08	±	1.0	OB,IB
^{132}Xe	8.46	±	1.7	5.88	±	1.2	OB,IB
^{133}Xe	18.6	±	3.7	17.2	±	3.4	OB,IB,RD
^{134}Xe	10.2	±	2.0	8.63	±	1.7	OB,IB
^{135}Xe	74.0	±	15	64.3	±	13	OB,IB,RD
^{136}Xe	31.4	±	6.3	30.4	±	6.1	OB,IB
^{137}Xe	1.48	±	0.30	1.46	±	0.29	OB,IB
^{138}Xe	3.26	±	0.65	3.26	±	0.65	IB
^{131}Cs	0.212	±	0.042	0.212	±	0.042	IB
^{132}Cs	1.69	±	0.34	1.69	±	0.34	IB,RD
^{133}Cs	1.70	±	0.34	0.750	±	0.15	IB
^{134}Cs	0.829	±	0.17	0.755	±	0.15	IB
^{136}Cs	15.5	±	3.1	15.5	±	3.1	RD
^{137}Cs	4.85	±	0.97	4.43	±	0.89	OB,IB
^{139}Cs	0.473	±	0.095	0.449	±	0.090	IB
^{141}Cs	0.0877	±	0.018	0.0867	±	0.017	IB
^{130}Ba	0.0057	±	0.0011	0.0057	±	0.0011	OB,IB
^{132}Ba	0.0816	±	0.016	0.0807	±	0.016	IB
^{134}Ba	0.664	±	0.13	0.651	±	0.13	OB,IB
^{136}Ba	1.82	±	0.36	1.59	±	0.32	OB,IB
^{138}Ba	7.97	±	1.6	6.04	±	1.2	OB,IB

Continued on next page

Continued from previous page

^{139}Ba	5.75	±	1.2	4.76	±	1.0	IB
^{140}Ba	3.96	±	0.79	3.30	±	0.66	OB,IB,RD
^{141}Ba	0.160	±	0.032	0.160	±	0.032	IB
^{142}Ba	0.163	±	0.033	0.159	±	0.032	IB
^{143}Ba	0.0296	±	0.0059	0.0293	±	0.0059	IB
^{132}La	0.0419	±	0.0084	0.0418	±	0.0084	IB
^{135}La	0.352	±	0.070	0.351	±	0.070	OB,IB
^{136}La	0.420	±	0.084	0.410	±	0.082	OB,IB
^{137}La	1.71	±	0.34	1.67	±	0.33	OB,IB
^{139}La	0.952	±	0.19	0.582	±	0.12	OB,IB
^{140}La	2.20	±	0.44	2.18	±	0.44	RD
^{143}La	0.144	±	0.029	0.144	±	0.029	IB
^{136}Ce	0.0829	±	0.017	0.0826	±	0.017	OB,IB
^{138}Ce	0.351	±	0.070	0.342	±	0.068	OB,IB
^{139}Ce	7.35	±	1.5	6.59	±	1.3	IB,RD
^{140}Ce	0.316	±	0.063	0.282	±	0.056	IB
^{141}Ce	5.65	±	1.1	3.41	±	0.68	IB,RD
^{142}Ce	2.24	±	0.45	1.69	±	0.34	IB
^{143}Ce	1.43	±	0.29	0.886	±	0.18	RD
^{144}Ce	0.598	±	0.12	0.536	±	0.11	IB
^{145}Ce	0.0345	±	0.0069	0.0324	±	0.0065	IB
^{146}Ce	0.0956	±	0.019	0.0956	±	0.019	IB
^{139}Pr	0.0284	±	0.0057	0.0280	±	0.0056	IB
^{141}Pr	0.342	±	0.068	0.326	±	0.065	IB
^{142}Pr	1.11	±	0.22	1.11	±	0.22	RD
^{140}Nd	0.0289	±	0.0058	0.0287	±	0.0057	OB
^{142}Nd	2.47	±	0.49	2.39	±	0.48	OB,IB
^{143}Nd	13.0	±	2.6	3.41	±	0.68	OB,IB
^{144}Nd	7.45	±	1.5	2.79	±	0.56	OB,IB
^{145}Nd	0.245	±	0.049	0.162	±	0.032	IB
^{146}Nd	0.311	±	0.062	0.250	±	0.050	IB
^{147}Nd	0.228	±	0.046	0.199	±	0.040	IB
^{148}Nd	0.276	±	0.055	0.253	±	0.051	IB

Continued on next page

Continued from previous page

^{149}Nd	0.134	±	0.027	0.131	±	0.026	IB
^{142}Pm	0.158	±	0.032	0.157	±	0.031	IB
^{143}Pm	0.0156	±	0.0031	0.0153	±	0.0031	IB
^{145}Pm	0.253	±	0.051	0.239	±	0.048	IB
^{147}Pm	0.147	±	0.029	0.0934	±	0.019	IB
^{149}Pm	0.124	±	0.025	0.114	±	0.023	IB
^{145}Sm	0.0516	±	0.010	0.0510	±	0.010	IB
^{146}Sm	1.59	±	0.32	1.52	±	0.30	IB
^{147}Sm	2.05	±	0.41	1.88	±	0.38	IB
^{148}Sm	1.11	±	0.22	0.512	±	0.10	IB
^{149}Sm	0.0557	±	0.011	0.0434	±	0.0087	IB
^{150}Sm	0.224	±	0.045	0.194	±	0.039	OB,IB
^{151}Sm	0.0348	±	0.0070	0.0322	±	0.0064	IB
^{152}Sm	0.0586	±	0.012	0.0542	±	0.011	OB,IB
^{154}Sm	0.203	±	0.041	0.191	±	0.038	IB
^{147}Eu	0.248	±	0.050	0.244	±	0.049	IB
^{149}Eu	0.146	±	0.029	0.145	±	0.029	IB
^{151}Eu	0.0305	±	0.0061	0.0305	±	0.0061	IB
^{152}Gd	0.0436	±	0.0087	0.0402	±	0.0080	OB,IB
^{154}Gd	0.0250	±	0.0050	0.0225	±	0.0045	OB,IB
^{156}Gd	0.0179	±	0.0036	0.0115	±	0.0023	IB
^{156}Dy	0.0468	±	0.0094	0.0453	±	0.0091	IB
^{158}Dy	0.0207	±	0.0041	0.0185	±	0.0037	IB
^{160}Dy	0.0173	±	0.0035	0.0130	±	0.0026	IB
^{162}Dy	0.0418	±	0.0084	0.0344	±	0.0069	IB
^{164}Dy	0.0529	±	0.011	0.0493	±	0.010	IB
^{160}Er	0.131	±	0.026	0.124	±	0.025	IB,RD
^{161}Er	0.0139	±	0.0028	0.0135	±	0.0027	IB
^{176}Yb	0.0069	±	0.0014	0.0067	±	0.0013	OB
^{176}Hf	0.0228	±	0.0046	0.0185	±	0.0037	OB
^{178}Hf	0.0781	±	0.016	0.0684	±	0.014	OB
^{180}Hf	0.482	±	0.096	0.474	±	0.095	OB,RD
^{181}Hf	0.0049	±	0.0010	0.0045	±	0.0009	OB

Continued on next page

Continued from previous page

^{182}Hf	0.0117	±	0.0023	0.0112	±	0.0022	OB
^{179}Ta	0.0245	±	0.0049	0.0156	±	0.0031	OB
^{181}Ta	0.0247	±	0.0049	0.0187	±	0.0037	OB
^{176}W	0.0179	±	0.0036	0.0174	±	0.0035	IB
^{180}W	0.0461	±	0.0092	0.0417	±	0.0083	OB,IB
^{182}W	0.0289	±	0.0058	0.0237	±	0.0047	OB,IB
^{184}W	0.0428	±	0.0086	0.0383	±	0.0077	OB,IB
^{186}W	0.0286	±	0.0057	0.0261	±	0.0052	OB,IB
^{187}W	0.0965	±	0.019	0.0965	±	0.019	IB
^{179}Re	0.0035	±	0.0007	0.0034	±	0.0007	OB
^{185}Re	0.0246	±	0.0049	0.0154	±	0.0031	OB
^{187}Re	0.0112	±	0.0022	0.0100	±	0.0020	OB
^{186}Os	0.0106	±	0.0021	0.0099	±	0.0020	OB,IB
^{188}Os	0.131	±	0.026	0.103	±	0.021	OB,IB
^{190}Os	1.20	±	0.24	0.557	±	0.11	OB,IB
^{191}Os	0.124	±	0.025	0.0804	±	0.016	OB,IB
^{192}Os	0.144	±	0.029	0.134	±	0.027	OB,IB
^{194}Os	0.0789	±	0.016	0.0789	±	0.016	OB,IB
^{197}Os	0.0035	±	0.0007	0.0035	±	0.0007	OB
^{188}Ir	0.1660	±	0.0230	0.1150	±	0.0230	RD
^{190}Ir	5.66	±	1.1	3.58	±	0.72	RD
^{192}Ir	0.322	±	0.064	0.322	±	0.064	RD
^{190}Pt	0.124	±	0.025	0.116	±	0.023	OB,IB
^{191}Pt	0.125	±	0.025	0.115	±	0.023	IB
^{192}Pt	0.473	±	0.095	0.427	±	0.085	OB,IB
^{194}Pt	1.60	±	0.32	1.28	±	0.26	OB,IB
^{196}Pt	4.97	±	0.99	4.21	±	0.84	OB,IB
^{197}Pt	4.81	±	0.96	3.51	±	0.70	OB,IB,RD
^{198}Pt	0.666	±	0.13	0.628	±	0.13	OB,IB
^{200}Pt	0.728	±	0.15	0.728	±	0.15	OB,IB,RD
^{201}Pt	0.0714	±	0.014	0.0714	±	0.014	OB,IB
^{202}Pt	0.178	±	0.036	0.178	±	0.036	OB
^{191}Au	0.514	±	0.10	0.469	±	0.094	OB,RD

Continued on next page

Continued from previous page

^{192}Au	0.168	±	0.034	0.155	±	0.031	RD
^{193}Au	1.390	±	0.280	1.27	±	0.21	RD
^{194}Au	1.31	±	0.26	1.26	±	0.25	RD
^{196}Au	4.05	±	0.81	3.34	±	0.67	RD
^{198}Au	2.81	±	0.56	2.77	±	0.55	RD
^{199}Au	8.57	±	1.7	6.23	±	1.2	RD
^{194}Hg	0.457	±	0.091	0.446	±	0.089	OB,IB
^{196}Hg	0.897	±	0.18	0.847	±	0.17	OB,IB
^{198}Hg	2.81	±	0.56	2.39	±	0.48	OB,IB
^{200}Hg	7.49	±	1.5	6.07	±	1.2	OB,IB
^{202}Hg	2.66	±	0.53	2.10	±	0.42	OB,IB
^{203}Hg	6.61	±	1.3	5.30	±	1.1	OB,IB,RD
^{204}Hg	8.68	±	1.7	6.75	±	1.3	OB,IB
^{205}Hg	5.93	±	1.2	4.95	±	1.0	OB
^{206}Hg	0.0093	±	0.0019	0.0093	±	0.0019	OB
^{208}Hg	0.0341	±	0.0068	0.0341	±	0.0068	OB
^{196}Tl	0.281	±	0.056	0.283	±	0.057	RD
^{197}Tl	0.564	±	0.11	0.521	±	0.10	IB,RD
^{198}Tl	0.386	±	0.077	0.342	±	0.068	RD
^{199}Tl	1.46	±	0.29	1.30	±	0.26	IB,RD
^{201}Tl	8.95	±	1.8	8.14	±	1.6	OB,IB,RD
^{202}Tl	0.754	±	0.15	0.754	±	0.15	IB
^{203}Tl	0.360	±	0.072	0.239	±	0.048	OB
^{204}Tl	1.68	±	0.34	1.68	±	0.34	OB,IB
^{205}Tl	9.93	±	2.0	6.39	±	1.3	OB,IB
^{206}Tl	10.5	±	2.1	9.03	±	1.8	OB,IB
^{207}Tl	0.145	±	0.029	0.129	±	0.026	OB,IB
^{198}Pb	0.0236	±	0.0047	0.0233	±	0.0047	OB
^{201}Pb	1.56	±	0.31	1.41	±	0.28	OB,IB,RD
^{202}Pb	4.84	±	0.97	4.55	±	0.91	OB,IB,RD
^{203}Pb	6.41	±	1.3	5.95	±	1.2	OB,RD
^{204}Pb	5.66	±	1.1	4.30	±	0.86	OB,IB,RD
^{206}Pb	17.20	±	3.4	8.59	±	1.7	OB,IB

Continued on next page

Continued from previous page

^{207}Pb	0.304	±	0.061	0.191	±	0.038	IB
^{208}Pb	25.8	±	5.2	20.6	±	4.1	OB,IB
^{209}Pb	2.20	±	0.44	1.89	±	0.38	OB,IB
^{210}Pb	0.345	±	0.069	0.312	±	0.062	OB,IB
^{211}Pb	0.760	±	0.15	0.760	±	0.15	OB,IB
^{199}Bi	0.0062	±	0.0012	0.0062	±	0.0012	OB
^{201}Bi	0.0299	±	0.0060	0.0296	±	0.0059	OB
^{202}Bi	0.0073	±	0.0015	0.0071	±	0.0014	OB
^{203}Bi	0.396	±	0.079	0.349	±	0.070	OB,RD
^{204}Bi	2.07	±	0.41	1.93	±	0.39	OB,RD
^{205}Bi	2.17	±	0.43	1.90	±	0.38	OB,IB,RD
^{206}Bi	2.96	±	0.59	2.95	±	0.59	OB,IB,RD
^{207}Bi	2.60	±	0.52	2.47	±	0.49	OB,IB
^{209}Bi	0.439	±	0.088	0.339	±	0.068	OB,IB
^{211}Bi	0.130	±	0.026	0.127	±	0.025	OB,IB
^{202}Po	0.0093	±	0.0019	0.0092	±	0.0018	OB
^{204}Po	0.104	±	0.021	0.103	±	0.021	OB,IB
^{205}Po	0.124	±	0.025	0.122	±	0.024	OB,IB
^{206}Po	0.815	±	0.16	0.755	±	0.15	OB,IB,RD
^{207}Po	0.818	±	0.16	0.817	±	0.16	OB,IB,RD
^{208}Po	5.02	±	1.0	4.58	±	0.92	OB,IB
^{209}Po	0.590	±	0.12	0.532	±	0.11	OB,IB
^{210}Po	2.20	±	0.44	1.19	±	0.24	OB,IB
^{212}Po	0.469	±	0.094	0.464	±	0.093	OB,IB
^{213}Po	0.193	±	0.039	0.190	±	0.038	OB,IB
^{214}Po	0.0767	±	0.015	0.0754	±	0.015	OB,IB
^{207}At	0.0102	±	0.0020	0.0101	±	0.0020	OB
^{208}At	0.0367	±	0.0073	0.0353	±	0.0071	OB
^{209}At	0.635	±	0.13	0.569	±	0.11	OB,RD
^{210}At	0.989	±	0.20	0.894	±	0.18	OB,RD
^{211}At	0.467	±	0.093	0.451	±	0.090	OB,IB
^{213}At	0.384	±	0.077	0.384	±	0.077	OB,IB
^{210}Rn	0.0700	±	0.014	0.0678	±	0.014	OB

Continued on next page

Continued from previous page

^{211}Rn	0.368	±	0.074	0.350	±	0.070	OB,RD
^{212}Rn	0.537	±	0.11	0.515	±	0.10	OB,IB
^{213}Rn	0.166	±	0.033	0.146	±	0.029	OB
^{214}Rn	0.324	±	0.065	0.324	±	0.065	OB,IB
^{215}Rn	0.343	±	0.069	0.343	±	0.069	OB,IB
^{216}Rn	0.112	±	0.022	0.112	±	0.022	IB
^{218}Rn	0.0214	±	0.0043	0.0191	±	0.0038	IB
^{211}Fr	0.0030	±	0.0006	0.0030	±	0.0006	OB
^{212}Fr	0.0512	±	0.010	0.0512	±	0.010	OB
^{213}Fr	0.0402	±	0.0080	0.0402	±	0.0080	OB
^{215}Fr	0.0167	±	0.0033	0.0167	±	0.0033	OB
^{216}Fr	0.0057	±	0.0011	0.0057	±	0.0011	OB
^{214}Ra	0.0034	±	0.0007	0.0033	±	0.0007	OB

5.2 Theory Evaluation Factor

In this experiment, measured cross sections are compared to theoretical predictions from GRAZING [23] as well as to the calculations of Zagrebaev and Greiner [6, 18]. To make these comparisons more quantitative instead of qualitative, the theory evaluation factor (tef) is used [81]. The tef for a single cross section is given by equation 5.1.

$$tef = \log\left(\frac{\sigma_{experimental}}{\sigma_{theory}}\right) \tag{5.1}$$

The average tef for each isotopic distribution is then determined.

$$\overline{tef} = \frac{1}{N_d}\sum_{i=1}^{N_d} tef_i \tag{5.2}$$

Here, N_d is the number of data points being compared. The variance in this value is then given by equation 5.3.

$$\sigma = \frac{1}{N_d}\sqrt{\sum_{i=1}^{N_d}\left(tef_i - \overline{tef}\right)^2} \quad (5.3)$$

Since the tef is a logarithmic value, integer tef values such as 1 or 2 equate to orders of magnitude difference between the experimental and predicted values. Also, the sign of the tef denotes whether the experimental values are generally greater than (-) or less than (+) the predicted values.

5.3 PLF Comparisons to Model Predictions

The GRAZING model is the only prediction model evaluated for the projectile-like fragments from this reaction. The pre- and post-neutron emission cross section predictions were calculated using the version of GRAZING implemented on the Nuclear Reactions Video Project website [23] using the standard input parameters provided.

Figure 5.4 shows the independent yield (IY) isotopic distributions for secondary (post-neutron emission) reaction products "south" of the ^{136}Xe projectile. These nuclides include isotopes of Sn (ΔZ=-4), Sb (ΔZ=-3), and Te (ΔZ=-2). It is clear that there is a very large discrepancy between the measured nuclidic cross sections and the predicted values in both magnitude and maximum peak position. The GRAZING code predicts peak maxima to occur at or near N=82, while the experimental values generally peak at much lower neutron numbers. Also, the magnitude of the predicted cross sections can be orders of magnitude lower than was experimentally observed.

The inability of the GRAZING code to accurately predict cross sections for large mass transfers is most likely due to the boundary condition of the grazing region

included in the model. The grazing region is the region outside the sum of the nuclear radii of the projectile and target (section 1.3). Reactions with impact parameters below this boundary, which lead to large projectile energy loss and mass transfers through deep inelastic collisions and quasifission, are not considered.

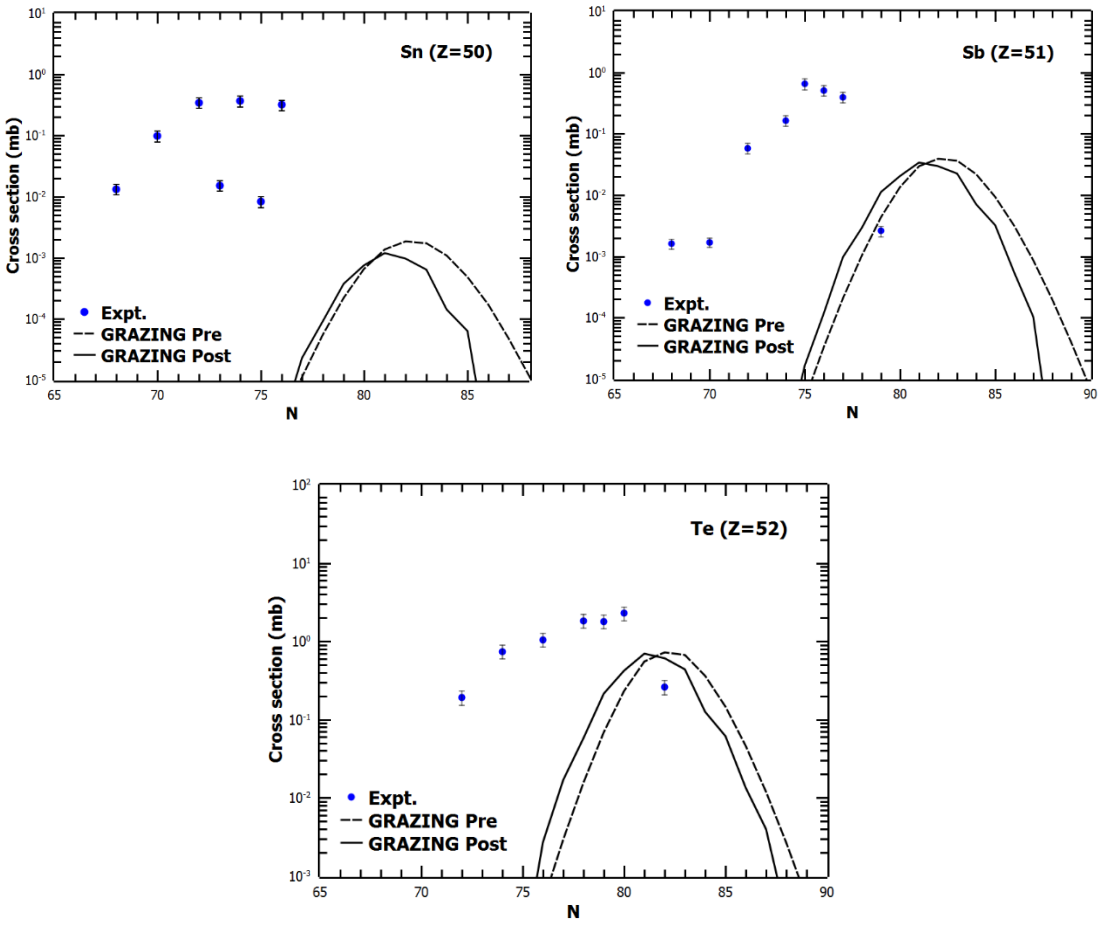

Figure 5.4: Secondary isotopic distributions for elements "south" of the ^{136}Xe projectile. The experimental data are compared to the pre- and post-neutron emission cross section predictions from the GRAZING code X.

Table 5.2 shows the tef values for these distributions. This quantitative measure confirms that the GRAZING predictions are not adequate for large mass transfer products, such as Sn and Sb isotopes. However, a trend can be noticed that as

Z increases toward the Z of the projectile, the average tef value approaches zero by a substantial amount.

Table 5.2: tef values for nuclides "south" of the ^{136}Xe projectile. The sign on the tef value denotes whether the experimental value(s) are greater than (-) or less than (+) the predicted value(s). As Z increases toward Z of the projectile, the agreement between theoretical and experimental values increases.

Element	ΔZ	tef_{ave}	σ_{tef}
Sn	-4	-6.21	0.65
Sb	-3	-3.65	1.01
Te	-2	-1.42	0.48

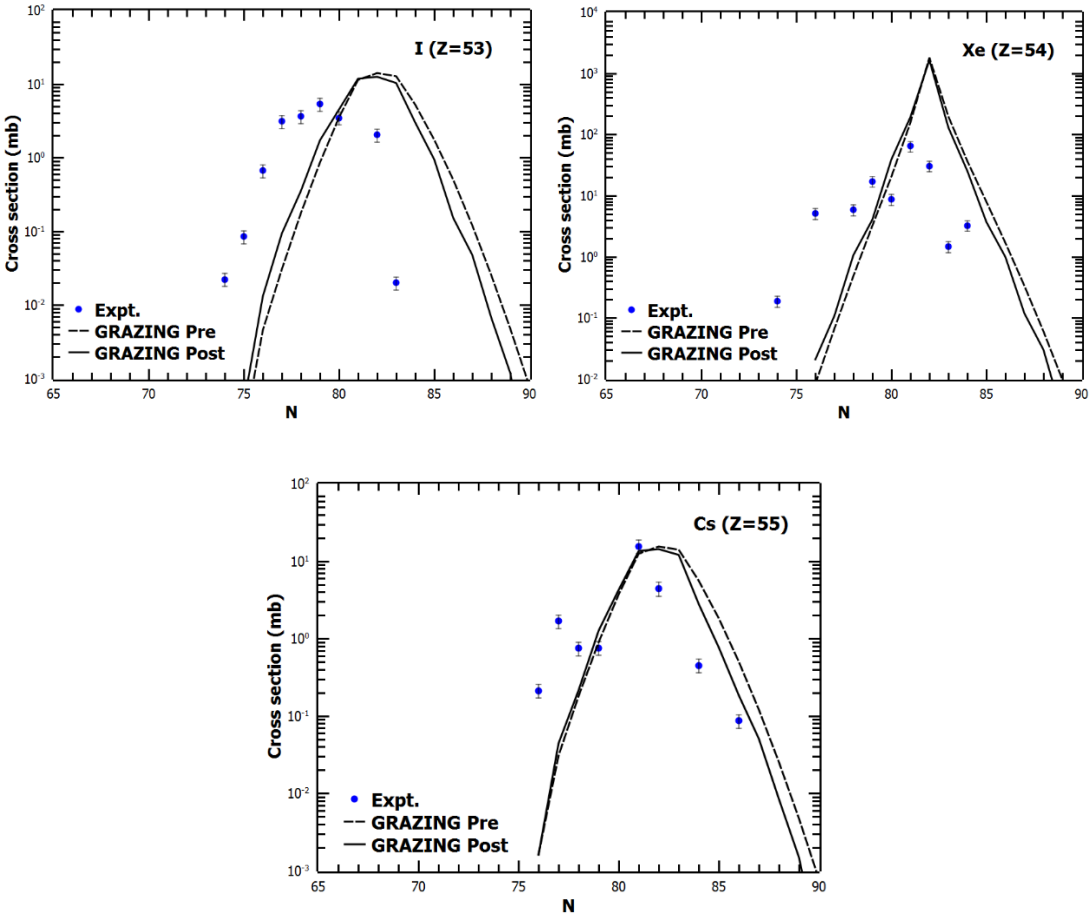

Figure 5.5: Secondary isotopic distributions for elements near the ^{136}Xe projectile. The experimental data are compared to the pre- and post-neutron emission cross section predictions from the GRAZING code X.

Figure 5.5 shows the IY isotopic distributions for elements near the projectile, including isotopes of I (ΔZ=-1), Xe (ΔZ=0), and Cs (ΔZ=+1). These distributions show increased agreement to the predicted values of GRAZING, both in the magnitude of the cross sections and location of peak maxima.

The tef values for the elements near the projectile are given in Table 5.3. The trend of increasing agreement as ΔZ approaches zero continues, with a minimum average tef value occurring for the Xe (ΔZ=0) isotopes. The agreement between the GRAZING predictions and the experimental data in this region show that GRAZING is adequate to predict formation cross sections for small mass transfer reaction products. These products are most likely to occur during more peripheral collisions with low projectile energy loss, for which GRAZING is well suited.

Table 5.3: tef values for nuclides near the ^{136}Xe projectile. As Z increases toward Z of the projectile, the agreement between theoretical and experimental values increases.

Element	ΔZ	tef_{ave}	σ_{tef}
I	-1	-0.49	0.50
Xe	0	0.29	0.42
Cs	+1	-0.48	0.37

Figure 5.6 shows the IY isotopic distributions for elements "north" of the projectile on the chart of nuclides, including Ba (ΔZ=+2), La (ΔZ=+3), and Ce (ΔZ=+4). The agreement between the predicted and experimental cross sections for Ba are in fair agreement, however, the difference increases again as Z increases away from the projectile. It is also observed that the location of the peak maximum for

these distributions appear to agree with those predicted by GRAZING, while this is not the case for the elements "south" of the projectile.

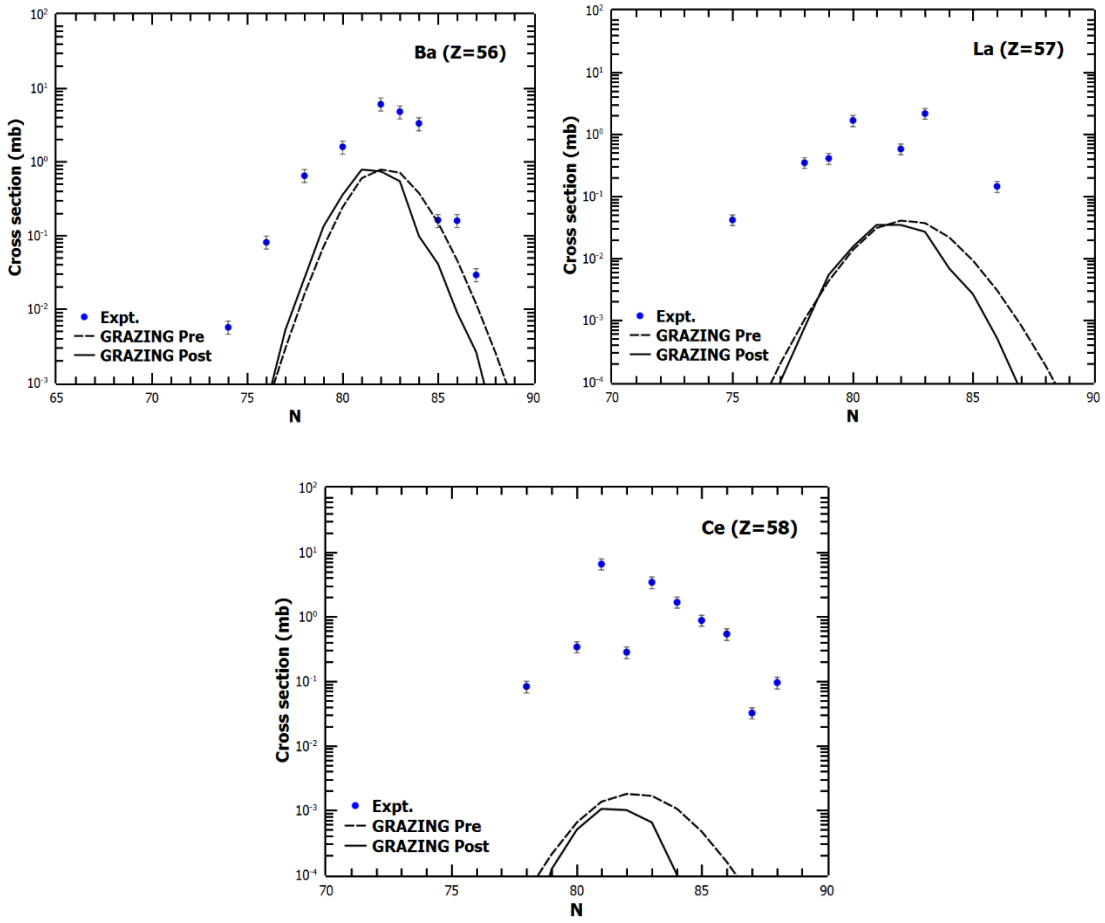

Figure 5.6: Secondary isotopic distributions for elements "north" of the ^{136}Xe projectile. The experimental data are compared to the pre- and post-neutron emission cross section predictions from the GRAZING code X.

The tef values for these distributions are given in Table 5.4. Again, the trend of larger magnitude tef values as ΔZ increases is observed. Overall, GRAZING does a reasonable job in predicting the cross sections for isotopes of the projectile and ΔZ= ±1. However, it does a poor job in predicting both the magnitude of the cross sections and location of the distribution maxima for ΔZ values greater than this.

Table 5.4: tef values for nuclides "north" of the ^{136}Xe projectile. The tef increases as ΔZ increases, showing a decrease in the agreement between theoretical and experimental cross sections.

Element	ΔZ	tef_{ave}	σ_{tef}
Ba	+2	-1.36	0.19
La	+3	-2.84	0.59
Ce	+4	-8.33	2.48

These discrepancies have been observed before in the reaction of ^{64}Ni + ^{238}U at E_{lab}=390 MeV (section 2.2.1). In that reaction, predictions from GRAZING were in good agreement with the experimental data for PLFs with Z=-2 to Z=+1. However, as more protons were transferred to or from the projectile, the predictions deviated by larger amounts from the experimentally measured cross sections.

Good agreement has been shown between the theoretical cross sections calculated using GRAZING and those determined through time-dependent Hartree-Fock calculations (section 1.3). TDHF calculations consider not only grazing collisions, but also deep inelastic collisions and quasifission reactions as well. Surprisingly, however, this formalism also fails to accurately predict cross sections for large transfer products. At present, it is unclear what physics are missing from these models in order to better account for these discrepancies.

5.4 TLF Comparisons to Model Predictions

Both the GRAZING predictions and those of Zagrebaev and Greiner are compared to experimentally determined cross sections for the TLFs. Figure 5.7 shows the IY isotopic distributions for elements "south" of the ^{208}Pb target, including W

(ΔZ=-8), Os (ΔZ=-6), and Pt (ΔZ=-4). In this group, GRAZING only predicts yields for isotopes of Pt.

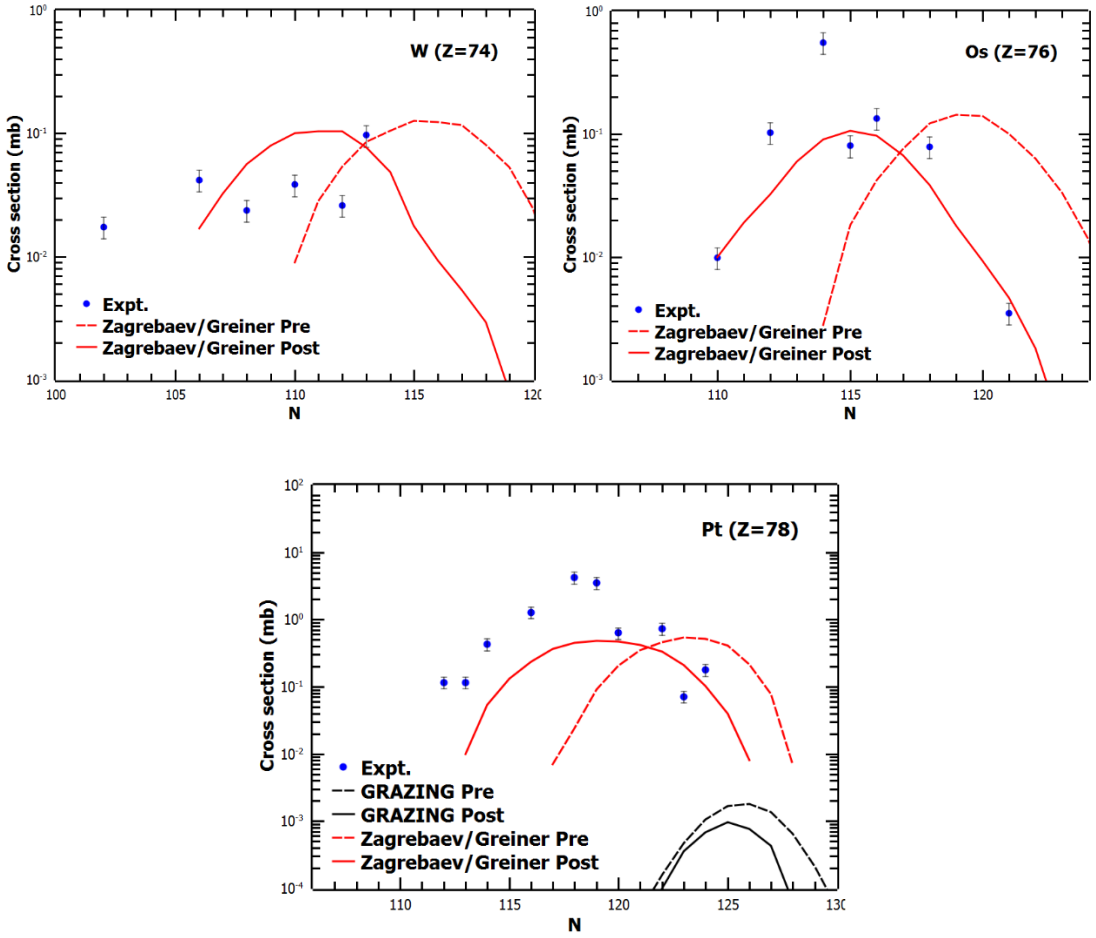

Figure 5.7: Secondary isotopic distributions for nuclei "south" of the ^{208}Pb target. The data are compared to pre- and post-neutron emission predictions from the GRAZING code and the model of Zagrebaev and Greiner.

The agreement between the experimentally determined cross sections and the predictions from [6, 18] are very different than the agreement with the GRAZING predictions. As was shown in the PLF predictions from GRAZING, at large ΔZ values relative to the target GRAZING is poor at predicting both the magnitude of the cross sections as well as the location of the distribution maximum. By contrast, the

predictions of Zagrebaev and Greiner are in fair agreement with observed experimental yields. The tef values for both the GRAZING predictions and those from [6, 18] are shown in Table 5.5.

Table 5.5: tef values for elements "south" of the ^{208}Pb target. No GRAZING predictions are available for W and Os isotopes.

GRAZING				Zagrebaev/Greiner	
Element	**ΔZ**	**tef_{ave}**	**σ_{tef}**	**tef_{ave}**	**σ_{tef}**
W	-8	-	-	0.19	0.15
Os	-6	-	-	-0.27	0.13
Pt	-4	-4.99	0.91	-0.54	0.15

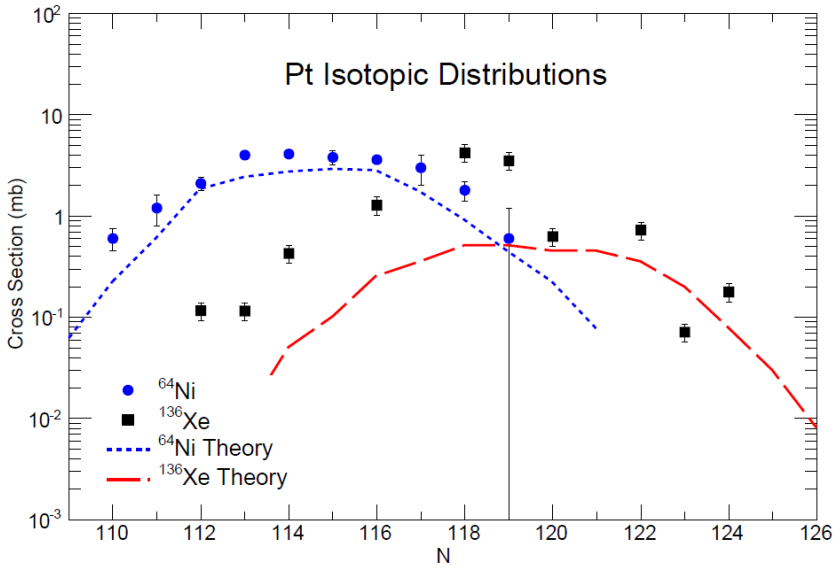

Figure 5.8: Comparison of Pt secondary isotopic distributions from the reactions of ^{136}Xe + ^{208}Pb and ^{64}Ni + ^{208}Pb. The more neutron-rich ^{136}Xe projectile produces more neutron-rich reaction products, consistent with previous observations. The ^{136}Xe data are from this experiment, the ^{64}Ni data was taken from [53], the ^{64}Ni theory was taken from [51], and the ^{136}Xe theory was taken from [18].

Figure 5.8 shows a comparison of Pt isotopic distributions from the ^{136}Xe + ^{208}Pb reaction as well as the reaction between ^{64}Ni + ^{208}Pb [53]. As is expected from

previous experiments [44, 45], the more neutron-rich projectile results in more neutron-rich reaction products, as seen by the location of the distribution peaks.

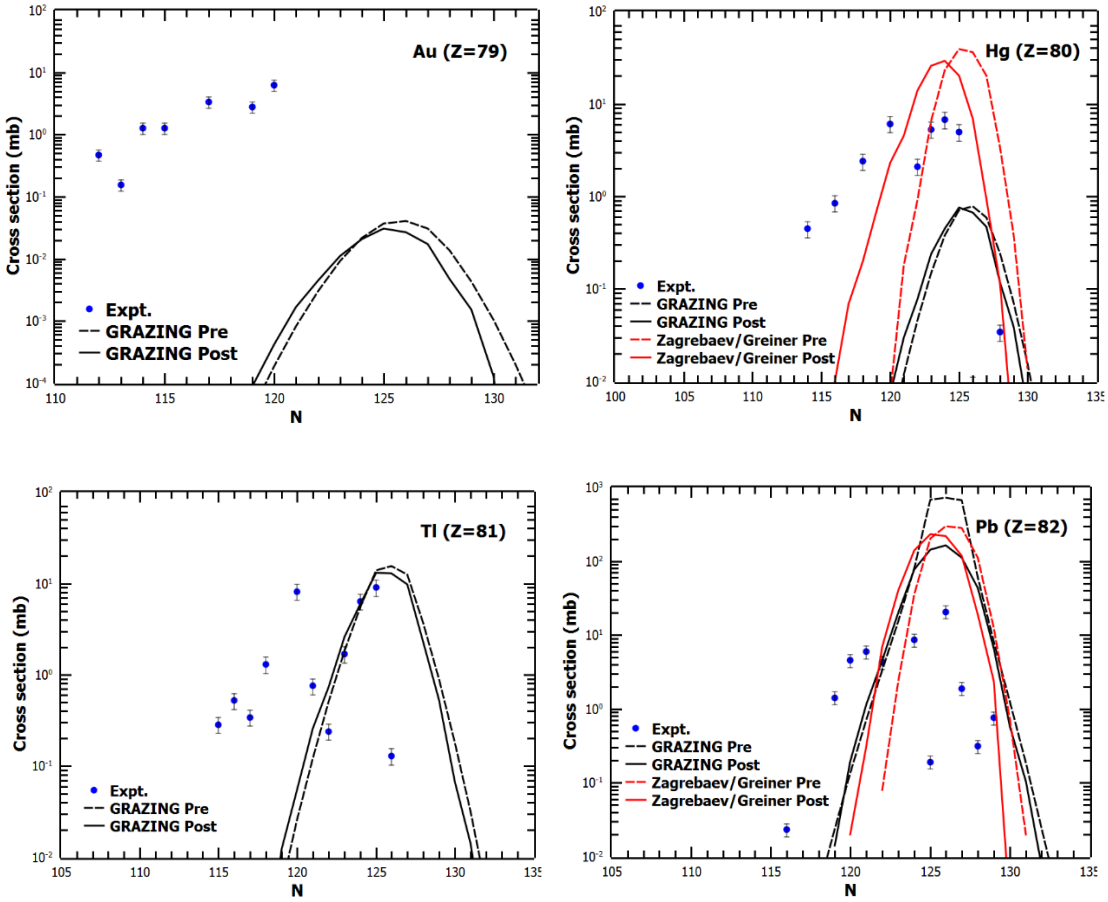

Figure 5.9: Secondary isotopic distributions for elements near the ^{208}Pb target. The data are compared to pre- and post-neutron emission predictions from the GRAZING code and the model of Zagrebaev and Greiner.

Figure 5.9 shows the IY isotopic distributions for elements near the target. Since Zagrebaev and Greiner do not have predictions for odd Z nuclei [6], only the GRAZING predictions will be compared in those cases. Once again, it is seen that as ΔZ from the target decreases, the agreement between the GRAZING predictions and the experimental cross sections improves. It can be seen that the predictions from Zagrebaev and Greiner [6] and those from GRAZING are similar for the Pb

distribution. However, the disagreement increases at the edges of the predicted distributions.

The Hg, Tl, and Pb data appear to have a bi-modal distribution. To determine if there is a true bi-modal distribution or if the measured cross sections are scattered about a single distribution, the data were fit assuming both a single and double Gaussian distribution. The reduced χ^2 was then calculated for both fits for each element. In each case, the reduced χ^2 for the single Gaussian fits were lower than the bi-modal fits (i.e. for Hg: single distribution reduced χ^2=1.268; bi-modal reduced χ^2=3.268), indicating that the cross sections lie along a single distribution.

The experimental cross sections for nuclei near the target are lower than the predicted values from both GRAZING and Zagrebaev and Greiner [6]. Lower experimental results in this region, compared to the model of Zagrebaev and Greiner, have previously been observed [5, 51]. Overall, however, the experimental values are in fair agreement with predicted cross sections, as can be seen by the tef values in Table 5.6.

Table 5.6: tef values for elements near the ^{208}Pb target. The agreement with the GRAZING predictions increases as ΔZ from the target decreases. The average tef values for the predictions of [6] show good overall agreement with experimental cross sections.

		GRAZING		Zagrebaev/Greiner	
Element	ΔZ	tef_{ave}	σ_{tef}	tef_{ave}	σ_{tef}
Au	-3	-5.55	0.67	-	-
Hg	-2	-1.22	0.64	0.16	0.40
Tl	-1	-0.86	0.62	-	-
Pb	0	0.36	0.48	0.32	0.55

The IY isotopic distributions for the odd Z nuclides "north" of the ^{208}Pb target are shown in Figure 5.10. As ΔZ continues to increase, the cross sections are once again underestimated. However, the location of the distribution maximum is more consistent with the measured results than for nuclei "south" of the target, as can be seen in the At (Z=85) distribution plot.

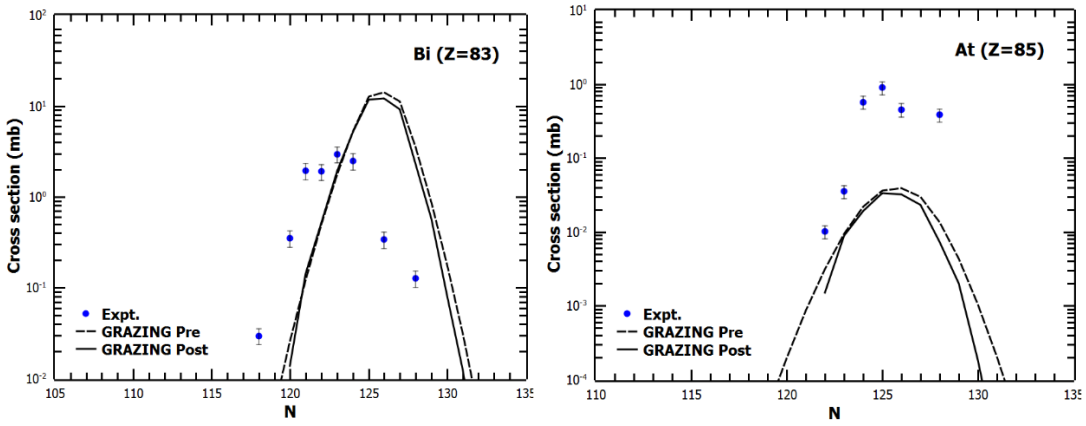

Figure 5.10: Secondary isotopic distributions for odd Z elements "north" of the ^{208}Pb target. No predictions from Zagrebaev and Greiner are available for these nuclei at E_{cm}=450 MeV.

While no predictions from the model of Zagrebaev and Greiner are available for trans-target nuclei for this reaction at E_{cm}=450 MeV [6], there are predictions for Po and Rn isotopes at E_{cm}=514 MeV from both the model of Zagrebaev and Greiner [5] and the DNS model [26]. Figure 5.11 shows the measured and predicted IY isotopic distributions for Po (Z=84) and Rn (Z=86), respectively. The predictions in this figure include those from GRAZING at E_{cm}=450 MeV [23] and GRAZING at E_{cm}=514 [23].

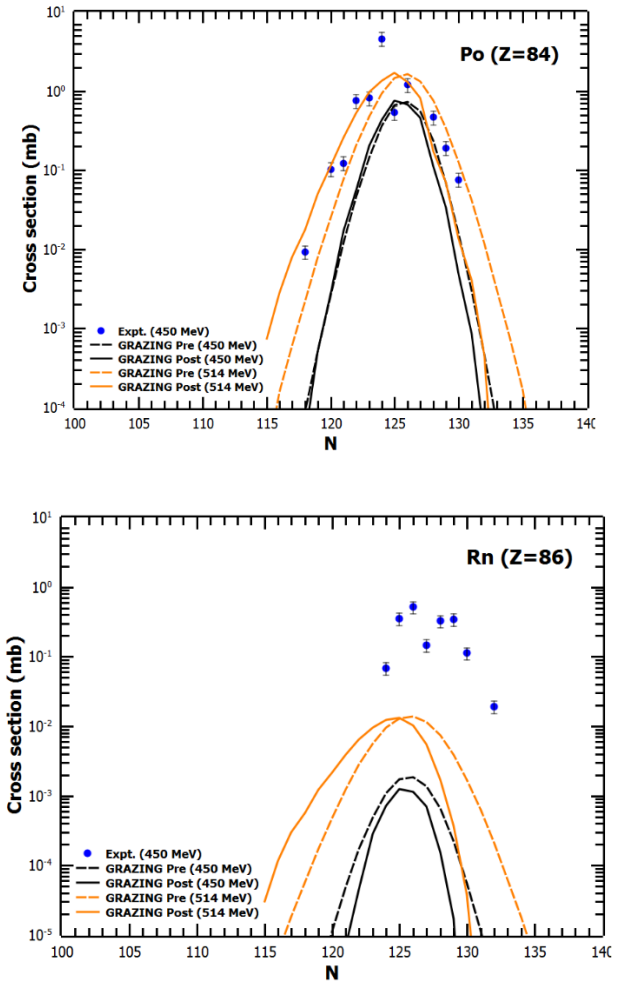

Figure 5.11: Secondary isotopic distributions of even Z trans-target nuclei compared to GRAZING predictions. The higher lying lines (orange) represent pre- (dashed) and post- (solid) neutron emission predictions from GRAZING at E_{cm}=514 MeV. The lower lines (black) represent the pre- and post-neutron emission predictions for E_{cm}=450 MeV.

Due to the difference in energies between the models and this experiment, only tef values were calculated for the GRAZING [23] predictions at E_{cm}=450 MeV. It is interesting to note that compared to the predictions from GRAZING at E_{cm}=450 and 514 MeV, the experimentally measured cross sections from this experiment at E_{cm}=450 still exceed the predictions by this model at a higher energy.

Figure 5.12 shows the predictions of Zagrebaev and Greiner [5] and those from the DNS model [10] to the cross sections from this experiment for Po and Rn isotopes. Both models predicted cross sections at an energy of E_{cm}=514 MeV, Also included are data points previously measured [5], also at E_{cm}=514 MeV.

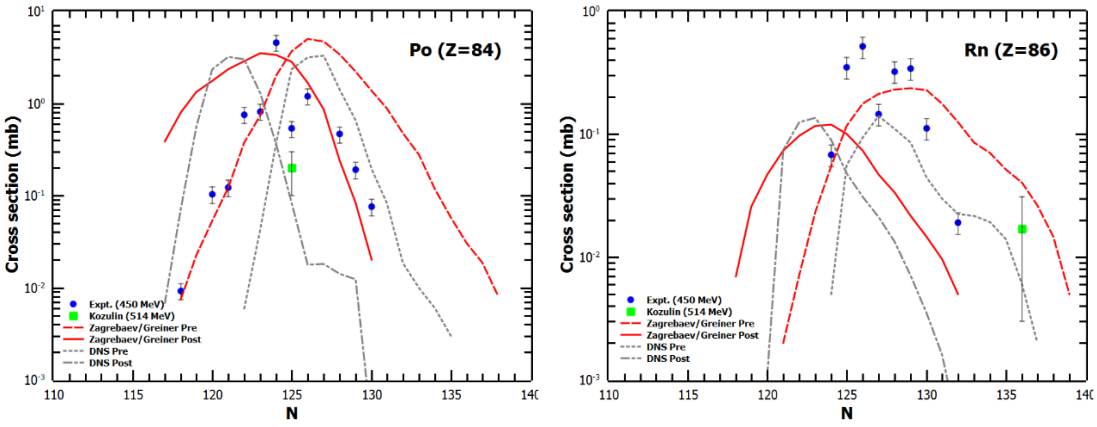

Figure 5.12: Secondary isotopic distribution of Po and Rn compared to predictions from Zagrebaev and Greiner and the DNS model. The data from this experiment at E_{cm}=450 MeV is compared to predictions for pre- and post-neutron emission cross sections from Zagrebaev and Greiner (red lines) and the DNS model (grey lines). Also shown are data points from a previous experiment of ^{136}Xe + ^{208}Pb at E_{cm}=514 MeV.

Since the reaction energy for this experiment differs from the energy at which the model predictions were calculated, a direct comparison is not possible. It is noteworthy, though, that even at a lower reaction energy, many of the experimental data points from Po, and almost all from Rn, still exceed the predicted secondary cross sections. In some cases for Rn isotopes the measured cross sections are nearly an order of magnitude higher than the predicted cross sections. This is consistent with results from previous experiments [5] and is encouraging for the production of trans-target nuclei in different systems.

The tef values for the trans-target nuclides are shown in Table 5.7. Only the tef values comparing the GRAZING predictions are presented. Similar to what is observed in the PLF data set, there was a minimum average tef for Pb (target) isotopes, then as ΔZ increases the GRAZING predictions increasingly disagree.

Table 5.7: tef values for elements "north" of the ^{208}Pb target. Only tef values for the GRAZING predictions are presented.

Element	ΔZ	tef_{ave}	σ_{tef}
Bi	+1	-0.45	0.41
Po	+2	-1.14	0.24
At	+3	-1.23	0.15
Rn	+4	-3.31	0.64

5.5 N=126 Nuclei

One particular area of interest are those nuclei produced with a closed neutron shell at N=126. Figure 5.13 shows the predictions from GRAZING, the predictions from Zagrebaev and Greiner [6], the measured cross sections from this experiment, as well as the measured cross sections from the ^{64}Ni + ^{208}Pb reaction [53] for these nuclei. No predictions are available for the production of N=126 nuclei using the ^{64}Ni projectile so no comment can be made on the agreement between those measurements and theory. Also, the Zagrebaev and Greiner predictions only extend to Z=82 and none are available for the neutron-deficient side of the distribution (higher Z).

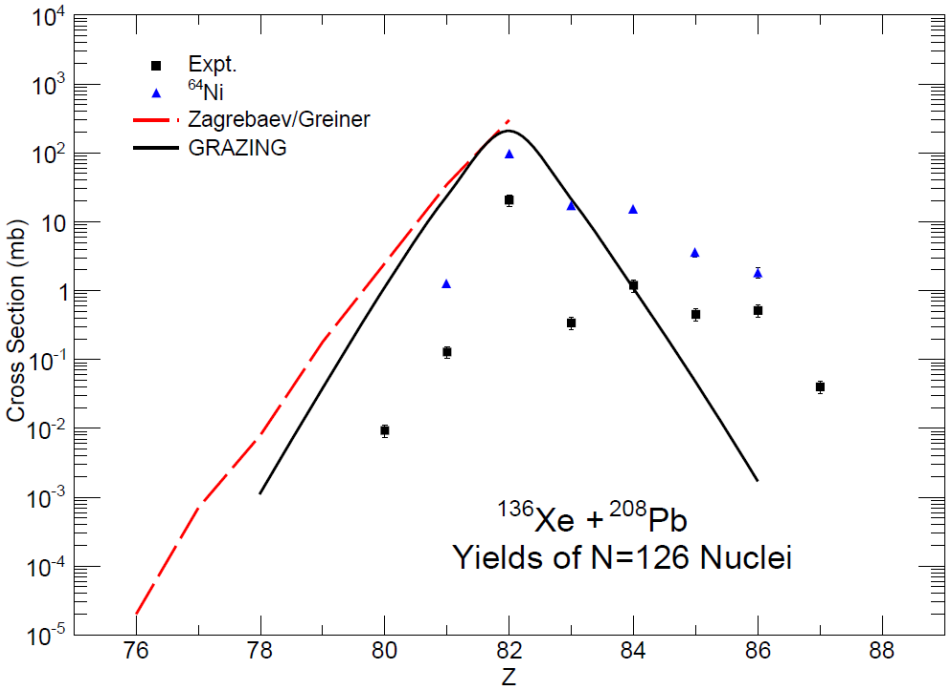

Figure 5.13: Comparison of predicted and measured cross sections for N=126 nuclei. The plot includes GRAZING predictions (solid line), Zagrebaev and Greiner predictions (dashed line), measurements from this experiment (black points), and measurements from the ^{64}Ni + ^{208}Pb experiment (blue points. The shapes of the measured distributions are similar. However on the neutron-rich side the measured cross sections are two orders of magnitude lower than predicted, and on the neutron-deficient side the measured cross sections are two orders of magnitude higher than predicted.

On the neutron-rich side of the distribution (lower Z), only Z=-1 and -2 nuclei were observed, and the measured cross sections are lower than the predictions by as much as two orders of magnitude. On the neutron-deficient side, the measurements also do not agree with the GRAZING predictions, though in this case the measurements are higher than predicted by almost two orders of magnitude. The general shape of the measured distributions using ^{136}Xe (black points) and ^{64}Ni (blue points) agree well. Considering the magnitude of the disagreements between theory

and the measurements, the outlook of producing new N=126 neutron-rich nuclei with high cross sections does not look promising.

5.6 Cross-Coincidence Analysis

Another exercise performed was a preliminary investigation of cross-coincidence events. This has been used before to develop γ-ray decay schemes for reaction products of transfer reactions [82]. Cross-coincidence events are observed by gating on a low lying γ-ray transition in either a PLF or TLF nuclide, then observing γ-emissions from the partner fragments formed in the reactions.

In this exercise, a gate was set on the $4^+ \rightarrow 2^+$ and the $2^+ \rightarrow 0^+$ transitions for ^{138}Ba ($\Delta Z = +2$, $\Delta N = 0$ from the projectile) of the PLF data set. Even with two gates set, a number of γ-rays appear in the coincidence spectrum. Through this analysis it was possible to determine γ-ray peaks originating from Hg nuclides, which would be the resulting partner nuclides ($\Delta Z = -2$ from the target).

The γ-ray peaks for the Hg isotopes were integrated and corrected for relative efficiency of Gammasphere in order to produce the distribution shown in Figure 5.14. This distribution shows the relative yields of the Hg isotopes in arbitrary units and is meant as a qualitative instead of quantitative comparison.

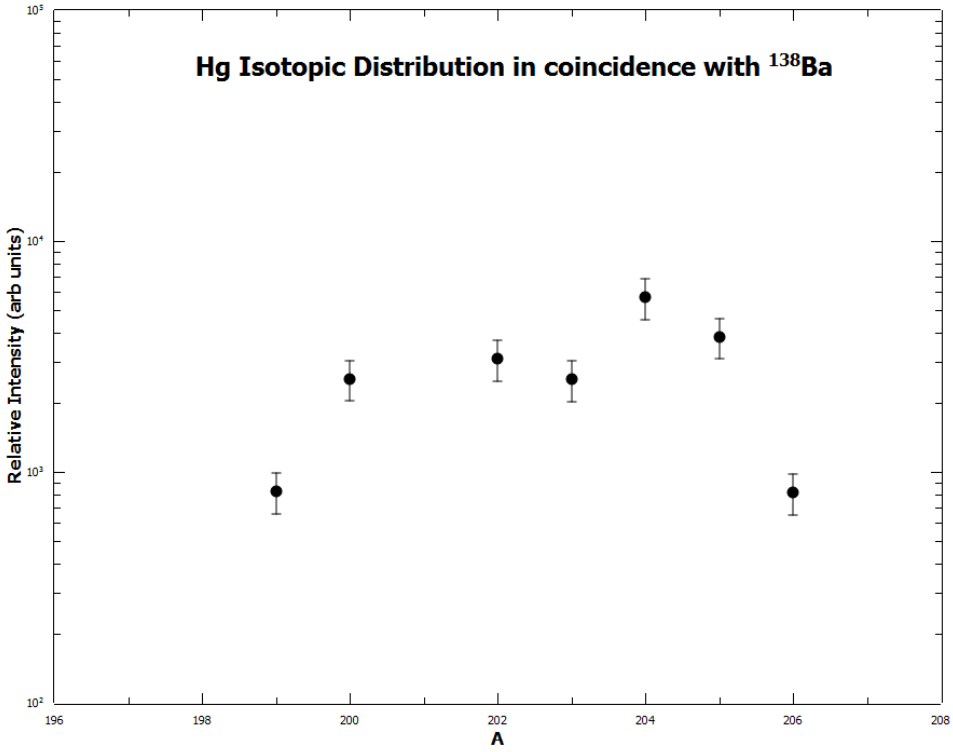

Figure 5.14: Cross-coincidence distribution of partner Hg isotopes when gating on ^{138}Ba. The peak of the distribution is at $^{202\text{-}203}$Hg, indicating that 3 – 4 neutrons were evaporated.

The distribution appears to peak near $^{202\text{-}203}$Hg. The partner fragment to ^{138}Ba would be ^{206}Hg, therefore there are approximately three to four neutrons emitted during de-excitation. If each neutron carries away 10 MeV, the excitation energy of these fragments would be approximately 30 – 40 MeV, which seems reasonable in this reaction [5]. It is also worth noting that ^{206}Hg was observed, which represents a cold process where no neutron evaporation occurs. As seen in the distribution of Figure 5.14, though, it is not a prevalent process.

Another partner pair that was investigated was that of ^{140}Ba and ^{204}Hg ($\Delta Z=\pm 2$, $\Delta N=\pm 2$). Again, gates were set on the $4^+ \rightarrow 2^+$ and the $2^+ \rightarrow 0^+$ transitions for ^{140}Ba. The distribution of the Hg isotopes is shown in Figure 5.15.

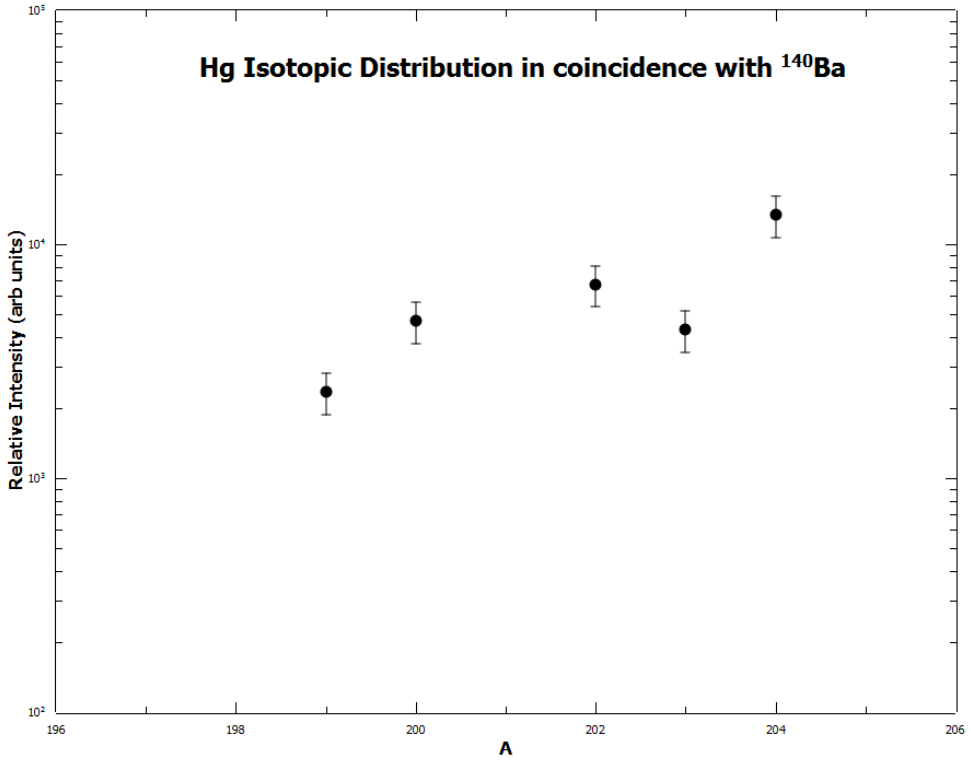

Figure 5.15: Cross-coincidence distribution of partner Hg isotopes when gating on ^{140}Ba. The peak of the distribution is at ^{201}Hg, indicating that 3 neutrons were evaporated. There is also a large number of cold transfer events (shown by A=204) resulting in no neutron emission.

The peak of this distribution occurs at ^{201}Hg, again showing that ~3 neutrons are evaporated. However, there are a relatively large number of events that produce the partner nucleus of ^{204}Hg. This nucleus is the direct partner of ^{140}Ba and is the result of a cold transfer process where no neutrons are emitted. It is also worth noting that the formation of this partner pair is the result of an α-particle transfer from ^{208}Pb to ^{136}Xe. At the present time, it is unclear if there is a correlation between α-particle transfer and the low excitation energy of the resulting fragments. It would be useful for future experiments to explore this phenomenon further.

5.7 Conclusions and Future Work

In this experiment a thick ^{208}Pb target was bombarded with ^{136}Xe at E_{cm}= 450 MeV. The resulting reaction products were stopped in the target and the γ-rays emitted by these nuclides were detected using Gammasphere, a large array of 90 HPGe detectors. The γ-γ-γ coincidences were then used to determine the cross sections of stable and very short-lived nuclei produced in the reaction. When bombardment had completed, radioactive decay data was recorded, first in Gammasphere, then using a calibrated single HPGe detector in the Argonne National Laboratory hot lab. The radioactive decay data from both sources were analyzed using standard γ-ray spectroscopy techniques and compared for consistency.

Cumulative and independent cross sections were determined for 235 nuclides split into two groups: projectile-like fragments (PLFs), ranging from Z=48 to Z=69, and target-like fragments (TLFs), ranging from Z=70 to Z=88. The results were then compared to two different prediction models for multi-nucleon transfer reactions. The first model utilizes the GRAZING code [22, 23], which uses grazing trajectories to predict transfer reactions. The second model is that of Zagrebaev and Greiner [6, 18], which includes the influence of shell effects during transfer reactions at low energy near the barrier.

From this experiment a number of conclusions can be made. First, the GRAZING model is only adequate for nuclides that are ΔZ=±1 away from the projectile and target. At greater ΔZ values, GRAZING greatly under-predicts the magnitude of the production cross sections as well as the location of the isotopic distribution maxima. Similar results have been previously observed in the ^{64}Ni + ^{238}U

reaction at E_{lab}=390 MeV and the $^{136}Xe + ^{198}Pt$ reaction at E_{lab}=1088 MeV. In both experiments GRAZING predictions began to deviate from experimental results starting at ΔZ=-3 and ΔZ=+2.

GRAZING does well for a wide range of neutron transfers for near projectile/target nuclei, which are small energy loss transitions, but does not do well for a wide range of proton transfers, which are higher energy transitions. The most likely cause of these discrepancies is the inability of GRAZING to deal with large energy loss collisions caused by small impact parameter collisions [12, 13, 47]. These collisions with large energy loss are very deep inelastic or quasifission reactions that result in a large number of nucleon transfers between the colliding nuclei. These collisions are inside the graing region and are not considered by GRAZING [13].

Second, the predictions of Zagrebaev and Greiner agree exceptionally well with measured cross sections, especially for large transfers “south” of the target on the chart of nuclides. However, no comparison could be made with their model for PLFs or neutron-deficient TLFs.

Finally, the measured cross sections for creating N=126 neutron-rich nuclei are two orders of magnitude below the predicted values. This is not an encouraging result in the effort to produce an “N=126 factory,” that is, to use transfer reactions to produce neutron-rich N=126 nuclei for further study.

There is still much work that can be done involving multi-nucleon transfer reactions. The technique of using large γ-ray detector arrays allows for relatively fast experiments and data analysis. This technique could be used to study a number of the surrogate reactions proposed by Zagrebaev and Greiner [13-20]. However, in future

experiments it would be of value to obtain a direct absolute efficiency measurement of Gammasphere, or any other detector array used. This would reduce the systematic error and help simplify the data analysis process.

Another area of investigation is the comparison of different experimentation/detection techniques. Since the beam is stopped in the target using thick target experiments, the energy of the reaction is really an integration from entrance energy down to the barrier. While simulations of this effect have been made [24], it would be better to compare actual experimental results. This is in contrast to thin target experiments where the resulting fragments are separated using either gas filled or velocity separators.

Given the enhanced production cross sections relative to theory, especially for larger nucleon transfers, it would be justified and worthwhile to begin experiments with heavier projectiles and targets. This would help fill out the chart of nuclides on the neutron-rich side of stability for heavy and super-heavy elements and aid in the improvement of models to predict multi-nucleon transfer reaction cross sections.

BIBLIOGRAPHY

[1] W. Loveland, D. J. Morrissey, and G. T. Seaborg, *Modern Nuclear Chemistry* (John Wiley & Sons, Inc., 2006).

[2] R. Bass, *Nuclear Reactions with Heavy Ions* (Springer-Verlag, 1980).

[3] R. Bass, Nuclear Physics **A231**, 45 (1974).

[4] R. Bass, Physical Review Letters **39**, 265 (1977).

[5] E. M. Kozulin *et al.*, Physical Review C **86**, 044611 (2012).

[6] V. Zagrebaev, and W. Greiner, Physical Review Letters **101**, 122701 (2008).

[7] V. V. Volkov, Physics Letters **44**, 93 (1978).

[8] C. Riedel, and W. Norenberg, Z. Phys. A **290**, 385 (1979).

[9] G. G. Adamian *et al.*, Journal of Physics: Conference Series **282**, 012002 (2011).

[10] L. Zhu, Z. Feng, and F. Zhang, arXiv, 1503.04421v1 (2015).

[11] K. Sekizawa, and K. Yabana, Physical Review C **88**, 014614 (2013).

[12] A. Winther, Nuclear Physics A **572**, 191 (1994).

[13] A. Winther, Nuclear Physics A **594**, 203 (1995).

[14] V. Zagrebaev, and W. Greiner, J. Phys. G: Nucl. Part. Phys. **34**, 1 (2007).

[15] V. Zagrebaev, and W. Greiner, J. Phys. G: Nucl. Part. Phys. **34**, 2265 (2007).

[16] V. Zagrebaev, and W. Greiner, J. Phys. G: Nucl. Part. Phys. **35**, 125103 (2008).

[17] V. Zagrebaev, and W. Greiner, Physical Review C **78**, 034610 (2008).

[18] V. Zagrebaev, and W. Greiner, Physical Review C **83**, 044618 (2011).

[19] V. Zagrebaev *et al.*, Physical Review C **84**, 044617 (2011).

[20] V. Zagrebaev, and W. Greiner, Physical Review C **87**, 034608 (2013).

[21] V. Zagrebaev, A. Karpov, and W. Greiner, Journal of Physics: Conference Series **420**, 012001 (2013).

[22] http://www.to.infn.it/nanni/grazing.

[23] http://nrv.jinr.ru/nrv/webnrv/grazing/.

[24] R. Yanez, and W. Loveland, Physical Review C **91**, 044608 (2015).

[25] J. V. Kratz, W. Loveland, and K. J. Moody, Nucl. Phys. A, http://dx.doi.org/10.1016/j.nuclphysa.2015.06.004 (2015).

[26] L. Zhu, Z.-Q. Feng, and F.-S. Zhang, J. Phys. G (Accepted for publication).

[27] H. Essel *et al.*, Z. Phys. A **289**, 265 (1978).

[28] K. E. Rehm *et al.*, Physical Review Letters **51**, 1426 (1983).

[29] H. Essel *et al.*, Physics Letters **81B**, 161 (1979).

[30] E. K. Hulet *et al.*, Physical Review Letters **39**, 385 (1977).

[31] J. V. Kratz *et al.*, Physical Review Letters **39**, 984 (1977).

[32] J. V. Kratz *et al.*, Physical Review C **13**, 2347 (1976).

[33] J. V. Kratz, A. E. Norris, and G. T. Seaborg, Physical Review Letters **33**, 502 (1974).

[34] R. J. Otto *et al.*, Physical Review Letters **36**, 135 (1976).

[35] H. Sohlbach *et al.*, Z. Phys. A **328**, 205 (1987).

[36] R. Vandenbosch *et al.*, Nuclear Physics **A269**, 210 (1976).

[37] D. C. Hoffman, M. M. Fowler, and W. R. Daniels, Physical Review C **31**, 1763 (1984).

[38] R. M. Chasteler *et al.*, Physical Review C **36**, 1820 (1987).

[39] H. Freiesleben *et al.*, Z. Phys. A **292**, 171 (1979).

[40] K. E. Gregorich *et al.*, Physical Review C **35**, 2117 (1987).

[41] K. J. Moody *et al.*, Physical Review C **33**, 1315 (1985).

[42] M. Schadel *et al.*, Physical Review Letters **48**, 852 (1982).

[43] M. Schadel *et al.*, Physical Review Letters **41**, 469 (1978).

[44] D. Lee *et al.*, Physical Review C **25**, 286 (1982).

[45] R. B. Welch *et al.*, Physical Review C **35**, 204 (1987).

[46] S. Szilner *et al.*, Physical Review C **76**, 024604 (2007).

[47] L. Corradi, A. M. Stefanini, and C. J. Lin, Physical Review C **59**, 261 (1999).

[48] Y. X. Watanabe *et al.*, Nucl. Inst. and Meth. in Phys. Res. B **317**, 752 (2013).

[49] W. Loveland *et al.*, Physical Review C **83**, 044610 (2011).

[50] V. F. Comas *et al.*, Eur. Phys. J. A **49**, 112 (2013).

[51] O. Beliuskina *et al.*, Eur. Phys. J. A **50**, 161 (2014).

[52] S. Heinz *et al.*, Journal of Physics: Conference Series **282**, 012007 (2011).

[53] W. Krolas *et al.*, Nuclear Physics A **724**, 289 (2003).

[54] B. Fornal *et al.*, Physical Review C **49**, 2413 (1994).

[55] B. Fornal *et al.*, Acta Physica Polonica B **26**, 357 (1995).

[56] B. Fornal *et al.*, Physical Review C **55**, 762 (1997).

[57] R. Broda *et al.*, Physics Letters B **251**, 245 (1990).

[58] J. F. C. Cocks *et al.*, Nuclear Physics A **645**, 61 (1999).

[59] J. F. C. Cocks *et al.*, J. Phys. G: Nucl. Part. Phys. **26**, 23 (2000).

[60] W. Krolas *et al.*, Nuclear Physics A **832**, 170 (2010).

[61] W. Krolas, Acta Physica Polonica B **42**, 689 (2011).

[62] J. S. Barrett *et al.*, Physical Review C **91**, 064615 (2015).

[63] R. V. F. Janssens, Nuclear Physics **A685**, 209c (2001).

[64] M. Devlin *et al.*, Nucl. Inst. and Meth. A **383**, 506 (1996).

[65] A. M. Baxter *et al.*, *Nuclear Structure at High Angular Momentum* Ottawa, 1992).

[66] I. Y. Lee, Prog. Part. Nucl. Phys. **38**, 65 (1997).

[67] http://www.phy.anl.gov/gammasphere/doc/efficiency/.

[68] http://www.radware.phy.ornl.gov/.

[69] http://srim.org.

[70] http://www.calel.org/range.html.

[71] http://www.jimfitz.demon.co.uk/fitzpeak.htm.

[72] U. Reus, and W. Westmeier, in *Atomic Data and Nuclear Data Tables*1983), pp. 1

[73] K. Aleklett, *Radiochemists' Gamma Ray Table* (Studsvik Neutron Research Laboratory, Nykoping, Sweden.

[74] http://www.nndc.bnl.gov/.

[75] http://www.phy.anl.gov/gammasphere/doc/index.html.

[76] D. J. Morrissey *et al.*, Physical Review C **21**, 1783 (1980).

[77] G. Friedlander *et al.*, *Nuclear and Radiochemistry* (John Wiley & Sons, Inc., 1981).

[78] D. C. Radford, Nucl. Inst. and Meth. **A361**, 297 (1995).

[79] A. Savitzky, and M. J. E. Golay, Analytical Chemistry **36**, 1627 (1964).

[80] W. W. Wilcke *et al.*, Atomic Data and Nuclear Data Tables **25**, 389 (1980).

[81] G. Bertsch *et al.*, J. Phys. G **42**, 077001 (2015).

[82] B. Fornal *et al.*, Physical Review C **72**, 044315 (2005).

[83] I. Binder *et al.*, in *LBL Annual Report No. LBL-2366* (Lawrence Berkely National Laboratory, 1974), p. 451.

APPENDIX

The following are the FORTRAN codes were developed at Lawerence Berkely National Laboratory [32, 83] to construct and analyze radioactive decay curves (analysis-rev-oo.for), calculate cross section (cross.for), and properly format an input file (massyprep.for) for the program used to determine charge distributions and independent yields (massywalt.for). Sample input and output files are shown after each program's code.

analysis-rev-oo.for

```
      Program dehl

! dehl is an error weighted least squares decay curve fitting program.
c      this modification is to replace binary table of nuclides--which seems to have
problems
c      with ascii table.
c

      Implicit Integer*2 (i-n)
      Implicit Character (g-h)
      Implicit Real*8 (a-f,r-z)

      Common /data/thlmin,thlmax,abumin,dgam,chilim,iamin,iamax
      Common /work/mass,enl,aie,the,gaie,ga,giso,gd,xths,xa0f,xa0s,
     * egam,iin,ier
      Common /work1/vel,zel,tct,adta,bdta,cdta,ddta,icm,icn,idt,ird,
     * frm,ipr
      Common /char/gnswer,gline

      Dimension mass(200),enl(200),aie(200),the(200),xths(200),
     1 xa0f(200),xa0s(200)
      Dimension vel(10,10),zel(10),wel(10,10),tct(100),eg(100),
     1 adta(100),bdta(100),cdta(100),ddta(100),frm(10),ipr(10)

      Character*78 glabel(2)
      Character*2 ga(200),giso(200)
      Character*1 gd(200),gaie(200),hfix(10),gnswer,gline(78)

! Call initial routine
      Call hlinit
```

```
! Prepare separation line
      Do 200 i=1,78
  200 gline(i)='-'

! Set flag for searching energy
      ier=0
            write(*,*)'got past hlinit'
  100 Read(1,*,End=999)egam,xidt
            write(*,*)egam,xidt
c 000 Format(F7.1,14X,I2)
      If(egam.EQ.0.)Go To 100
            write(*,*)'read idt'
            idt=xidt
            write(*,*)xidt,idt
      Do 6969 i=1,idt
 1    READ(1,*)EG(I), ADTA(I), BDTA(I), CDTA(I)
 2    FORMAT(F6.1, 36X, E8.3, 2E9.3)
c      cdta(i)=cdta(i)+ddta(i)
      WRITE(*,2)EG(I), ADTA(I), BDTA(i), cdta(i)
 6970 FORMAT(5E10.3)
c     IF(E(I).EQ.0.0)GO TO 3
c     I=I+1
c     GO TO 1
 6969  continue
      IMAX=I
c      OPEN(2,FILE='NEW.DAAT', STATUS='NEW')
c      WRITE(2,4) E(IMAX-1),IMAX
c 4    FORMAT(1X, F8.1, I6)
c      DO 5 I=1,IMAX-1
c      WRITE(2,6)E(I), ADTA(I), BDTA(I), CDTA(I), ddta(i)
c 6    FORMAT(1X, 5E10.3)
c 5    CONTINUE


! Read in the data
!   adta = counts/min
!   bdta = sigma(counts/min)
!   cdta = time at beginning of count
!   ddta = length of count

c     Do 101 i=1,idt
c     Read(1,1001)cdta(i),ddta(i),adta(i),bdta(i)
c101 cdta(i)=cdta(i)+ddta(i)/2.
c
c001 Format(13X,4E12.5)
```

```
      If(idt.LT.2)Go To 100

      Call clrscr
      Write(*,1002)egam,idt
 1002 Format('  Analyze of ',F6.1,' keV, ',I2,' points')

! Search for gamma-lines near egam
      Call gamlist

      icn=1
      icomp=0
      iter=0

      If(adta(1).LT.adta(idt))Then
        hfix(1)='Y'
        frm(1)=100000.
      Else
        hfix(1)='N'
        frm(1)=dlog(2.d0)*(cdta(idt)-cdta(1))/dlog(adta(1)/adta(idt))
        If(frm(1).LT.thlmin)frm(1)=thlmin
      Endif

      hfix(2)='N'
      frm(2)=adta(2)*dexp(dlog(2.d0)*cdta(2)/frm(1))

  102 icm=icn
      frm(1)=dlog(2.d0)/frm(1)
      If(icm.GT.1)frm(3)=dlog(2.d0)/frm(3)
      If(icm.GT.2)frm(5)=dlog(2.d0)/frm(5)

! Locate and count the variable parameters
      ird=0
      Do 103 i=1,icm*2
      If(hfix(i).EQ.'N')Then
        ird=ird+1
        ipr(ird)=i
      Endif
  103 Continue

! Go take derivatives and build matrix
  104 If(icn.LT.6)Call deriv
      If(icn.GT.5)Call gderiv

! Go solve the matrix
```

```
      Call matrix(vel,wel,zel,ird)
      iter=iter+1

! Convergence check
      iconv=0
      Do 105 i=1,ird
      frm(ipr(i))=frm(ipr(i))+zel(i)
  105 If(dabs(zel(i)).GT.dabs(frm(ipr(i)))/10000.)iconv=1

      ika=0
      Do 106 ik=1,icm*2
  106 If(frm(ik).LT.0.)ika=1

      If(ika.EQ.1)Then
        Write(*,1003)
 1003   Format('  Problems in the fit have been noticed')
        Go To 111
      Endif

      If(iter.LT.2)Go To 104
      If(iter.GT.50)Go To 107
      If(iconv.EQ.1)Go To 104
      Go To 108

  107 Write(*,1003)
      Write(*,1004)
 1004 Format('  It has not converged after 50 iterations')

  108 Do 109 i=1,icm
      iin=iin+1
      If(hfix(2*i-1).EQ.'N'.AND.hfix(2*i).EQ.'N')Then
        x1=dlog(2.d0)/frm(2*i-1)
        mass(iin)=0
        ga(iin)='XX'
        giso(iin)='mm'
        gd(iin)=' '
        enl(iin)=0.
        aie(iin)=100.
        gaie(iin)=' '
        the(iin)=0.
        xths(iin)=x1
        xa0f(iin)=0.
        xa0s(iin)=frm(2*i)
      Endif
```

```
If(hfix(2*i-1).EQ.'Y'.AND.hfix(2*i).EQ.'N')Then
  x1=dlog(2.d0)/frm(2*i-1)
  mass(iin)=0
  ga(iin)='XX'
  giso(iin)='mm'
  gd(iin)=' '
  enl(iin)=0.
  aie(iin)=100.
  gaie(iin)=' '
  the(iin)=0.
  xths(iin)=x1
  xa0f(iin)=frm(2*i)
  xa0s(iin)=0.
Endif

If(hfix(2*i-1).EQ.'N'.AND.hfix(2*i).EQ.'Y')Then
  x1=dlog(2.d0)/frm(2*i-1)
  mass(iin)=0
  ga(iin)='XX'
  giso(iin)='mm'
  gd(iin)=' '
  enl(iin)=0.
  aie(iin)=100.
  gaie(iin)=' '
  the(iin)=x1
  xths(iin)=0.
  xa0f(iin)=0.
  xa0s(iin)=frm(2*i)
Endif

If(hfix(2*i-1).EQ.'Y'.AND.hfix(2*i).EQ.'Y')Then
  x1=dlog(2.d0)/frm(2*i-1)
  mass(iin)=0
  ga(iin)='XX'
  giso(iin)='mm'
  gd(iin)=' '
  enl(iin)=0.
  aie(iin)=100.
  gaie(iin)=' '
  the(iin)=0.
  xths(iin)=x1
  xa0f(iin)=0.
  xa0s(iin)=frm(2*i)
Endif
```

```
  109 Continue

      If(idt.GT.2)Then
        chi=0.
        Do 110 i=1,idt
  110   chi=chi+(dabs(tct(i)-adta(i)))**2./bdta(i)**2.
        chir=chi/(idt-ird)
      Else
        chir=0.
      Endif

      If(chir.GT.chilim)Then
        If(icomp.EQ.2.OR.idt.LT.5.OR.adta(1).LT.adta(2))Go To 111
        icomp=icomp+1

! Fit two components
        If(icomp.EQ.1)Then
          icn=2
          iter=0
          hfix(1)='N'
          t11=(cdta(2)-cdta(1))*dlog(2.d0)/dlog(adta(1)/adta(2))
          frm(1)=t11
          If(adta(idt-1).LT.adta(idt))Then
            hfix(3)='N'
            frm(3)=100000.
          Else
            hfix(3)='N'
            frm(3)=dlog(2.d0)*(cdta(idt)-cdta(idt-1))/dlog(adta(idt-1)
     *       /adta(idt))
          Endif
          If(frm(1).LT.thlmin)frm(1)=thlmin
          If(frm(3).LT.thlmin)frm(1)=thlmin
          rem1=frm(3)
          hfix(2)='N'
          frm(2)=adta(2)*dexp(dlog(2.d0)*cdta(2)/frm(1))
          hfix(4)='N'
          frm(4)=adta(idt)*dexp(dlog(2.d0)*cdta(idt)/frm(3))
          frm(2)=frm(2)-frm(4)
          rem2=frm(4)
          Go To 102
        Endif

! Fit three components
        If(idt.LT.6.OR.adta(1).LT.adta(idt))Go To 111
        icn=3
```

```
        iter=0

        hfix(1)='Y'
        frm(1)=dlog(2.d0)/frm(1)
        hfix(3)='N'
        frm(3)=dlog(2.d0)/frm(3)*1.2
        hfix(5)='N'
        frm(5)=rem1*2
        If(frm(1).LT.thlmin)frm(1)=thlmin
        hfix(2)='N'
        frm(2)=frm(2)-rem2*0.9
        hfix(4)='N'
        frm(4)=frm(4)-rem2*0.9
        hfix(6)='N'
        frm(6)=rem2*.9
        Go To 102
      Endif
C
  111 Write(*,*)
  112 Write(*,1005)
 1005 Format('  (F)it, New (E)nergy, (D)elete data point, (C)ontinue,',
     * ' (Q)uit: F; ',$)
      Read(*,'(A1)')gnswer
      If(gnswer.EQ.'C'.OR.gnswer.EQ.'c')Go To 100
      If(gnswer.EQ.'Q'.OR.gnswer.EQ.'q')Go To 999

! If new energy is requested
      If(gnswer.EQ.'E'.OR.gnswer.EQ.'e')Then
        Write(*,1006)
 1006   Format(/'  Please give new energy: ',$)
        Read(*,'(F6.0)',Err=100)enew
        If(enew.LE.egam)Then
          Rewind(1)
          Read(1,'(A78)')glabel
        Endif
  113   Read(1,'(F7.1)',End=999)efind
        If(efind.EQ.0..OR.efind.LT.enew)Go To 113
        Backspace(1)
        ier=0
        Go To 100
      Endif

! If delete a point is requested
      If(gnswer.EQ.'D'.OR.gnswer.EQ.'d')Then
  114   Call clrscr
```

```
! Write points on screen
      Write(*,1007)
 1007   Format('  Points'/)
      Do 115 i=1,idt
  115   Write(*,1008)i,cdta(i)-ddta(i)/2.,ddta(i),adta(i),bdta(i)
 1008   Format(I4,1P4E13.5)

! Give point to delete, ENTER to quit
      Write(*,1009)
 1009   Format(/'  Enter point to delete or ENTER for no delete: ',$)
      Read(*,'(I2)',Err=114)idel
      If(idel.EQ.0)Go To 117
      If(idel.LT.1.OR.idel.GT.idt)Go To 114

! Locate point and delete it
      j=0
      Do 116 i=1,idt
      If(i.EQ.idel)Go To 116
      j=j+1
      adta(j)=adta(i)
      bdta(j)=bdta(i)
      cdta(j)=cdta(i)
      ddta(j)=ddta(i)
  116   Continue
      idt=idt-1
      Go To 114
    Endif

  117 Call dehl2
    If(gnswer.EQ.'C')Go To 100
    Go To 112

  999 Continue
    If(gnswer.EQ.'E'.OR.gnswer.EQ.'e')Then
      Rewind(1)
      Read(1,'(A78)')glabel
      Go To 100
    Endif
    Write(*,1010)
 1010 Format(/'  End-of-Job')
    End

    Subroutine clrscr
```

```
! This routine clears the screen and sets the cursor to first position in first
! line. Routine requires ANSI device driver.

      Character*1 astr(5),char
      Data astr/' ',' ','[','2','J'/

      astr(2)=char(27)
      Write(*,'(5A1)')astr
      Return
      End
      Subroutine dehl2

      Implicit Integer*2 (i-n)
      Implicit Character (g-h)
      Implicit Real*8 (a-f,r-z)

      Common /work/mass,enl,aie,the,gaie,ga,giso,gd,xths,xa0f,xa0s,
     * egam,iin,ier
      Common /work1/vel,zel,tct,adta,bdta,cdta,ddta,icm,icn,idt,ird,
     * frm,ipr
      Common /char/gnswer,gline

      Dimension mass(200),enl(200),aie(200),the(200),xths(200),
     * xa0f(200),xa0s(200)
      Dimension vel(10,10),zel(10),wel(10,10),tct(100),
     * adta(100),bdta(100),cdta(100),ddta(100),frm(10),ipr(10)
      Dimension abu(200),ab0(200),sab0(200),efx(10),mas(10),a00(5),kz(5)

      Character*2 ga(200),giso(200),gid(200),gis(200)
      Character*1 gline(78),gnswer,gsave,gfit
      Character*1 gd(200),gaie(200),gabu(200),hfix(10)

  100 Call clrscr

! Write isotopes found in ID-search
      Write(*,1000)egam,idt
 1000 Format('  Analyze of ',F6.1,' keV, ',I2,' points')
      If(iin.GT.22)Then
        jnuc=iin-22
        Do 102 i=1,22
        If(the(i).LT.999.9.AND.xths(i).LT.999.9)Then
          Write(*,1001)i,mass(i),ga(i),giso(i),gd(i),enl(i),aie(i),
     *    gaie(i),the(i),xths(i),xa0f(i),xa0s(i)
 1001     Format(I4,I4,A2,1X,A2,1X,A1,F7.1,F7.2,A1,F7.3,5X,F7.3,
     *    4X,1P2E11.4)
```

```
      Else
        Write(*,1002)i,mass(i),ga(i),giso(i),gd(i),enl(i),aie(i),
     *    gaie(i),the(i),xths(i),xa0f(i),xa0s(i)
 1002    Format(I4,I4,A2,1X,A2,1X,A1,F7.1,F7.2,A1,1PE11.3,E12.3,2E11.4)
      Endif
  102  Continue

      Write(*,1003)
 1003  Format('  ENTER for more: ',$)
      Read(*,'(A1)')gnswer
      Do 103 i=jnuc,iin
      If(the(i).LT.999.9.AND.xths(i).LT.999.9)Then
        Write(*,1001)i,mass(i),ga(i),giso(i),gd(i),enl(i),aie(i),
     *    gaie(i),the(i),xths(i),xa0f(i),xa0s(i)
      Else
        Write(*,1002)i,mass(i),ga(i),giso(i),gd(i),enl(i),aie(i),
     *    gaie(i),the(i),xths(i),xa0f(i),xa0s(i)
      Endif
  103  Continue
     Else
      Do 104 i=1,iin
      If(the(i).LT.999.9.AND.xths(i).LT.999.9)Then
        Write(*,1001)i,mass(i),ga(i),giso(i),gd(i),enl(i),aie(i),
     *    gaie(i),the(i),xths(i),xa0f(i),xa0s(i)
      Else
        Write(*,1002)i,mass(i),ga(i),giso(i),gd(i),enl(i),aie(i),
     *    gaie(i),the(i),xths(i),xa0f(i),xa0s(i)
      Endif
  104  Continue
     Endif

! Ask type of fit wanted
     Write(*,1004)
 1004 Format('  (0)No fit; (1)One comp.; (2)Two comp.;',
     *' (3)Three comp.; (4)Four comp.'/'  (6)Growth and decay;',
     *' (7)G&D. + one comp.; (8)G&D. + two comp. Type?: ',$)
     Read(*,'(I2)',Err=100)icn
     If(icn.EQ.0)Then
       gnswer='C'
       Return
     Endif
     If(icn.LT.0)Go To 100
     If(icn.GT.8)Go To 100
     If(icn.EQ.5)Go To 100
     iicn=icn
```

```
      If(icn.GT.5)iicn=iicn-4

      Do 105 i=1,5
  105 kz(i)=0

      Write(*,*)
      Do 106 i=1,iicn
      Write(*,1005)i
 1005 Format('  ENTER or give number for component No ',I1,': ',$)
      Read(*,'(I2)',Err=100)kz(i)
      If(kz(i).GT.iin)kz(i)=iin
      If(kz(i).EQ.0)Then
        Write(*,1006)i
 1006   Format(5X,'Guess of half-life of component No ',I1,': ',$)
        Read(*,'(F10.0)',Err=100)xth
        If(xth.EQ.0.)Go To 100
        Write(*,1007)i
 1007   Format(4X,'Guess of 0-activity of component No ',I1,': ',$)
        Read(*,'(F10.0)',Err=100)xa0
        If(xa0.EQ.0.)Go To 100
        iin=iin+1
        kz(i)=iin
        mass(iin)=0
        ga(iin)='XX'
        giso(iin)='mm'
        enl(iin)=0.
        aie(iin)=100.
        gaie(iin)=' '
        the(iin)=0.
        gd(iin)=' '
        xths(iin)=xth
        xa0f(iin)=0.
        xa0s(iin)=xa0
      Endif
  106 Continue
C
      Call clrscr
C
C     Reset variables
      Do 107 i=1,10
      hfix(i)=' '
      ipr(i)=0
      efx(i)=0.
      mas(i)=0
      gid(i)='XX'
```

```
      gis(i)='mm'
  107 Continue

      If(icn.LT.5)Then
        icm=icn
        If(icm.EQ.1)gfit='A'
        If(icm.EQ.2)gfit='B'
        If(icm.EQ.3)gfit='C'
        If(icm.EQ.4)gfit='D'
      Else
        If(icn.EQ.6)gfit='F'
        If(icn.EQ.7)gfit='G'
        If(icn.EQ.8)gfit='H'
        icm=icn-4
      Endif

! Input initial values for parameters
      If(icm.EQ.1)a01=adta(1)

      If(icm.EQ.2)Then
        a02=adta(idt)
        a01=adta(1)-a02
      Endif

      If(icm.EQ.3)Then
        a03=adta(idt)*0.7
        km=idt/2
        a02=adta(km)-a03
        a01=adta(1)-a02-a01
        If(a01.LT.0.)a01=adta(1)/2.
      Endif

      a00(1)=a01
      a00(2)=a02
      a00(3)=a03

      Do 108 i=1,icm
      mas(i)=mass(kz(i))
      gid(i)=ga(kz(i))
      gis(i)=giso(kz(i))
      abu(i)=aie(kz(i))
      gabu(i)=gaie(kz(i))
      efx(i)=enl(kz(i))
      x1=xths(kz(i))
      x2=xa0s(kz(i))
```

```
      x3=the(kz(i))
      x4=xa0f(kz(i))*abu(i)/100.

      If(x2.EQ.0..AND.x4.EQ.0.)x2=a00(i)

      If(x1.EQ.0.)Then
        hfix(2*i-1)='Y'
        frm(2*i-1)=x3
      Else
        hfix(2*i-1)='N'
        frm(2*i-1)=x1
      Endif

      If(x2.EQ.0.)Then
        hfix(2*i)='Y'
        frm(2*i)=x4
      Else
        hfix(2*i)='N'
        frm(2*i)=x2
      Endif
  108 Continue

      iter=0
      Do 109 i=1,icm
  109 frm(2*i-1)=dlog(2.d0)/frm(2*i-1)

! Locate and count the variable parameters
      ird=0
      Do 110 i=1,icm*2
      If(hfix(i).EQ.'N')Then
        ird=ird+1
        ipr(ird)=i
      Endif
  110 Continue

! Go take derivatives and build matrix
  111 If(icn.LT.5)Call deriv
      If(icn.GT.5)Call gderiv

! Go solve the matrix
      Call matrix(vel,wel,zel,ird)
      iter=iter+1

! Convergence check
      iconv=0
```

```
      Do 112 i=1,ird
      frm(ipr(i))=frm(ipr(i))+zel(i)
  112 If(dabs(zel(i)).GT.dabs(frm(ipr(i)))/10000.)iconv=1

! Check if there are problems in the fit
      ika=0
      If(frm(1).LT.0.)ika=1
      Do 113 i=2,icm*2
  113 If(frm(i).LT.0.AND.hfix(i-1).EQ.'N')ika=1
      If(ika.EQ.1)Then
        Write(*,1008)
 1008   Format('  ********* problem in the fit *********')
        Go To 117
      Endif

      If(iter.LT.2)Go To 111
      If(iter.GT.50)Go To 114
      If(iconv.EQ.1)Go To 111
      Go To 115

  114 Write(*,1009)
 1009 Format('  It has not converged after 50 iterations')

! Calculate red. CHI squared
  115 If(idt.EQ.2)Then
        chir=0.
      Else
        chi=0.
        Do 116 i=1,idt
  116   chi=chi+(dabs(tct(i)-adta(i)))**2./bdta(i)**2.
        chir=chi/(idt-ird)
      Endif

! Print results on the screen
  117 Call graph(chir)

      If(ika.EQ.1)Return

      itype=0
      If(gfit.EQ.'F')itype=1
      If(gfit.EQ.'G')itype=1
      If(gfit.EQ.'H')itype=1
      If(itype.EQ.1)abu(1)=(abu(1)*abu(2)/100.)

      gpr='N'
```

```
118 m=1
    Do 119 i=1,icm
    If(hfix(2*i-1).EQ.'N'.AND.hfix(2*i).EQ.'N')Then
      x1=dlog(2.d0)/frm(2*i-1)
      x2=dlog(2.d0)*wel(m,m)**.5/frm(2*i-1)**2.
      If(abu(i).EQ.0.)Then
        If(gpr.EQ.'N')Write(*,1010)
        abu(i)=100.
      Endif
      ab0(i)=frm(2*i)/abu(i)*100.
      sab0(i)=wel(m+1,m+1)**.5/abu(i)*100.
      If(x1.GT.999.)Then
        If(gpr.EQ.'N')Write(*,1011)egam,mas(i),gid(i),gis(i),efx(i),
     *    abu(i),gabu(i),x1,ab0(i),sab0(i)/ab0(i)*100.,gfit
        If(gpr.EQ.'Y')Write(11,1012)mas(i),gid(i),gis(i),efx(i),
     *    abu(i),gabu(i),x1,x2,ab0(i),sab0(i)/ab0(i)*100.
        If(gpr.EQ.'Y')Write(12,1013)egam,mas(i),gid(i),gis(i),efx(i),
     *    abu(i),gabu(i),x1,ab0(i),sab0(i),gfit
      Else
        If(gpr.EQ.'N')Write(*,1014)egam,mas(i),gid(i),gis(i),efx(i),
     *    abu(i),gabu(i),x1,ab0(i),sab0(i)/ab0(i)*100.,gfit
        If(gpr.EQ.'Y')Write(11,1015)mas(i),gid(i),gis(i),efx(i),
     *    abu(i),gabu(i),x1,x2,ab0(i),sab0(i)/ab0(i)*100.
        If(gpr.EQ.'Y')Write(12,1016)egam,mas(i),gid(i),gis(i),efx(i),
     *    abu(i),gabu(i),x1,ab0(i),sab0(i),gfit
      Endif
      m=m+2
    Endif

    If(hfix(2*i-1).EQ.'Y'.AND.hfix(2*i).EQ.'N')Then
      x1=dlog(2.d0)/frm(2*i-1)
      x2=dlog(2.d0)*wel(m,m)**.5/frm(2*i-1)**2.
      If(abu(i).EQ.0)Then
        If(gpr.EQ.'N')Write(*,1010)
        abu(i)=100.
      Endif
      ab0(i)=frm(2*i)/abu(i)*100.
      sab0(i)=wel(m,m)**.5/abu(i)*100.
      If(x1.GT.999.)Then
        If(gpr.EQ.'N')Write(*,1011)egam,mas(i),gid(i),gis(i),efx(i),
     *    abu(i),gabu(i),x1,ab0(i),sab0(i)/ab0(i)*100.,gfit
        If(gpr.EQ.'Y')Write(11,1012)mas(i),gid(i),gis(i),efx(i),
     *    abu(i),gabu(i),x1,0.,ab0(i),sab0(i)/ab0(i)*100.
        If(gpr.EQ.'Y')Write(12,1013)egam,mas(i),gid(i),gis(i),efx(i),
     *    abu(i),gabu(i),x1,ab0(i),sab0(i),gfit
```

```
   Else
    If(gpr.EQ.'N')Write(*,1014)egam,mas(i),gid(i),gis(i),efx(i),
*    abu(i),gabu(i),x1,ab0(i),sab0(i)/ab0(i)*100.,gfit
    If(gpr.EQ.'Y')Write(11,1015)mas(i),gid(i),gis(i),efx(i),
*    abu(i),gabu(i),x1,0.,ab0(i),sab0(i)/ab0(i)*100.
    If(gpr.EQ.'Y')Write(12,1016)egam,mas(i),gid(i),gis(i),efx(i),
*    abu(i),gabu(i),x1,ab0(i),sab0(i),gfit
   Endif
   m=m+1
  Endif

  If(hfix(2*i-1).EQ.'N'.AND.hfix(2*i).EQ.'Y')Then
   x1=dlog(2.d0)/frm(2*i-1)
   x2=dlog(2.d0)*wel(m,m)**.5/frm(2*i-1)**2.
   ab0(i)=frm(2*i)/abu(i)*100.
   If(x1.GT.999.)Then
    If(gpr.EQ.'N')Write(*,1011)egam,mas(i),gid(i),gis(i),efx(i),
*    abu(i),gabu(i),x1,ab0(i),0.,gfit
    If(gpr.EQ.'Y')Write(11,1012)mas(i),gid(i),gis(i),efx(i),
*    abu(i),gabu(i),x1,x2,ab0(i),0.
    If(gpr.EQ.'Y')Write(12,1013)egam,mas(i),gid(i),gis(i),efx(i),
*    abu(i),gabu(i),x1,ab0(i),0.,gfit
   Else
    If(gpr.EQ.'N')Write(*,1014)egam,mas(i),gid(i),gis(i),efx(i),
*    abu(i),gabu(i),x1,ab0(i),0.,gfit
    If(gpr.EQ.'Y')Write(11,1015)mas(i),gid(i),gis(i),efx(i),
*    abu(i),gabu(i),x1,x2,ab0(i),0.
    If(gpr.EQ.'Y')Write(12,1016)egam,mas(i),gid(i),gis(i),efx(i),
*    abu(i),gabu(i),x1,ab0(i),0.,gfit
   Endif
   m=m+1
  Endif

  If(hfix(2*i-1).EQ.'Y'.AND.hfix(2*i).EQ.'Y')Then
   x1=dlog(2.d0)/frm(2*i-1)
   x2=dlog(2.d0)*wel(m,m)**.5/frm(2*i-1)**2.
   ab0(i)=frm(2*i)/abu(i)*100.
   If(x1.GT.999.)Then
    If(gpr.EQ.'N')Write(*,1011)egam,mas(i),gid(i),gis(i),efx(i),
*    abu(i),gabu(i),x1,ab0(i),0.,gfit
    If(gpr.EQ.'Y')Write(11,1012)mas(i),gid(i),gis(i),efx(i),
*    abu(i),gabu(i),x1,0.,ab0(i),0.
    If(gpr.EQ.'Y')Write(12,1013)egam,mas(i),gid(i),gis(i),efx(i),
*    abu(i),gabu(i),x1,ab0(i),0.,gfit
   Else
```

```
          If(gpr.EQ.'N')Write(*,1014)egam,mas(i),gid(i),gis(i),efx(i),
     *    abu(i),gabu(i),x1,ab0(i),0.,gfit
          If(gpr.EQ.'Y')Write(11,1015)mas(i),gid(i),gis(i),efx(i),
     *    abu(i),gabu(i),x1,0.,ab0(i),0.
          If(gpr.EQ.'Y')Write(12,1016)egam,mas(i),gid(i),gis(i),efx(i),
     *    abu(i),gabu(i),x1,ab0(i),0.,gfit
        Endif
      Endif
  119 Continue
      If(gpr.EQ.'Y')Return

! Format statements
 1010 Format('  Abundance of gamma can not be zero! It is set to 100%')
 1011 Format(1X,F7.1,I4,A2,1X,A2,F6.1,'keV , ',F6.2,A1,', HL=',E10.4,
     1 ', A0=',E11.5,'+/-',F5.1,'%',1X,A1)
 1012 Format(I4,A2,1X,A2,F7.1,'keV,',F6.2,A1,',HL=',1PE10.4,'+/-',
     1 1PE9.3,',A= ',1PE10.4,'+/-',0PF6.2,'%')
 1013 Format(F7.1,I4,A2,1X,A2,F7.1,'keV,',F6.2,A1,',HL=',E10.4,
     1',A0=',E11.5,'+/-',E11.5,1X,A1)
 1014 Format(1X,F7.1,I4,A2,1X,A2,F6.1,'keV , ',F6.2,A1,', HL=',F10.4,
     1', A0=',E11.5,'+/-',F5.1,'%',1X,A1)
 1015 Format(I4,A2,1X,A2,F7.1,'keV,',F6.2,A1,',HL=',F10.4,'+/-',F9.4,
     1',A= ',1PE10.4,'+/-',0PF6.2,'%')
 1016 Format(1X,F6.1,I4,A2,1X,A2,F7.1,'keV,',F6.2,A1,',HL=',F10.4,
     1',A0=',E11.5,'+/-',E11.5,1X,A1)

! Prompt if results are to be saved, if yes flag for printing
      Write(*,1017)
 1017 Format('  Do you like to save this(these)',
     * ' result(s)? (Y/N): N; ',$)
      Read(*,'(A1)')gsave
      If(gsave.EQ.'Y'.OR.gsave.EQ.'y'.AND.ika.NE.1)Then
        Write(11,'(1X,78A1)')(gline(i),i=1,78)
        Write(11,1018)egam,idt,gfit,chir
 1018   Format(1X,F6.1,' keV: No data points=',I2,', ',A1,' fit, ',
     *  'Reduced CHI Squared= ',F9.5)
        gpr='Y'
        Go To 118
      Endif

      Return
      End
      Subroutine deriv

! This subroutine is used to take the derivatives of the decay curve functions
```

```
! for all but the growth and decay derivatives.

      Implicit Integer*2 (i-n)
      Implicit Real*8 (a-f,r-z)

      Common /work1/vel,zel,tct,adta,bdta,cdta,ddta,icm,icn,idt,ird,
     * frm,ipr

      Dimension vel(10,10),zel(10),tct(100),
     * adta(100),bdta(100),cdta(100),ddta(100),frm(10),ipr(10)
      Dimension ed(10)

! First clear out the old matrix
      Do 110 j=1,ird
      Do 100 k=1,ird
  100 vel(j,k)=0.
  110 zel(j)=0.

      Do 160 i=1,idt
      Do 120 j=1,2*icm
  120 ed(j)=0.
      tct(i)=0.

! Now take the derivatives
      Do 130 j=1,icm
        texp=dexp(-frm(2*j-1)*cdta(i))
        ed(2*j-1)=-cdta(i)*frm(2*j)*texp
        ed(2*j)=texp
  130 tct(i)=frm(2*j)*texp+tct(i)

! Now build the matrix
      Do 150 j=1,ird
        zel(j)=zel(j)+ed(ipr(j))*(adta(i)-tct(i))/bdta(i)**2.
        Do 140 k=1,ird
  140   vel(j,k)=vel(j,k)+ed(ipr(j))*ed(ipr(k))/bdta(i)**2.
  150 Continue

  160 Continue

      Return
      End
      Subroutine gamlist

      Implicit Integer*2 (i-n)
      Implicit Character (g-h)
```

```
      Implicit Real*8 (a-f,r-z)

      Common /data/thlmin,thlmax,abumin,dgam,chilim,iamin,iamax
      Common /work/mass,enl,aie,the,gaie,ga,giso,gd,xths,xa0f,xa0s,
     * egam,iin,ier
      Common /gd/mad(150),gad,gid,mam(150),gam,gim,abum(150),
     * xhlm(150),xhld(150),jn

      Dimension mass(200),enl(200),aie(200),the(200),xths(200),
     * xa0f(200),xa0s(200)

      Character*1 gd(200),gaie(200)
      Character*2 gad(150),gid(150),gam(150),gim(150),ga(200),giso(200)

      If(ier.EQ.1)Go To 106
  102 i=1

c  103 Read(3,Rec=i,err=104)eny
   103 Read(3,*)eny
  6969 format(f6.1)
      i=i+1
      If(eny.LT.egam-dgam)Go To 103

   104 ilow=i-1
      Do 105 i=10,150
c      Do 105 i=101,200
c      Read(3,Rec=ilow+i-101,err=106)enl(i),aie(i),gaie(i),the(i),
c     * mass(i),ga(i),giso(i),gd(i)
       Read(3,*)enl(i),aie(i),the(i),mass(i),ga(i)
       giso(i)='  '
       gd(i)=' '
  6970 format(f6.1,f8.2,f15.4,i6,a2,a3,a2)
      write(*,6970)enl(i),aie(i),the(i),mass(i),ga(i),giso(i),gd(i)
   105 Continue

      ier=1
   106 If(enl(150).LE.egam+dgam)Then
c  106 If(enl(200).LE.egam+dgam)Then
        i=ilow
        Go to 103
      Endif

      iin=0
          Do 108 i=10,150
c      Do 108 i=101,200
```

```
      If(enl(i).GE.egam-dgam.AND.enl(i).LE.egam+dgam)Then
       If(the(i).GE.thlmin.AND.the(i).LE.thlmax)Then
        If(mass(i).GE.iamin.AND.mass(i).LE.iamax)Then
         If(aie(i).GE.abumin)Then
          iin=iin+1
          mass(iin)=mass(i)
          ga(iin)=ga(i)
          giso(iin)=giso(i)
          gd(iin)=gd(i)
          enl(iin)=enl(i)
          aie(iin)=aie(i)
c           gaie(iin)=gaie(i)
          the(iin)=the(i)
          xths(iin)=0.
          xa0f(iin)=0.
          xa0s(iin)=0.

          If(gd(i).EQ.'*'.OR.gd(i).EQ.'#')Then
           Do 107 j=1,jn
           If(mass(i).EQ.mad(j).AND.ga(i).EQ.gad(j).AND.
     *      giso(i).EQ.gid(j))Then
            iin=iin+1
            mass(iin)=mam(j)
            ga(iin)=gam(j)
            giso(iin)=gim(j)
            gd(iin)='M'
            enl(iin)=enl(i)
            aie(iin)=abum(j)
            gaie(iin)='%'
            the(iin)=xhlm(j)
            xths(iin)=0.
            xa0f(iin)=0.
            xa0s(iin)=0.
           Endif
  107       Continue
          Endif
         Endif
        Endif
       Endif
      Endif
  108 Continue

      If(iin.EQ.0.AND.ini.EQ.0)Then
       ini=1
       Go To 102
```

```
      Endif
      ini=0

      iin=iin+1
      mass(iin)=0.
      ga(iin)='BG'
      giso(iin)='  '
      gd(iin)=' '
      enl(iin)=0.
      aie(iin)=100.
      gaie(iin)=' '
      the(iin)=0.
      xths(iin)=1000000.
      xa0f(iin)=0.
      xa0s(iin)=0.

      Return
      End
      Subroutine gderiv

! This subroutine is to take the derivatives for the growth and decay cases .

      Implicit Integer*2 (i-n)
      Implicit Real*8 (a-f,r-z)

      Common /work1/vel,zel,tct,adta,bdta,cdta,ddta,icm,icn,idt,ird,
     * frm,ipr

      Dimension vel(10,10),zel(10),tct(100),
     * adta(100),bdta(100),cdta(100),ddta(100),frm(10),ipr(10)
      Dimension ed(10)

! First clear out the old matrix
      Do 110 j=1,ird
      Do 100 k=1,ird
  100 vel(j,k)=0.
  110 zel(j)=0.

      Do 180 i=1,idt
      Do 120 j=1,2*icm
  120 ed(j)=0.
      tct(i)=0.

! Now take the derivatives
      j=1
```

```
  130 texp1=dexp(-frm(4*j-1)*cdta(i))
      texp3=dexp(-frm(4*j-3)*cdta(i))
      e1me2=texp3-texp1
      el2ml1=frm(4*j-1)-frm(4*j-3)
      ed(4*j-3)=frm(4*j-2)*frm(4*j-1)/el2ml1*(e1me2
     * /el2ml1-cdta(i)*texp3)
      ed(4*j-2)=frm(4*j-1)/el2ml1*e1me2
      ed(4*j-1)=frm(4*j-2)*frm(4*j-1)/el2ml1*(e1me2/frm(4*j-1)
     * -e1me2/el2ml1+cdta(i)*texp1)-frm(4*j)*cdta(i)*texp1
      ed(4*j)=texp1
      tct(i)=tct(i)+frm(4*j-1)/el2ml1*e1me2*frm(4*j-2)
     * +frm(4*j)*texp1

! If two G&D's then do it again
      If((icn.GT.9).AND.(j.EQ.1))Then
        j=2
        Go To 130
      Endif
      If(icn.EQ.10)Go To 150
      If(icn.EQ.6)Go To 150

! If any independent components, get their derivatives too
      j=3
      If(icn.EQ.11)j=5
      Do 140 l=j,icm
        texp=dexp(-frm(2*l-1)*cdta(i))
        ed(2*l-1)=-cdta(i)*frm(2*l)*texp
        ed(2*l)=texp
  140   tct(i)=tct(i)+frm(2*l)*texp
  150 Continue

! Build the matrix
      Do 170 j=1,ird
        zel(j)=zel(j)+ed(ipr(j))*(adta(i)-tct(i))/bdta(i)**2.
        Do 160 k=1,ird
  160   vel(j,k)=vel(j,k)+ed(ipr(j))*ed(ipr(k))/bdta(i)**2.
  170 Continue
  180 Continue

      Return
      End
      Subroutine graph(chi)

! This is a semi-log plotter routine
```

```
      Implicit Integer*2 (i-n)
      Implicit Character (g-h)
      Implicit Real*8 (a-f,r-z)

      Common /work1/vel,zel,tct,adta,bdta,cdta,ddta,icm,icn,idt,ird,
     * frm,ipr

      Dimension vel(10,10),zel(10),tct(100),
     * adta(100),bdta(100),cdta(100),ddta(100),frm(10),ipr(10)
      Dimension ea(100),sil(100),sih(100)

      Character*1 char,gr(125),grm(80,20)

! Take logs
      Do 102 i=1,idt
      If(tct(i).LE.0.)Then
        tct(i)=-1.
        Go To 100
      Endif
      tct(i)=dlog10(tct(i))
  100 If(adta(i)+bdta(i).LE.0.)Then
        ea(i)=-1.
        sil(i)=-1.
        sih(i)=-1.
        Go To 102
      Endif
      sih(i)=dlog10(adta(i)+bdta(i))
      If(adta(i).LE.0.)Then
        ea(i)=-1.
        sil(i)=-1.
        Go To 102
      Endif
      If(adta(i)-bdta(i).LE.0.)Then
        sil(i)=-1.
        Go To 101
      Endif
      sil(i)=dlog10(adta(i)-bdta(i))
  101 ea(i)=dlog10(adta(i))
  102 Continue

! Find extrema XMAX,XMIN,YMAY,YMIN
      xmax=cdta(1)
      xmin=cdta(1)
      ymax=ea(1)
      ymin=ea(1)
```

```
      Do 104 i=1,idt
        If(cdta(i).GT.xmax)xmax=cdta(i)
        If(cdta(i).LT.xmin)xmin=cdta(i)
        If(sih(i).GT.ymax)ymax=sih(i)
        If(tct(i).GT.ymax)ymax=tct(i)
        If(sil(i).EQ.-1.)Go To 103
        If(sil(i).LT.ymin)ymin=sil(i)
  103   If(tct(i).EQ.-1)Go To 104
        If(tct(i).LT.ymin)ymin=tct(i)
  104 Continue

! Make the plot line by line

! Reset arrays
      Do 106 i=1,78
      Do 105 j=1,20
      grm(i,j)=' '
  105 Continue
  106 Continue

! Make frame
      Do 107 i=1,78
      grm(i,1)=char(18)
  107 grm(i,20)=char(18)
      Do 108 j=1,20
      grm(1,j)=char(25)
  108 grm(78,j)=char(25)
      grm(1,1)=char(24)
      grm(1,20)=char(23)
      grm(78,1)=char(24)
      grm(78,20)=char(23)

! Make info display
      grm(62,2)='*'
      grm(64,2)='='
      grm(66,2)='C'
      grm(67,2)='a'
      grm(68,2)='l'
      grm(69,2)='c'
      grm(70,2)='.'
      grm(72,2)='D'
      grm(73,2)='a'
      grm(74,2)='t'
      grm(75,2)='a'
```

```
      grm(62,3)='+'
      grm(64,3)='='
      grm(66,3)='A'
      grm(67,3)='c'
      grm(68,3)='t'
      grm(69,3)='u'
      grm(70,3)='a'
      grm(71,3)='l'
      grm(73,3)='D'
      grm(74,3)='a'
      grm(75,3)='t'
      grm(76,3)='a'

      grm(62,4)='-'
      grm(64,4)='='
      grm(66,4)='E'
      grm(67,4)='r'
      grm(68,4)='r'
      grm(69,4)='o'
      grm(70,4)='r'
      grm(72,4)='L'
      grm(73,4)='i'
      grm(74,4)='m'
      grm(75,4)='i'
      grm(76,4)='t'

      scx=(xmax-xmin)/73.
      scy=(ymax-ymin)/17.

      Do 112 i=1,75
      Do 109 iw=1,20
  109 gr(iw)=' '
      Do 111 j=1,idt
      If((cdta(j).GE.xmin+scx*dble(i-1)).AND.(cdta(j).LT.xmin+
     * scx*dble(i)))Then
        If(sih(j).NE.-1.)gr(int((sih(j)-ymin)/scy+1.))=char(24)
        If(sil(j).NE.-1.)gr(int((sil(j)-ymin)/scy+1.))=char(23)
        If(ea(j) .NE.-1.)gr(int((ea(j) -ymin)/scy+1.))='+'
        If(tct(j).NE.-1.)gr(int((tct(j)-ymin)/scy+1.))='*'
      Endif
      Do 110 ii=1,18
  110 grm(i+2,20-ii)=gr(ii)
  111 Continue
  112 Continue
```

```
      Write(*,1000)ymin,ymax,xmin,xmax,chi
 1000 Format('  LogYMIN=',F4.2,' / LogYMAX=',F4.2,' / XMIN=',F6.2,
     1' / XMAX=',F6.2,'   CHI Sqrd=',F8.4)

      Do 113 j=1,20
      Write(*,1001)(grm(i,j),i=1,78)
 1001 Format(1X,78A1)
  113 Continue

      Return
      End

      Subroutine hlinit

      Implicit Integer*2 (i-n)
      implicit Character (g-h)
      implicit Real*8 (a-f,r-z)

      Common /data/thlmin,thlmax,abumin,dgam,chilim,iamin,iamax
      Common /gd/mad(150),gad,gid,mam(150),gam,gim,abum(150),
     * xhlm(150),xhld(150),jn

      Character*78 glabel(2)
      Character*2 gad(150),gid(150),gam(150),gim(150)
      Character*1 gnswer

      Logical finns

      Call clrscr

! Check if all necessary files are present
      Inquire(File='NewGS2.OUT',Exist=finns)
      If(.NOT.finns)Then
        Write(*,1000)
 1000   Format(/15X,'NewGS2.OUT file could not be found'/)
        Stop ' End-of-Job'
      Endif

c      Inquire(File='degamlib.dat',Exist=finns)
       Inquire(File='denuclib1-a-q.csv',Exist=finns)
```

```
      If(.NOT.finns)Then
        Write(*,1001)
c 1001   Format(/15X,'degamlib.dat file could not be found'/)
 1001   Format(/15X,'denuclib1-a-q.csv file could not be found'/)
        Stop ' End-of-Job'
      Endif

      Inquire(File='degd.dat',Exist=finns)
      If(.NOT.finns)Then
        Write(*,1002)
 1002   Format(/15X,'degd.dat file could not be found'/)
        Stop ' End-of-Job'
      Endif

      Open(1,File='NewGS2.OUT',Status='OLD')
c      Open(3,File='degamlib.dat',Status='OLD',
      Open(3,File='denuclib1-a-q.csv',Status='OLD')
c     * Access='DIRECT',Recl=32)
      Open(4,File='degd.dat',Status='OLD')

      Write(*,1003)
 1003 Format(///
     * 15X,'DDDDDD    EEEEEEEE  HH    HH  LL'/
     * 15X,'DD    DD  EE        HH    HH  LL'/
     * 15X,'DD    DD  EE        HH    HH  LL'/
     * 15X,'DD    DD  EEEEEE    HHHHHHHH  LL'/
     * 15X,'DD    DD  EE        HH    HH  LL'/
     * 15X,'DD    DD  EE        HH    HH  LL'/
     * 15X,'DDDDDD    EEEEEEEE  HH    HH  LLLLLLLL'//
     * 15X,'Version 1.00B  07-OCT-1992'/)

      Write(*,1004)
 1004 Format(15X,'Welcome to DEHL, an error weighted least',/,
     * 15X,'squares decay curve fitting program.')

      i=1
  100 Read(4,1005,End=101)mad(i),gad(i),gid(i),xhld(i),mam(i),gam(i),
     1 gim(i),abum(i),xhlm(i)
 1005 Format(I4,A2,1X,A2,F8.3,I4,A2,1X,A2,F8.2,F8.3)
      i=i+1
      Go To 100
  101 jn=i-1

      Write(*,1006)
 1006 Format(/15X,'Hit any key to continue...',$)
```

```
      Read(*,'(A1)')gnswer

! Check if .dehlrc is present, if not create it
      Inquire(File='.dehlrc',Exist=finns)

! Read .dehlrc
      If(finns)Then
        Open(99,File='.dehlrc',Status='OLD')
        Read(99,1007)thlmin,thlmax,iamin,iamax,abumin,dgam,chilim
 1007   Format(F7.1/F7.1,2(/4X,I3)/F7.0,2(/F6.2))
        Go To 103
      Else
        Open(99,File='.dehlrc',Status='NEW')
        thlmin=0.
        thlmax=1.E+15
        iamin=5
        iamax=230
        abumin=1.
        dgam=1.5
        chilim=4.
      Endif

  102 Call clrscr
      Write(*,1008)
 1008 Format(///5X,'Please give new parameters or ENTER for no change:')

      arem=thlmin
      Write(*,1009)arem
 1009 Format(//25X,'MIN value of half-life: ',F5.1,'; ',$)
      Read(*,1)thlmin
    1 Format(F7.0)

      arem=thlmax
      Write(*,1010)arem
 1010 Format(25X,'MAX value of half-life: ',1PE7.1,'; ',$)
      Read(*,1)thlmax
      If(thlmax.EQ.0.)thlmax=arem

      irem=iamin
      Write(*,1011)irem
 1011 Format(32X,'MIN mass-number:   ',I3,'; ',$)
      Read(*,'(I3)')iamin
      If(iamin.EQ.0)iamin=irem

      irem=iamax
```

```
      Write(*,1012)irem
 1012 Format(32X,'MAX mass-number:   ',I3,'; ',$)
      Read(*,'(I3)')iamax
      If(iamax.EQ.0)iamax=irem

      arem=abumin
      Write(*,1013)arem
 1013 Format(8X,'MIN value of abundance in ID-search (%): ',F5.1,'; ',$)
      Read(*,1)abumin
      If(abumin.EQ.0.)abumin=arem

      arem=dgam
      Write(*,1014)arem
 1014 Format(10X,'Deviation of gamma in ID-search (keV): ',F5.1,'; ',$)
      Read(*,1)dgam
      If(dgam.EQ.0.)dgam=arem

      arem=chilim
      Write(*,1015)arem
 1015 Format(7X,'Red CHI sqrd limit for more than 1 comp: ',F5.1,'; ',$)
      Read(*,1)chilim
      If(chilim.EQ.0.)chilim=arem

  103 Call clrscr

      Write(*,1016)thlmin,thlmax,iamin,iamax,abumin,dgam,chilim
 1016 Format(//////
     * 25X,'MIN value of half-life: ',F5.1/
     * 25X,'MAX value of half-life: ',E7.1/
     * 19X,'MIN mass-number in ID-search:   ',I3/
     * 19X,'MAX mass-number in ID-search:   ',I3/
     * 25X,'MIN value of abundance: ',F5.1/
     * 16X,'Deviation of gamma in ID-search: ',F5.1,' keV'/
     * 22X,'Reduced CHI squared limit: ',F5.1//
     * 23X,'Are these data OK? (Y/N): Y; ',$)
      Read(*,2)gnswer
    2 Format(A1)
      If(gnswer.EQ.'N'.OR.gnswer.EQ.'n')Go To 102

! Save parameters
      Rewind(99)
      Write(99,1017)thlmin,thlmax,iamin,iamax,abumin,dgam,chilim
 1017 Format(F7.1,' ;MIN value of half-life.'/
     * E7.1,' ;MAX value of half-life.'/
     * 4X,I3,' ;MIN mass-number in ID-search.'/
```

```
     * 4X,I3,' ;MAX mass-number in ID-search.'/
     * F7.0,' ;MIN value of abundance.'/
     * F7.2,' ;Deviation of gamma in ID-search (keV).'/
     * F7.2,' ;Reduced CHI squared limit for more than 1 comp.')
      Close(99)

      Call clrscr

! Read headings
      Read(1,3)glabel
    3 Format(A30)
      write(*,3)glabel
          WRITE(*,*)'****************************************'
! Check if defit.res is present
      Inquire(File='defit.res',Exist=finns)
      If(finns)Then
        Open(11,File='defit.res',Status='OLD')
        Write(*,1018)
 1018   Format(//22X,'The file defit.res already exist.'/8X,'Do you',
     *  ' like to (D)elete it or (C)ontinue on the same file? : C; ',$)
        Read(*,2)gnswer
        If(gnswer.NE.'D'.AND.gnswer.NE.'d')Then
          Call Set_End_File(11)
        Else
          Write(11,3)glabel
        Endif
      Else
        Open(11,File='defit.res',Status='NEW')
        Write(11,3)glabel
      Endif

! Check if desort.dat is present
      Inquire(File='desort.dat',Exist=finns)
      If(finns)Then
        Open(12,File='desort.dat',Status='OLD')
        Write(*,1019)
 1019   Format(//22X,'The file desort.dat already exist.'/8X,'Do you',
     *  ' like to (D)elete it or (C)ontinue on the same file? : C; ',$)
        Read(*,2)gnswer
        If(gnswer.NE.'D'.AND.gnswer.NE.'d')Then
          Call Set_End_File(12)
        Else
          Write(12,3)glabel
        Endif
      Else
```

```
      Open(12,File='desort.dat',Status='NEW')
      Write(12,3)glabel
    Endif



    Return
    End

    Subroutine Set_End_File(iunit)
    Character*1 gline
  1 Read(iunit,'(A1)',End=2)gline
    Go To 1
  2 Backspace(iunit)
    Return
    End

    Subroutine matrix(vel,wel,zel,iord)

! This is the matrix diagonalization and inversion routine. Solution and
! inversion is done by Gauss-Jordan elimination below the diagonal, reflecting
! through the center, repeating the Gauss-Jordan elimination and re-reflecting.

!   vel(i,j) are the elements of the matrix
!   wel(i,j) are the elements of the inverse matrix
!   zel(i)   are the elements of the vector
!   iord is the order of the matrix

    Implicit Character (g-h)
    Implicit Integer*2 (i-n)
    Implicit Real*8 (a-f,r-z)

    Dimension vel(10,10),wel(10,10),zel(10),usum(10)

! Scale the matrix, the inverse, and the vector to prevent overflow and
! underflow and to enhance accuracy
    Do 30 iz1=1,iord
    usum(iz1)=0.
    Do 10 iz2=1,iord
    usum(iz1)=usum(iz1)+vel(iz1,iz2)
 10 wel(iz1,iz2)=0.
    Do 20 iz2=1,iord
 20 vel(iz1,iz2)=vel(iz1,iz2)*dble(iord)/usum(iz1)
    zel(iz1)=zel(iz1)*dble(iord)/usum(iz1)
 30 wel(iz1,iz1)=dble(iord)/usum(iz1)
```

```
      iz4=1

! Check for zeroes on the diagonal
   40 Do 120 iz1=1,iord
        If(vel(iz1,iz1).EQ.0.)Then
          If(iz4.EQ.2)Go To 180
          Do 60 iz5=iz1+1,iord
          Do 50 iz6=1,iord
          vel(iz1,iz6)=vel(iz1,iz6)+vel(iz5,iz6)
   50     wel(iz1,iz6)=wel(iz1,iz6)+wel(iz5,iz6)
          zel(iz1)=zel(iz1)+zel(iz5)
   60     If(vel(iz1,iz1).NE.0.)Go To 70
          Go to 180
   70   Endif

! Gauss-Jordan elimination
   80   ebug=vel(iz1,iz1)
        Do 90 iz2=1,iord
        vel(iz1,iz2)=vel(iz1,iz2)/ebug
   90   wel(iz1,iz2)=wel(iz1,iz2)/ebug
        zel(iz1)=zel(iz1)/ebug
        If(iz1.EQ.iord)Go To 130
        Do 110 iz2=iz1+1,iord
        If(vel(iz2,iz1).EQ.0.)Go To 110
        ebug=-vel(iz2,iz1)/vel(iz1,iz1)
        Do 100 iz3=1,iord
        vel(iz2,iz3)=vel(iz2,iz3)+ebug*vel(iz1,iz3)
  100   wel(iz2,iz3)=wel(iz2,iz3)+ebug*wel(iz1,iz3)
  110   zel(iz2)=zel(iz2)+ebug*zel(iz1)
  120   Continue

! Reflect through the center
  130   If(iord/2.EQ.(iord+1)/2)Then
          iz1=int(iord/2)
        Else
          iz1=int((iord-1)/2)
        Endif
        Do 150 iz2=1,iz1
        Do 140 iz3=1,iord
        store=vel(iz2,iz3)
        vel(iz2,iz3)=vel(iord+1-iz2,iz3)
        vel(iord+1-iz2,iz3)=store
        store=wel(iz2,iz3)
        wel(iz2,iz3)=wel(iord+1-iz2,iz3)
  140   wel(iord+1-iz2,iz3)=store
```

```
      store=zel(iz2)
      zel(iz2)=zel(iord+1-iz2)
  150 zel(iord+1-iz2)=store
      Do 170 iz2=1,iz1
      Do 160 iz3=1,iord
      store=vel(iz3,iz2)
      vel(iz3,iz2)=vel(iz3,iord+1-iz2)
      vel(iz3,iord+1-iz2)=store
      store=wel(iz3,iz2)
      wel(iz3,iz2)=wel(iz3,iord+1-iz2)
  160 wel(iz3,iord+1-iz2)=store
  170 Continue
      iz4=iz4+1
      If(iz4.EQ.2)Go To 40
      Return

! If all else fails, give up
  180 Stop ' Matrix wont solve...'
      End
```

Sample input file for analysis-rev-oo.for

The first column contains the average peak energy from the various runs in keV. The second column contains first, the number of points at that particular energy, and second, the activities of each point in γps. The third column is the error in the activities and the fourth column are the time points of each sample in days relative to end of bombardment.

Pb sample

```
 338.1770          13
 338.1770     2.50176     0.21544     0.03333
 338.1770     2.95602     0.17738     0.16806
 338.1770     2.87689     0.19043     0.30278
 338.1770     3.18800     0.14935     0.39444
 338.1770     3.06862     0.14236     0.51042
 338.1770     3.09835     0.12408     0.62639
 338.1770     3.47554     0.14452     0.74236
 338.1770     3.13488     0.14613     0.85833
 338.1770     3.49336     0.14799     0.99514
```

338.1770	3.21434	0.10692	1.15278
338.1770	3.16671	0.11996	1.31042
338.1770	2.87038	0.09943	1.46806
338.1770	3.54708	0.13497	1.62569
374.6191	15		
374.6191	154.0683	0.60506	0.03333
374.6191	89.17410	0.36657	0.10069
374.6191	62.62191	0.30792	0.16806
374.6191	48.40187	0.27468	0.23542
374.6191	42.71033	0.26099	0.30278
374.6191	35.91476	0.18655	0.39444
374.6191	29.92546	0.17129	0.51042
374.6191	25.05410	0.15942	0.62639
374.6191	21.63012	0.16959	0.74236
374.6191	17.74342	0.14076	0.85833
374.6191	14.70776	0.30104	0.99514
374.6191	11.62781	0.10421	1.15278
374.6191	8.85484	0.09799	1.31042
374.6191	7.09926	0.09010	1.46806
374.6191	5.57210	0.08512	1.62569
441.9420	11		
441.9420	3.22856	0.21807	0.03333
441.9420	3.12197	0.18749	0.10069
441.9420	2.30789	0.17988	0.16806
441.9420	1.77497	0.16790	0.23542
441.9420	1.91929	0.16130	0.30278
441.9420	1.92919	0.13487	0.39444
441.9420	1.71743	0.11912	0.51042
441.9420	1.23253	0.12666	0.74236
441.9420	0.84161	0.08935	0.99514
441.9420	0.98494	0.14203	1.31042
441.9420	0.71411	0.07549	1.62569
515.8436	15		
515.8436	24.73998	0.32537	0.03333
515.8436	24.43145	0.29404	0.10069
515.8436	24.28720	0.27114	0.16806
515.8436	22.41433	0.25426	0.23542
515.8436	23.25464	0.24462	0.30278
515.8436	24.87313	0.18324	0.39444
515.8436	23.90817	0.19862	0.51042
515.8436	24.15236	0.19027	0.62639
515.8436	22.88415	0.21885	0.74236
515.8436	25.46755	0.17556	0.85833
515.8436	25.73842	0.14993	0.99514
515.8436	24.52354	0.14534	1.15278

515.8436	24.65684	0.14381	1.31042
515.8436	24.31179	0.14485	1.46806
515.8436	23.84003	0.14434	1.62569
674.0704	6		
674.0704	4.84860	0.18307	0.16806
674.0704	3.63783	0.16619	0.23542
674.0704	3.49939	0.16054	0.30278
674.0704	3.06117	0.11727	0.39444
674.0704	3.41684	0.11645	0.51042
674.0704	1.97741	0.10176	0.85833
802.8085	15		
802.8085	62.58968	0.41394	0.03333
802.8085	64.60686	0.55552	0.10069
802.8085	64.12534	0.37394	0.16806
802.8085	64.85789	0.36932	0.23542
802.8085	65.44346	0.41241	0.30278
802.8085	64.76823	0.27676	0.39444
802.8085	63.13363	0.32127	0.51042
802.8085	61.14476	0.26877	0.62639
802.8085	60.45771	0.26431	0.74236
802.8085	60.10896	0.26252	0.85833
802.8085	59.64418	0.22485	0.99514
802.8085	57.62016	0.38564	1.15278
802.8085	56.66501	0.66213	1.31042
802.8085	57.29828	0.21766	1.46806
802.8085	56.90846	0.24382	1.62569
807.4398	11		
807.4398	3.53183	0.20213	0.10069
807.4398	4.05803	0.19287	0.30278
807.4398	3.33907	0.12760	0.39444
807.4398	3.16243	0.12760	0.51042
807.4398	1.92781	0.12317	0.62639
807.4398	2.16398	0.11690	0.85833
807.4398	2.40245	0.10685	0.99514
807.4398	2.27320	0.10422	1.15278
807.4398	2.11314	0.09569	1.31042
807.4398	2.35629	0.09373	1.46806
807.4398	3.17872	0.09766	1.62569
880.8128	15		
880.8128	46.78455	0.41600	0.03333
880.8128	47.83079	0.43047	0.10069
880.8128	49.77894	0.33731	0.16806
880.8128	49.58912	0.32285	0.23542
880.8128	47.09239	0.51722	0.30278
880.8128	48.91855	0.23780	0.39444

880.8128	47.32731	0.36507	0.51042
880.8128	46.80014	0.33071	0.62639
880.8128	47.43822	0.23130	0.74236
880.8128	46.48447	0.22943	0.85833
880.8128	46.47150	0.19581	0.99514
880.8128	44.04799	0.32613	1.15278
880.8128	43.36901	0.28382	1.31042
880.8128	42.90414	0.38891	1.46806
880.8128	41.77921	0.32478	1.62569
898.7786	15		
898.7786	177.82661	0.59642	0.03333
898.7786	104.84813	0.82011	0.10069
898.7786	80.90712	0.40518	0.16806
898.7786	66.47706	0.37276	0.23542
898.7786	55.17466	0.57050	0.30278
898.7786	48.82794	0.42553	0.39444
898.7786	40.69047	0.46116	0.51042
898.7786	35.64703	0.38149	0.62639
898.7786	32.03242	0.20057	0.74236
898.7786	27.28187	0.18744	0.85833
898.7786	21.19026	0.61612	0.99514
898.7786	17.01724	0.55485	1.15278
898.7786	13.38910	0.52113	1.31042
898.7786	13.84557	0.12252	1.46806
898.7786	9.62300	0.78132	1.62569
983.6456	15		
983.6456	43.01224	0.33006	0.03333
983.6456	42.22937	0.31154	0.10069
983.6456	38.69523	0.36543	0.16806
983.6456	35.39601	0.36543	0.23542
983.6456	33.91395	0.31827	0.30278
983.6456	30.00445	0.19867	0.39444
983.6456	26.42405	0.20549	0.51042
983.6456	23.05707	0.20549	0.62639
983.6456	20.43934	0.18211	0.74236
983.6456	18.66687	0.16165	0.85833
983.6456	16.20301	0.14377	0.99514
983.6456	13.81245	0.13447	1.15278
983.6456	12.18222	0.12803	1.31042
983.6456	10.95205	0.11802	1.46806
983.6456	10.18604	0.11373	1.62569
992.0335	15		
992.0335	39.17537	0.31767	0.03333
992.0335	35.05794	0.28895	0.10069
992.0335	29.14316	0.37346	0.16806

992.0335	24.68485	0.28220	0.23542
992.0335	21.20180	0.22981	0.30278
992.0335	16.13300	0.15636	0.39444
992.0335	12.02135	0.17298	0.51042
992.0335	8.97624	0.13682	0.62639
992.0335	6.65109	0.11434	0.74236
992.0335	4.97891	0.10554	0.85833
992.0335	3.60743	0.08326	0.99514
992.0335	2.31033	0.07392	1.15278
992.0335	1.66959	0.11700	1.31042
992.0335	1.31922	0.06747	1.46806
992.0335	1.14049	0.06460	1.62569
1181.2328	15		
1181.2328	45.60668	0.32843	0.03333
1181.2328	40.71835	0.30317	0.10069
1181.2328	35.44228	0.28513	0.16806
1181.2328	31.07289	0.26708	0.23542
1181.2328	27.81214	0.25445	0.30278
1181.2328	23.07014	0.17846	0.39444
1181.2328	18.13614	0.16072	0.51042
1181.2328	14.33973	0.14611	0.62639
1181.2328	11.26913	0.13254	0.74236
1181.2328	9.07619	0.12314	0.85833
1181.2328	6.64726	0.09275	0.99514
1181.2328	4.74021	0.08355	1.15278
1181.2328	3.28386	0.07589	1.31042
1181.2328	2.30424	0.06899	1.46806
1181.2328	1.76541	0.06439	1.62569
1436.4781	9		
1436.4781	25.78126	0.48351	0.10069
1436.4781	11.34601	0.26096	0.16806
1436.4781	8.29147	0.20916	0.23542
1436.4781	7.96113	0.15542	0.30278
1436.4781	6.68243	0.10875	0.39444
1436.4781	5.44396	0.09876	0.51042
1436.4781	4.35655	0.09321	0.62639
1436.4781	2.68336	0.10654	0.74236
1436.4781	2.78063	0.07989	0.85833
1483.2464	14		
1483.2464	17.70641	0.21293	0.03333
1483.2464	16.24312	0.20132	0.10069
1483.2464	14.40427	0.18777	0.16806
1483.2464	11.91685	0.44524	0.23542
1483.2464	11.07652	0.17228	0.30278
1483.2464	9.13501	0.11979	0.39444

1483.2464	7.14800	0.10747	0.51042
1483.2464	5.56845	0.09852	0.62639
1483.2464	4.19366	0.08620	0.74236
1483.2464	3.41887	0.08284	0.85833
1483.2464	2.31464	0.06331	0.99514
1483.2464	1.50556	0.05674	1.15278
1483.2464	0.97521	0.05098	1.31042
1483.2464	0.68907	0.04523	1.46806

Sample output file from analysis-rev-oo.for

The output of the program is arranged by increases γ-ray energy, followed by the nuclide identity, the literature γ-ray energy for each nuclide, the γ intensity, the half-life, and the EOB activity, A_0 with the uncertainty.

```
GS sample analysis

  338.2 206 PO      338.4 keV,  19.40 ,HL=  0.880E+01 ,1x,A0= 0.17619E+02 +/- 0.24668E+00 A
  374.6 204 BI      374.7 keV,  81.00 ,HL=  0.468E+00 ,1x,A0= 0.78280E+02 +/- 0.16779E+00 B
  441.9 211 RN      442.2 keV,  23.50 ,HL=  0.608E+00 ,1x,A0= 0.11841E+02 +/- 0.37339E+00 A
  515.8 206 BI      516.2 keV,  40.70 ,HL=  0.624E+01 ,1x,A0= 0.58092E+02 +/- 0.11351E+01 B
  515.8 206 BI      516.2 keV,  40.70 ,HL=  0.624E+01 ,1x,A0= 0.69778E+02 +/- 0.17240E+00 A
  674.1 211 RN      674.1 keV,  46.00 ,HL=  0.608E+00 ,1x,A0= 0.88325E+01 +/- 0.69501E+00 B
  802.8 206 BI      803.1 keV,  98.90 ,HL=  0.624E+01 ,1x,A0= 0.65895E+02 +/- 0.27370E+00 B
  807.4 206 PO      807.4 keV,  23.00 ,HL=  0.880E+01 ,1x,A0= 0.11129E+02 +/- 0.20557E+00 B
  807.4 206 PO      807.4 keV,  23.00 ,HL=  0.880E+01 ,1x,A0= 0.73155E+01 +/- 0.14251E+01 C
  880.8 206 BI      881.1 keV,  66.20 ,HL=  0.624E+01 ,1x,A0= 0.77045E+02 +/- 0.14164E+00 A
  898.8 204 BI      899.2 keV,  98.50 ,HL=  0.468E+00 ,1x,A0= 0.65572E+02 +/- 0.87735E+00 C
  983.6 204 BI      984.1 keV,  58.00 ,HL=  0.468E+00 ,1x,A0= 0.60409E+02 +/- 0.54137E+00 B
  992.0 211 RN      992.4 keV,  27.10 ,HL=  0.608E+00 ,1x,A0= 0.12213E+02 +/- 0.62990E+00 B
 1181.2 210 AT     1181.4 keV,  99.30 ,HL=  0.338E+00 ,1x,A0= 0.51753E+02 +/- 0.17428E+00 A
 1436.5 210 AT     1436.7 keV,  29.00 ,HL=  0.338E+00 ,1x,A0= 0.53036E+02 +/- 0.43726E+00 A
 1483.2 210 AT     1483.3 keV,  46.50 ,HL=  0.338E+00 ,1x,A0= 0.43392E+02 +/- 0.23282E+00 A
```

cross.for

```
      program crsplt
C
C     CODE REVISED FOR ATLAS W + GD DATA
C     WDL--8/2010
C
      DIMENSION TIM(60), CUR(60), A0I(60), ERRI(60), BRNCHI(60),
     1          FLUXI(60), TIAB(60), TITLE(8)
      INTEGER Z, ZP, ZGP
      character*10 title,targ,proj
      character*3 A
      COMMON / TABL / NAT(900), ELT(900), ISOMT(900), Z(900), ZP(900),
```

```
     1              ZGP(900), HL(900), HLP(900), HLGP(900), ITOT
      DATA BLANK / 1H /
C
CCCCCCCCCCCCCCCCCCCCCCCCCCCCCCCCCCCCCCCCCCCCCCCC
CCCCCCCCCCCCCCCCCCCCCC
C
C   CROS CALCULATES CROSS SECTIONS FOR NUCLIDES BASED UPON
THE GAMMA-
C  ASSIGNMENTS MADE FROM DECAY DATA. CROSS SECTIONS MAY BE
CALCULATED
C  BASED UPON SINGLE GAMMAS OR UPON SEVERAL GAMMA LINES
IDENTIFIED FOR A
C  GIVEN NUCLIDE.  IN THE FIRST CASE, THE INPUT DATA
C  ARE NOT (NECESSARILY) SORTED IN A PARTICULAR ORDER, AND NO
SEPARATORS
C   SHOULD BE USED.  IN THE SECOND CASE ( >= 1 GAMMA PER
NUCLIDE)
C  THE INPUT DATA SHOULD BE SORTED BY NUCLIDE AND EACH SET
OF DATA FOR
C  ANY GIVEN NUCLIDE SHOULD BE SEPARATED BY A BLANK RECORD.
C
C  IN ANY CASE, A SUMMARY TABLE IS GENERATED BY SPECIFYING
THAT OPTION
C  THE PROGRAM IS TERMINATED WITH AN EOF AFTER THE LAST INPUT
CARD OR
C  AFTER THE SUMMARY TABLE SPECIFIER.
C
C  CROSS SECTION CALCULATIONS INCLUDE VARIABLE FLUX
FACTORS.
C
C  THIS CODE DOES
C  WEIGHTED MEAN CALCULATION BASED UPON
C
C                     W(I) = BR(I) / ERR(I)**2
C
C  WHERE W(I) IS THE WEIGHT LINEARLY DEPENDANT ON THE
BRANCHING RATIO,
C  BR(I) AND ON THE SQUARE OF THE ERROR, ERR(I).  THE CODE ALSO
USES
C  A CORRECT ERROR ANALYSIS AND ERROR REJECTION FOR CROSS
SECTION
C  CALCULATIONS BASED UPON MORE THAN 1 GAMMA LINE.
C
C  THE STANDARD ERROR IS CALCULATED BY...
C
```

```
C           S.E. = SQRT((SUM(NU(I)*W(I)) / SUM(W(I)))
C
C  WHERE SUM INDICATES A SUM OVER ALL N MEMBERS OF THE
SAMPLE, W(I)
C  IS THE WEIGHT, NU THE DEVIATION, X(I)-<X>, AND N IS THE NUMBER
OF
C  LINES FOR A GIVEN NUCLIDE.
C
C
C
C  DATA INPUT
C
C    CARD 1......TITLE CARD (8A10)
C    CARD 2......BBDT INFORMATION CARD (A10,2F10.4,A10,2F10.1)
C           TARG....TARGET
C           TGTWT...TARGET THICKNESS (MG/CM**2)
C           TGMASS..TARGET MASS (MG/MMOL - SAME AS G/MOL)
C           PROJ....PROJECTILE
C           HICHRG..CHARGE OF PROJECTILE
C           TOB.....TOTAL TIME OF BOMBARDMENT (MIN)
C    CARD 3-N....BOMBARDMENT HISTORY CARDS (2F10.4)
C           TIM(I)...TIME OF I-TH BEAM FLUX INTERVAL (MIN)
C           CUR(I)...DOSE IN ITH INTERVAL IN PARTICLES
C    CARD N+1....BLANK
C    CARD N+2....CHEMICAL YIELD DATA (2E10.3)
C           YIELD, ERROR IN YIELD
C    CARDS N+3-M..EITHER SINGLE TAU2 CARDS WITH NO SEPARATORS
C              OR CARDS SORTED BY NUCLIDE AND SEPARATED BY
BLANKS.
C
C    CARD M+1...AFTER LAST CARD, A SUMMARY TABLE MAY BE
GENERATED WITH
C             A 1.0 IN COLS 1-3.
C
C  THIS PROGRAM WILL OUTPUT RESULTS TO "MASIN.DAT"
COMPATIBLE WITH THE
C  INPUT FORMAT TO   MASSY   .
C
C
C  READ IN THE   ISOTABLE   FOR DECAY INFORMATION TO BE
MATCHED UP TO
C  CROSS SECTIONS IN CPREP FOR GENERATION OF MASSY CARDS.
C
CCCCCCCCCCCCCCCCCCCCCCCCCCCCCCCCCCCCCCCCCCCCCCCCCCCCCCCCCCCCCCC
CCCCCCCCCCCCCCCCCCCC
```

```
C
      OPEN(4,FILE='library.dat',STATUS='OLD')
      I = 0
  100 I = I + 1
        READ(4,805) ELT(I), NAT(I), ISOMT(I), Z(I), ZP(I), ZGP(I),
     1            HL(I), HLP(I), HLGP(I)
        IF(Z(I) .NE. 0.0) GOTO 100
          ITOT = I - 1
C
C OPEN FILE: inputa.dat - OLD
      OPEN(5,FILE='ThinGSinput.dat',STATUS='OLD')
  105 READ(5,800) TITLE
      write(*,800)title
      READ(5,801) TARG,TGTWT,TGMASS,PROJ,HICHRG,TOB
           write(*,801) TARG,TGTWT,TGMASS,PROJ,HICHRG,TOB
        IFLAG = 0
        TOTCUR = 0.0
        TOTTIM = 0.0

      I = 1
c          write(*,*) 'got here'
  110 READ(5,802) TIM(I), CUR(I)
      write(*,802)TIM(I), CUR(I)
C       write(*,*) I,TGTWT,TGMASS
        IF(TIM(I) .EQ. 0.0) GOTO 120
          FLUXI(I) = CUR(I)/(TIM(I)*60)
C     Added "*60" to convert FLUX to part/sec to match A0
          TOTTIM = TOTTIM + TIM(I)
          TOTCUR = TOTCUR + CUR(I)
          TIAB(I) = TOB - TOTTIM
      write(*,*) 'entry ok'
          I = I + 1
          GOTO 110

  120 INTRVLS = I - 1
      TGTN = TGTWT*6.0220E20 / TGMASS
C     Avogadro's number units (above) = ATOMS/MMOL
      TFLUX = TOTCUR/TOTTIM
           write(*,*)'got to another place'
C
      READ(5,806) YIELD, ERRYLD
      IF(YIELD .EQ. 0.0) YIELD = 100.0
      IF(ERRYLD .EQ. 0.0  .AND.  YIELD .NE. 100.0) ERRYLD = 5.0
      YIELD = YIELD / 100.
      ERRYLD = ERRYLD / 100.0
```

```
          write(*,*)'got yield'
C
     OPEN(7,FILE='THINOUTPUT.dat',STATUS='NEW')
     WRITE (7,900) TITLE
     WRITE (7,901) TARG,PROJ
     WRITE(7,902)
TGTWT,TGMASS,TOTCUR,HICHRG,TOTTIM,TGTN,TFLUX,
    1          YIELD,ERRYLD

  130 LINE = 0
     TSEP = 0.0
     HLFSAV = 0.0


CCCCCCCCCCCCCCCCCCCCCCCCCCCCCCCCCCCCCCCCCCCCCCCCCCCCCCCCCCCCCCCCCCC
CCCCCCCCCCCCCC
C
C  E1....MEASURED GAMMA RAY ENERGY
C  E2....KNOWN GAMMA RAY ENERGY
C  A0....A0(CPM)
C  ERR...ERROR IN A0(CPM)
C  EL....ELEMENT SYMBOL
C  A.....MASS NUMBER
C  ISOM..M OR G
C       BE CAREFUL THAT YOUR FORM OF ISOM MATCHES ISOTAB.DAT
C  HLF...T1/2(DAY)
C  BRNCH..BRANCHING RATIO OF GAMMA RAY(%)
C  FRAC...SEPARATION TIME OF NUCLIDE FROM PARENT.  IF NO
CHEMICAL
C        SEPARATION WAS MADE, FRAC=0.0
C
C  FORMAT(1X,F6.1,1X,A3,2A2,2X,F6.1,4X,F6.2,5X,F10.4,4X,E11.5,3X,E11.5)
C
C
CCCCCCCCCCCCCCCCCCCCCCCCCCCCCCCCCCCCCCCCCCCCCCCCCCCCCCCCCCCCCCCCCCC
CCCCCCCCCCCCCCCCC
C
C             IN W + GD AO VALUES GIVEN IN BQ, MUST MULTIPLY BY 60.

c             this was edited out for Xe + Pb
C
C
```

```
 140 READ(5,803)E1,A,EL,ISOM,E2,BRNCH,HLF,A0,ERR
c      a0=a0*60.
c          ERR = ERR*60.
c          write(*,803)E1,A,EL,ISOM,E2,BRNCH,HLF,A0,ERR
     FRAC=0.0
 3334        IF(E1 .EQ. 0.0) GOTO 170
         IF(E1 .EQ. 1.0) GOTO 200
C            DECODE(3,700,A) C1,C2,C3
C            DECODE(3,701,A) I1,I2,I3
           READ(A, 700) C1,C2,C3
           READ(A, 701) I1,I2,I3
           NA = I1*100 + I2*10 + I3
           IF(C3 .EQ. BLANK) NA = I1*10 + I2
           IF(C2 .EQ. BLANK) NA = I1
 150       IF(LINE .EQ. 0) write (7,903) EL,NA,ISOM
           LINE = LINE + 1
           IF(HLFSAV .NE. 0.0) GOTO 155
             HLFSAV = HLF
             ELSAV = EL
             NASAV = NA
             ISOMSAV = ISOM
 155       IF(HLFSAV .NE. HLF) GOTO 160
           WRITE(7,904) E1,E2,A0,ERR,EL,NA,ISOM,HLF,BRNCH,FRAC
           A0I(LINE) = A0
           ERRI(LINE) = ERR
           BRNCHI(LINE) = BRNCH
           IF (FRAC.GT.TSEP) TSEP=FRAC
           GOTO 140

 160       WRITE (7,905)
           LINE = LINE - 1
           IFLAG = 1

 170 IF(LINE .EQ. 1) GOTO 180
       NLINS = LINE
       CALL ERROR(A0I,ERRI,BRNCHI,A0AVE,ERRAVE,NLINS)
       GOTO 190

 180 A0AVE = A0I(1)
     ERRAVE = ERRI(1)
     NLINS = 1
 190 HLF = HLFSAV * 1440.
```

```
      SUM = 0.0
          DO 10 I = 1,INTRVLS
        SUM = SUM + FLUXI(I) * (1.0 - EXP(-0.693 * TIM(I)/HLF)) *
     1                    EXP(-0.693 * TIAB(I)/HLF)
    10 CONTINUE


C     write(*,*) sum,a0ave
      SIGMA = A0AVE*1.0E27 / (SUM*TGTN)
      ERRSIG = ERRAVE*1.0E27 / (SUM*TGTN)
      SIGY = SIGMA / YIELD
      ERRSIGY = SIGY * SQRT((ERRYLD/YIELD)**2 + (ERRSIG/SIGMA)**2)
      WRITE (7,906) NLINS, LINE, ELSAV, NASAV, ISOMSAV
      WRITE (7,907) SIGMA, ERRSIG
      CALL RESULT(ELSAV,NASAV,ISOMSAV,SIGMA,ERRSIG,LINE,NLINS,
     1          SIGY,ERRSIGY,TSEP,0)
      IF(IFLAG .NE. 1) GOTO 130
        IFLAG = 0
        LINE = 0
        HLFSAV = 0.0
        GOTO 150

    200 CALL RESULT(ELSAV,NASAV,ISOMSAV,SIGMA,ERRSIG,LINE,NLINS,
     1          SIGY,ERRSIGY,TSEP,1)
      GOTO 105

    298 WRITE (7,908)
    299 STOP
C
C
C  FORMAT STATEMENTS
C
C
    700 FORMAT(3A1)
    701 FORMAT(3I1)
    800 FORMAT(8A10)
    801 FORMAT(A10,2F10.4,A10,2F10.4)
    802 FORMAT(2E15.4)
C   803 FORMAT(1X,F6.1,1X,A3,2A2,2X,F6.1,4X,F5.1,4X,e9.3,4X,E11.5,3X,
C     XE11.5)
    803 FORMAT(1X,F6.1,1X,A3,1x,2A2,3X,F6.1,6X,F6.2,7X,e9.3,9X,E11.5,5X,
     X E11.5)
    805 FORMAT(1X,A2,I3,A2,I3,2I5,3E10.3)
    806 FORMAT(2E10.3)
C
```

```
 900 FORMAT(1H1, 10X, 6(10H**********), //, 14X,
   1      'C R O S S   S E C T I O N   C A L C U L A T I O N S',//,
   2      11X,6(10H**********),//,10X,8A10,//)
 901 FORMAT(1H0,/,
   1      ' REVISED ERROR ANALYSIS FOR FINITE DATA SET,',/,
   4      ' CROSS SECTIONS FOR THE REACTION OF ',/,
   5      5X,A10,'  WITH  ',A10,///)
 902 FORMAT(1H0,10X,'I N P U T   P A R A M E T E R S',//,
   1      10X,'TARGET THICKNESS   =',F10.4,10H MG/CM**2  ,/,
   2      10X,'TARGET MASS        =',F10.4, /,
   3      10X,'TOTAL BEAM CURRENT =',G12.5,' MICROCOUL.',/,
   4      10X,'PROJECTILE CHARGE  =',F10.3, /,
   5      10X,'TOTAL BBDT TIME    =',F10.2,' MINUTES', /,
   6      10X,'TARGET ATOMS (N)   =',G12.5,' ATOMS',/,
   7      10X,'TOTAL BEAM FLUX    =',G12.5,' H.I. / MIN.',/,
   8      10X,'YIELD FOR SAMPLE   =',G11.4,' +/- ',G11.4,/////)
 903 FORMAT(1H0,'I S O T O P E ...',A2,'-',I3,A2,/)
 904 FORMAT(1H ,2F7.1,2(1X,E11.4),1X,1X,A2,'-',I3,A3,
   1      F8.3,F7.1,E10.3)
 905 FORMAT(1H0, 'HEY TURKEY, YOU NEED A BLANK CARD TO
SEPARATE ', /,
   1      ' THE NUCLIDES HERE, BUT YOU ARE FORGIVEN THIS TIME.',//)
 906 FORMAT(1H0,3X,I3,' OUT OF',I3,' GAMMA LINE(S) WERE USED TO ',
   1      'CALCULATE THE  ',A2,'-',I3,A2,' CROSS SECTION.',/)
 907 FORMAT(1H0,10X,'CROSS SECTION= ',G12.5,' +/- ',G12.5,
   1      /,11X,6(7H*******),///)
 908 FORMAT(1H0,4(10H**********),/,
   1      ' EOF ON CARD INPUT DETECTED AT INTERMEDIATE STAGE.',/,
   2      ' PROGRAM ABORTED.')
      END

      SUBROUTINE ERROR(A0I,ERRI,BRI,A0AVE,ERRAVE,NLINS)

C
CCCCCCCCCCCCCCCCCCCCCCCCCCCCCCCCCCCCCCCCCCCCCCCC
CCCCCCCCCCCCCCCCCCCCC
C  ERROR IS CALLED WHEN THERE ARE AT LEAST TWO POINT IN THE
SET OF
C  DATA FOR A GIVEN NUCLIDE.  IF THERE ARE MORE THAN TWO
POINTS,
C  THEN ERROR WILL TEST THE POINTS FOR THE REJECTION CRITERIA
AS
C  FOR SETS OF DATA WITH FEWER THAN 10 MEASUREMENTS, WE
HAVE DECIDED
```

```
C  TO USE THE  2-SIGMA  REJECTION LIMIT SINCE CHAUVENETS
CRITERION
C  ELIMINATES FAR TOO MANY POINTS IN SMALL DATA SETS.
CCCCCCCCCCCCCCCCCCCCCCCCCCCCCCCCCCCCCCCCCCCCCCCCCC
CCCCCCCCCCCCCCCCCCCC
C
      DIMENSION A0I(1),ERRI(1),BRI(1),A0REJ(50),ERREJ(50),CHAUV(25)

      DATA CHAUV/ 0.000, 0.000, 1.380, 1.535, 1.645, 1.730,
     1           1.800, 1.862, 1.915, 1.960, 2.001, 2.038,
     2           2.070, 2.100, 2.127, 2.155, 2.178, 2.200,
     3           2.220, 2.240, 2.260, 2.278, 2.293, 2.310, 2.327/

      N = 0
      IREJ = 0
      IF(NLINS .EQ. 2) GOTO 120
      IF(NLINS .LE. 25) CRIT = CHAUV(NLINS)
      IF(NLINS .LE. 10) CRIT = 2.0
      IF(NLINS .GT. 25) CRIT = CHAUV(25) + 0.12*(NLINS-25)
      CALL MEAN(A0I,ERRI,BRI,A0AVE,ERRAVE,NLINS)
      WRITE (7,900) A0AVE,ERRAVE,CRIT
      DO 10 I = 1,NLINS
        DEV = ABS(A0AVE-A0I(I))
        IF(DEV .GT. CRIT*ERRAVE) GOTO 100
          N = N + 1
          A0I(N) = A0I(I)
          ERRI(N) = ERRI(I)
          BRI(N) = BRI(I)
          GOTO 10
  100   IREJ = IREJ + 1
        A0REJ(IREJ) = A0I(I)
        ERREJ(IREJ) = ERRI(I)
   10 CONTINUE
      IF(IREJ .EQ. 0) GOTO 110
        WRITE (7,901)
        WRITE (7,902) (A0REJ(J),ERREJ(J), J=1,IREJ)
  110 NLINS = N
  120 CALL MEAN(A0I,ERRI,BRI,A0AVE,ERRAVE,NLINS)
      WRITE(7,903) A0AVE,ERRAVE
      RETURN


  900 FORMAT(1H0,' CALCULATION OF INITIAL MEAN',/,10X,'MEAN =
',G12.5,
     1      5X,'STD. DEV.= ',G12.5,5X,'REJECTION PARAM.= ',F5.3,/)
```

```
  901 FORMAT(1H0,'REJECTED DATA POINTS, CHAUVENETS
CRITERION',//)
  902 FORMAT(2(5X,G12.5))
  903 FORMAT(1H0,' FINAL MEAN= ',G12.5,5X,'STD. DEV.= ',G12.5,/)
      END

      SUBROUTINE MEAN(A0I,ERRI,BRI,A0AVE,ERRAVE,NLINS)

      DIMENSION A0I(1), ERRI(1), BRI(1), WTI(50)

      SUMXW = 0.0
      SUMW  = 0.0
      SUMWNU = 0.0
      IF(NLINS .GT. 1) GOTO 100
        A0AVE = A0I(1)
        ERRAVE = ERRI(1)
        RETURN
  100 DO 10 I = 1,NLINS
        WTI(I) = BRI(I) / ERRI(I)**2
        SUMW = SUMW + WTI(I)
        SUMXW = SUMXW + A0I(I)*WTI(I)
   10 CONTINUE
      A0AVE = SUMXW / SUMW
      DO 20 I = 1,NLINS
        SUMWNU = SUMWNU + WTI(I) * (A0AVE-A0I(I))**2
   20 CONTINUE
      ERRAVE = SQRT(SUMWNU / SUMW)
      RETURN
      END

      SUBROUTINE RESULT(EL,NA,ISOM,SIG,ERC,NF,NU,Y,EY,
     1                  TSEP,IEND)

      DIMENSION ELN(900),NAN(900),ISOMN(900),SIGX(900),ESIGN(900),
     1          NGAMF(900),NGAMU(900),CSY(900),ECSY(900),TREC(900)

      DATA N/0/
      IF(IEND .EQ. 1) GOTO 100
        N = N + 1
        ELN(N) = EL
        NAN(N) = NA
        ISOMN(N) = ISOM
        SIGX(N) = SIG
        ESIGN(N) = ERC
        NGAMF(N) = NF
```

```
      NGAMU(N) = NU
      CSY(N) = Y
      ECSY(N) = EY
      TREC(N) = TSEP
      RETURN
 100     WRITE(7,900)
      DO 10 I = 1,N
       WRITE(7,901) ELN(I),NAN(I),ISOMN(I),SIGX(I),ESIGN(I),
     1            NGAMF(I),NGAMU(I),CSY(I),ECSY(I)
   10 CONTINUE                                              280
C     CALL CPREP(ELN,NAN,ISOMN,CSY,ECSY,TREC,N)
      CALL CPREP(ELN,NAN,ISOMN,SIGX,ERRN,TREC,N)
      IEND = 0
      N = 0
      RETURN
C
C
  900 FORMAT(1H1,1X,'RESULTS OF  ',//,1X,'ISOTOPES',2X,'CROSS-',
     1      'SECTION(MB)',5X,'ERROR(MB)',5X,'GAMMAS FOUND, USED',
     2      2X,'YIELD(MB)',5X,'ERROR(MB)',//)
  901 FORMAT(1X,A2,1X,I3,A2,4X,2(E10.4,10X),I2,10X,I2,2(5X,E10.4),/)
      END


      SUBROUTINE CPREP(ELN,NAN,ISOMN,SIGX,ERRN,TREC,N)

      DIMENSION ELN(600), NAN(600), ISOMN(600), SIGX(600),
     1         ERRN(600), TREC(600)
      INTEGER Z, ZP, ZGP
      COMMON / TABL / NAT(900), ELT(900), ISOMT(900), Z(900), ZP(900),
     1               ZGP(900), HL(900), HLP(900), HLGP(900), ITOT

      OPEN(8,FILE='MASSYIN',STATUS='NEW')
      WRITE (7,902)
      DO 10 I = 1,N
       DO 20 J = 1,ITOT
        IF(ELN(I) .EQ. ELT(J)  .AND.  NAN(I) .EQ. NAT(J)  .AND.
     1      ISOMN(I) .EQ. ISOMT(J)) GOTO 100
   20  CONTINUE
       WRITE (7,900) ELN(I),NAN(I),ISOMN(I)
       GOTO 10
  100  IF(HLP(J) .EQ. -0) HLP(J) = 0.0
       IF(HLGP(J) .EQ. -0) HLGP(J) = 0.0
C     OPEN(8,FILE='MASSYIN',STATUS='NEW')
      WRITE(8,901) ELT(J),NAT(J),ISOMT(J),Z(J),ZP(J),ZGP(J),HL(J),
```

```
     1          HLP(J),HLGP(J),SIGX(I),ERRN(I),TREC(I)
      WRITE (7,901) ELT(J),NAT(J),ISOMT(J),Z(J),ZP(J),ZGP(J),HL(J),
     1          HLP(J),HLGP(J),SIGX(I),ERRN(I),TREC(I)
    10 CONTINUE
      RETURN                                        394

   900 FORMAT(' $$$$$$$$$$MISSING NUCLIDE FROM ISOTABLE  ',A2,'-
',I3,A2)
   901 FORMAT(1X,A2,I3,A1,I4,2I5,5E10.4,1X,F8.4)
   902 FORMAT(1H1, '  MASSY CARD IMAGES',/)
      END
```

Sample input file for cross.for

After the title row, the next row gives the target, target thickness in mg/cm^2, target A, projectile, projectile charge, and total time of bombardment. The next rows contain the beam history. The first column shows the time interval of each beam on/beam off cycle in minutes, while the second column shows the total number of particles per time period. The following rows contain the specific nuclide information obtained from running analysis-rev-oo.for

```
GS sample analysis
 208Pb     3.100      208.       136Xe     41.66     5526.
 308.          5.38e13
 21.             0.0
 379.          6.39e13
 144.            0.0
 16.           5.89e12
 51.             0.0
 1.            3.68e11
 45.             0.0
 29.           1.07e13
 9.              0.0
 6.            2.21e12
 4.              0.0
 47.           1.76e13
 6.              0.0
 170.          6.37e13
 4.              0.0
 19.           7.12e12
 9.              0.0
 41.           1.54e13
 7.              0.0
 57.           2.13e13
 6.              0.0
 382.          1.43e14
 18.             0.0
 27.           1.01e13
 15.             0.0
 3.            1.12e12
 49.             0.0
```

```
 7.            2.45e12
 88.             0.0
 451.          1.58e14
 57.             0.0
 20.           6.99e12
 31.             0.0
 39.           1.36e13
 7.              0.0
 7.            2.45e12
 55.             0.0
 10.           3.37e12
 5.              0.0
 21.           7.34e12
 4.              0.0
 849.          3.07e14
 74.             0.0
 497.          1.74e14
 9.              0.0
 1075.         3.76e14
 24.             0.0
 29.           1.01e13
 11.             0.0
 12.           4.19e12
 6.              0.0
 250.          7.49e13
 6.              0.0
 9.            3.15e12
0.0            0.0
100.        0.0
  983.6 204 BI      984.1 keV,  58.00 ,HL=  0.468E+00 ,1x,A0= 0.60409E+02 +/- 0.54137E+00 B
  374.6 204 BI      374.7 keV,  81.00 ,HL=  0.468E+00 ,1x,A0= 0.78280E+02 +/- 0.16779E+00 B
  898.8 204 BI      899.2 keV,  98.50 ,HL=  0.468E+00 ,1x,A0= 0.65572E+02 +/- 0.87735E+00 C

  802.8 206 BI      803.1 keV,  98.90 ,HL=  0.624E+01 ,1x,A0= 0.65895E+02 +/- 0.27370E+00 B
  515.8 206 BI      516.2 keV,  40.70 ,HL=  0.624E+01 ,1x,A0= 0.58092E+02 +/- 0.11351E+01 B
  515.8 206 BI      516.2 keV,  40.70 ,HL=  0.624E+01 ,1x,A0= 0.69778E+02 +/- 0.17240E+00 A
  343.3 206 BI      343.5 keV,  23.40 ,HL=  0.624E+01 ,1x,A0= 0.70294E+02 +/- 0.41410E+00 A
  880.8 206 BI      881.1 keV,  66.20 ,HL=  0.624E+01 ,1x,A0= 0.77045E+02 +/- 0.14164E+00 A

  807.4 206 PO      807.4 keV,  23.00 ,HL=  0.880E+01 ,1x,A0= 0.11129E+02 +/- 0.20557E+00 B
  338.2 206 PO      338.4 keV,  19.40 ,HL=  0.880E+01 ,1x,A0= 0.17619E+02 +/- 0.24668E+00 A
  807.4 206 PO      807.4 keV,  23.00 ,HL=  0.880E+01 ,1x,A0= 0.73155E+01 +/- 0.14251E+01 C

 1181.2 210 AT     1181.4 keV,  99.30 ,HL=  0.338E+00 ,1x,A0= 0.51753E+02 +/- 0.17428E+00 A
 1483.2 210 AT     1483.3 keV,  46.50 ,HL=  0.338E+00 ,1x,A0= 0.43392E+02 +/- 0.23282E+00 A
 1436.5 210 AT     1436.7 keV,  29.00 ,HL=  0.338E+00 ,1x,A0= 0.53036E+02 +/- 0.43726E+00 A

  992.0 211 RN      992.4 keV,  27.10 ,HL=  0.608E+00 ,1x,A0= 0.12213E+02 +/- 0.62990E+00 B
  674.1 211 RN      674.1 keV,  46.00 ,HL=  0.608E+00 ,1x,A0= 0.88325E+01 +/- 0.69501E+00 B
  441.9 211 RN      442.2 keV,  23.50 ,HL=  0.608E+00 ,1x,A0= 0.11841E+02 +/- 0.37339E+00 A

    1.0 211 RN      442.2 keV,  23.50 ,HL=  0.608E+00 ,1x,A0= 0.11841E+02 +/- 0.37339E+00 A
 AQUI =  T
```

Sample output from cross.for

The output file shows target and projectile information, such as effective target thickness (in mg/cm^2), target mass (amu), total bombardment time, and total number of target atoms. Cross section results for each nuclide are reported as well as the number of γ-rays used to calculate the result.

```
1          ************************************************************

             C R O S S   S E C T I O N   C A L C U L A T I O N S

           ************************************************************

          GS sample analysis


0
 REVISED ERROR ANALYSIS FOR FINITE DATA SET,
 CROSS SECTIONS FOR THE REACTION OF
      208Pb      WITH     136Xe



0          I N P U T   P A R A M E T E R S

          TARGET THICKNESS   =    3.1000 MG/CM**2
          TARGET MASS        =  208.0000
          TOTAL BEAM CURRENT = 0.15597E+16 MICROCOUL.
          PROJECTILE CHARGE  =    41.660
          TOTAL BBDT TIME    =   5526.00 MINUTES
          TARGET ATOMS (N)   = 0.89751E+19 ATOMS
          TOTAL BEAM FLUX    = 0.28226E+12 H.I. / MIN.
          YIELD FOR SAMPLE   =  1.000     +/-   0.000




0I S O T O P E ...BI-204

   983.6  984.1  0.6041E+02  0.5414E+00  BI-204      0.468   58.0 0.000E+00
   374.6  374.7  0.7828E+02  0.1678E+00  BI-204      0.468   81.0 0.000E+00
   898.8  899.2  0.6557E+02  0.8773E+00  BI-204      0.468   98.5 0.000E+00
0 CALCULATION OF INITIAL MEAN
          MEAN =   76.668         STD. DEV.=   4.8566         REJECTION PARAM.= 2.000

0REJECTED DATA POINTS, CHAUVENETS CRITERION


       60.409          0.54137
       65.572          0.87735
0 FINAL MEAN=   78.280         STD. DEV.=  0.16779

0     1 OUT OF  3 GAMMA LINE(S) WERE USED TO CALCULATE THE  BI-204   CROSS SECTION.

0          CROSS SECTION=   1.6571     +/-  0.35518E-02
           ****************************************



0I S O T O P E ...BI-206

   802.8  803.1  0.6589E+02  0.2737E+00  BI-206      6.240   98.9 0.000E+00
   515.8  516.2  0.5809E+02  0.1135E+01  BI-206      6.240   40.7 0.000E+00
   515.8  516.2  0.6978E+02  0.1724E+00  BI-206      6.240   40.7 0.000E+00
   343.3  343.5  0.7029E+02  0.4141E+00  BI-206      6.240   23.4 0.000E+00
   880.8  881.1  0.7704E+02  0.1416E+00  BI-206      6.240   66.2 0.000E+00
0 CALCULATION OF INITIAL MEAN
          MEAN =   72.791         STD. DEV.=   4.8125         REJECTION PARAM.= 2.000

0REJECTED DATA POINTS, CHAUVENETS CRITERION


       58.092           1.1351
0 FINAL MEAN=   72.867         STD. DEV.=   4.7074

0     4 OUT OF  5 GAMMA LINE(S) WERE USED TO CALCULATE THE  BI-206   CROSS SECTION.

0          CROSS SECTION=   4.8707     +/-  0.31466
           ****************************************
```

```
0I S O T O P E ...PO-206

   807.4  807.4  0.1113E+02  0.2056E+00  PO-206      8.800   23.0 0.000E+00
   338.2  338.4  0.1762E+02  0.2467E+00  PO-206      8.800   19.4 0.000E+00
   807.4  807.4  0.7315E+01  0.1425E+01  PO-206      8.800   23.0 0.000E+00
0 CALCULATION OF INITIAL MEAN
          MEAN =   13.446         STD. DEV.=   3.1902         REJECTION PARAM.= 2.000

0 FINAL MEAN=   13.446         STD. DEV.=   3.1902

0     3 OUT OF  3 GAMMA LINE(S) WERE USED TO CALCULATE THE  PO-206   CROSS SECTION.

0          CROSS SECTION=   1.2028     +/-  0.28539
           ****************************************



0I S O T O P E ...AT-210

  1181.2 1181.4  0.5175E+02  0.1743E+00  AT-210      0.338   99.3 0.000E+00
  1483.2 1483.3  0.4339E+02  0.2328E+00  AT-210      0.338   46.5 0.000E+00
  1436.5 1436.7  0.5304E+02  0.4373E+00  AT-210      0.338   29.0 0.000E+00
0 CALCULATION OF INITIAL MEAN
          MEAN =   50.122         STD. DEV.=   3.3785         REJECTION PARAM.= 2.000

0 FINAL MEAN=   50.122         STD. DEV.=   3.3785

0     3 OUT OF  3 GAMMA LINE(S) WERE USED TO CALCULATE THE  AT-210   CROSS SECTION.

0          CROSS SECTION=   1.0648     +/-  0.71772E-01
           ****************************************



0I S O T O P E ...RN-211

   992.0  992.4  0.1221E+02  0.6299E+00  RN-211      0.608   27.1 0.000E+00
   674.1  674.1  0.8833E+01  0.6950E+00  RN-211      0.608   46.0 0.000E+00
   441.9  442.2  0.1184E+02  0.3734E+00  RN-211      0.608   23.5 0.000E+00
0 CALCULATION OF INITIAL MEAN
          MEAN =   11.055         STD. DEV.=   1.4163         REJECTION PARAM.= 2.000

0 FINAL MEAN=   11.055         STD. DEV.=   1.4163

0     3 OUT OF  3 GAMMA LINE(S) WERE USED TO CALCULATE THE  RN-211   CROSS SECTION.

0          CROSS SECTION=  0.23680     +/-  0.30338E-01
           ****************************************
```

massyprep.for

```
      program crsplt
C
      DIMENSION eln(300),nan(300),isomn(300),sigx(300),errn(300),
     1   trec(300),     TITLE(8)
      INTEGER Z, ZP, ZGP
      character*10 title,targ,proj
      COMMON / TABL / NAT(900), ELT(900), ISOMT(900), Z(900), ZP(900),
     1            ZGP(900), HL(900), HLP(900), HLGP(900), ITOT
      DATA BLANK / 1H /
```

```
C
CCCCCCCCCCCCCCCCCCCCCCCCCCCCCCCCCCCCCCCCCCCCCCCCC
CCCCCCCCCCCCCCCCCCCC
C
C  THIS PROGRAM WILL OUTPUT RESULTS TO "MASIN.DAT"
COMPATIBLE WITH THE
C  INPUT FORMAT TO   MASSY   .
C
C
C  READ IN THE   ISOTABLE   FOR DECAY INFORMATION TO BE
MATCHED UP TO
C  CROSS SECTIONS IN CPREP FOR GENERATION OF MASSY CARDS.
C
CCCCCCCCCCCCCCCCCCCCCCCCCCCCCCCCCCCCCCCCCCCCCCCCC
CCCCCCCCCCCCCCCCCCCC
C
      OPEN(4,FILE='library.dat',STATUS='OLD')
      I = 0
  100 I = I + 1
        READ(4,805) ELT(I), NAT(I), ISOMT(I), Z(I), ZP(I), ZGP(I),
     1              HL(I), HLP(I), HLGP(I)
        IF(Z(I) .NE. 0.0) GOTO 100
          ITOT = I - 1
C
C
      OPEN(7,FILE='OUTPUT',STATUS='NEW')
 805  format(1x,a2,i3,a2,i3,2i5,3e10.3)
      open(5,file='massyprepin.dat',status='old')
 806  FORMAT(1X,A2,I3,A2,2F10.3)
      i=1
 121  READ(5,806)eln(i),nan(i),isomn(i),sigx(i),errn(i)
      if(SIGX(i) .eq. 0.0)go to 120
      i=i+1
      goto 121
 120  continue
      N=I-1
      do 122 i=1,n
      WRITE(7,806)ELN(I),NAN(I),ISOMN(I),SIGX(I),ERRN(I)
      trec(i)=0.0
 122  continue
      call cprep(eln,nan,isomn,sigx,errn,trec,n)
      stop
      end

      SUBROUTINE CPREP(ELN,NAN,ISOMN,SIGX,ERRN,TREC,N)
```

```
      DIMENSION ELN(300), NAN(300), ISOMN(300), SIGX(300),
     1         ERRN(300), TREC(300)
      INTEGER Z, ZP, ZGP
      COMMON / TABL / NAT(900), ELT(900), ISOMT(900), Z(900), ZP(900),
     1               ZGP(900), HL(900), HLP(900), HLGP(900), ITOT

      OPEN(8,FILE='MASSYIN.dat',STATUS='NEW')
      WRITE (7,902)
      DO 10 I = 1,N
        DO 20 J = 1,ITOT
          IF(ELN(I) .EQ. ELT(J)  .AND.  NAN(I) .EQ. NAT(J)  .AND.
     1      ISOMN(I) .EQ. ISOMT(J)) GOTO 100
   20   CONTINUE
        WRITE (7,900) ELN(I),NAN(I),ISOMN(I)
        GOTO 10
  100   IF(HLP(J) .EQ. -0) HLP(J) = 0.0
        IF(HLGP(J) .EQ. -0) HLGP(J) = 0.0
C       OPEN(8,FILE='MASSYIN',STATUS='NEW')
      WRITE(8,901) ELT(J),NAT(J),ISOMT(J),Z(J),ZP(J),ZGP(J),HL(J),
     1           HLP(J),HLGP(J),SIGX(I),ERRN(I),TREC(I)
      WRITE (7,901) ELT(J),NAT(J),ISOMT(J),Z(J),ZP(J),ZGP(J),HL(J),
     1           HLP(J),HLGP(J),SIGX(I),ERRN(I),TREC(I)
   10 CONTINUE
      RETURN                                          394

  900 FORMAT(' $$$$$$$$$$MISSING NUCLIDE FROM ISOTABLE  ',A2,'-
',I3,A2)
  901 FORMAT(A2,I3,A1,I4,2I5,5E10.4,1X,F8.4)
  902 FORMAT(1H1, '  MASSY CARD IMAGES',/)
      END
```

Sample input for massyprep.for

The first column contains the nuclide element symbol followed by the mass number, A. The next column contains symbols for ground state or metastable state isomers (indicated by the G next to ^{83}Rb). The next two columns contain the cumulative cross sections and the associated errors, respectively. These FORTRAN programs are fixed-format programs, meaning that the input and output files have specific formatting requirements. The spacing of each element must remain constant

to the sample shown. The last row of the file is zeroed out to indicate the end of the file.

```
 BI204  1.5197E+004.2555E-02
 BI206  4.6900E+004.3976E-01
 PO206  1.1149E+001.5337E-01
 AT210  1.0650E+007.1770E-02
 RN211  2.3910E-013.6800E-02
```

Sample output from massyprep.for

The output file gives the nuclide identity, the Z of the nuclide, Z of the parent and grandparent, half-life of the nuclide, parent, and grandparent, as well as the cross section and uncertainty.

```
CD115G  48   47   460.3211E+040.2000E+020.7877E+000.1143E+000.1740E-03   0.0000
SB116M  51    0    00.6030E+020.0000E+000.0000E+000.4416E+000.4766E+00   0.0000
TE119M  52    0    00.6754E+040.0000E+000.0000E+000.1197E+000.2770E-01   0.0000
SB120B  51    0    00.8294E+040.0000E+000.0000E+000.1931E+000.9732E-01   0.0000
TE121M  52   53   540.2218E+060.1272E+030.4010E+020.4408E+000.6248E-02   0.0000
SB122G  51    0    00.3888E+040.0000E+000.0000E+000.1351E+000.8552E-02   0.0000
I 123   53   54   550.7920E+030.1248E+030.5970E+010.2106E+010.4342E+00   0.0000
```

massywalt.for

```
      PROGRAM ISOBAR
      COMMON ITAPE,JTAPE,IPUN
      COMMON/BINPUT/ NA(200),NZD(200),NZP(200),NZG(200),HLD(200),
     1HLP(200),HLG(200),ST(200),SIG(200),ESIG(200),EL(200),ELM(200)
      COMMON/BCORECT/ C(5,200),BBDT(4,50),NBBDT(4)
      COMMON/CPDSYS/ KZP,KAP,KZT,KAT,KZCN,KACN
      COMMON/BCHARGE/ ZMP(200),CC(200),ZMPP(200),ZMPG(200),
     X ZMZMP(200),CCB(200)
      COMMON/CHARGEa/ WHAT(20),ZMPB(200),ZMZMPB(200),ZMPPB(200),
     X ZMPGB(200)
      COMMON/BTITLE/ TITLE(20)
      COMMON/BRATES/ RD(200),RP(200),RG(200),IYD(200),IYP(200),
     1 IYG(200),NTRIAL,RDB(200),RPB(200),RGB(200),FIYA(200),
     2 FIYB(200)
      COMMON/BRESULT/ FIY(200),FC(200),SIGIY(200),SIGA(200),
     X ESIGIY(200)
```

```
      COMMON/RESULTSa/ ESIGA(200),SIGC(200),ESIGC(200),
     X SIGIYA(200),SIGIYB(200),ESIGIYA(200),ESIGIYB(200)
      COMMON/BRACH/ BRACH(200)
      DIMENSION NO(4)
      REAL ZAP,ZAT,ZACN
      DATA BLANK/4H    /
CCCCCCCCCCCCCCCCCCCCCCCCCCCCCCCCCCCCCCCCCCCCCCCCCCCCCCCCCCCCCCCCCCCC
CCCCCCCCCCCCCCCCCC
C                                          C
C       READ THE BBDT HISTORY CARDS                    C
C                    FORMAT 2 F10.0     (50 CARDS MAX)   C
C                               (BLANK CARD TERM.)  C
C                                          C
C    READ TITLE CARD         FORMAT 8 A10                C
C                                          C
C    READ BBDT. CARD         FORMAT   E10.4, 4 I5          C
C                                          C
C                                          C
C     BT = TOTAL LENGTH OF BOMBARDMENT                  C
C    KAT = A OF TARGET                            C
C    KZT = Z OF TARGET                            C
C    KAP = A OF PROJECTILE                          C
C    KZP = Z OF PROJECTILE                          C
C                                          C
CCCCCCCCCCCCCCCCCCCCCCCCCCCCCCCCCCCCCCCCCCCCCCCCCCCCCCCCCCCCCCCCCCCC
CCCCCCCCCCCCCCCCCC
      KK=0
      NO(4)=199
      NO(3)=199
      NO(2)=199
      K=0
      NBBDT(1)=0
      NC=1
  501 TB = 0.
      flux=0.
      NC=NC+1
      OPEN(2,FILE='MASSYIN.dat',STATUS='OLD')
      OPEN(3,FILE='RESULT.dat',STATUS='NEW')
   10 K=K+1
      READ (2,94) BBDT(1,K), BBDT(2,K)
      write(*,*) bbdt(1,k),bbdt(2,k)
      IF( BBDT(1,K).EQ.0.) GO TO 13
      TB = TB + BBDT(1,K)
      FLUX = FLUX + BBDT(2,K)
      GO TO 10
```

```
 13 K=K-1
    NBBDT(NC)=K
    NOB=K
    PRIOR = 0.
    DO 15 J=NBBDT(NC-1)+1, NBBDT(NC)
    PRIOR = PRIOR + BBDT(1,J)
    BBDT(3,J) = TB - PRIOR
 15 BBDT(4,J) = BBDT(2,J) / FLUX
 19 READ(2,96,END=132) (TITLE(I),I=1,20)
    write (*,*) (title(i), i=1,20)
    IF((TITLE(1) .EQ. BLANK) .AND. (TITLE(2) .EQ. BLANK))
   X GO TO 501
    READ(2,99) BT,KAT,KZT,KAP,KZP,FMUP
    write(*,*) bt,kat,kzt,kap,kzp,fmup
    IF (FMUP.EQ.0.)FMUP=1.
    WRITE(3,98)
    WRITE(3,95)(TITLE(I),I=1,20)
    KZCN = KZP + KZT
    KACN = KAP + KAT
    REKZP = FLOAT(KZP)
    REKAP = FLOAT(KAP)
    ZAP = REKZP / REKAP
    REKZT = FLOAT(KZT)
    REKAT = FLOAT(KAT)
    ZAT = REKZT / REKAT
    REKZCN = FLOAT(KZCN)
    REKACN = FLOAT(KACN)
    ZACN = REKZCN / REKACN
    WRITE(3,97) BT,KZP,KAP,ZAP,KZT,KAT,ZAT,KZCN,KACN,ZACN
    write(*,*)bt,kzp,kap,zap,kzt,kat,kzcn,kacn,zacn
    IF(int( TB).EQ.int(BT) ) GO TO 38
    WRITE (3,102) BT, TB
    GO TO 132
 38 I=KK
 39 I=I+1
    BRACH(I)=1.
    READ(2,100) EL(I),NA(I),ELM(I),NZD(I),NZP(I),NZG(I),
   1 HLD(I),HLP(I),HLG(I),SIG(I),ESIG(I),ST(I)
    write(*,*)el(i), na(i), elm(i), nzd(i), nzp(i),nzg(i),
   1 hld(i),hlp(i), hlg(i), sig(i), esig(i), st(i)
    SIG(I)=SIG(I)*FMUP
    ESIG(I)=ESIG(I)*FMUP
C     IF((ELM(I).NE.1H ).AND.(HLP(I).NE.0.))READ(2,840)BRACH(I)
 840 FORMAT(F10.5)
    IF(ST(I).EQ.0.) GO TO 841
```

```
      GO TO 842
  841 IF((HLD(I).GT.10.*HLG(I)).AND.(HLP(I).GT.10.*HLG(I)))
     X ST(I) = 5.*HLG(I)
      IF(HLD(I).GT.10.*HLP(I))ST(I)=5.*HLP(I)
  842 CONTINUE
      IF(NA(I).NE. 0.0) GO TO 39
      L = 1
      M = 45
      N = I - 1
      NO(NC)=N
      KK=N
   25 WRITE(3,301)
      DO 27 I = L, M
      IF(I .EQ. KK+1) GO TO 30
      WRITE (3,101) EL(I),NA(I),ELM(I),NZD(I),NZP(I),NZG(I),
     X HLD(I),HLP(I),HLG(I),SIG(I),ESIG(I),ST(I),I
   27 CONTINUE
      L = L + 44
      M = M + 44
      WRITE(3,109)
      GO TO 25
   30 NTRIAL=0
      CALL CORRECT(NOB,KK,NO(3),NO(2))
C
C     READ CHARGE DISPERSION PARAMETERS SPECIFIED IN
C     SUBROUTINE CHARGE
C     BLANK CARD ENDS THE DATA SET AND RETURNS TO READ
C     NEXT DATA SET
C
    42 READ(2,104)(WHAT(I),I=1,9)
      write(*,*)(what(i), i=1,9)
C***BLANK CARD START NEW MASS INTERVAL SAME CURRENT***
      IF((WHAT(1).EQ.-0.0).AND.(WHAT(2).EQ.-0.0)) GO TO 843
      GO TO 844
  843 KK=0
      GO TO 19
  844 CONTINUE
      NTRIAL=NTRIAL+1
      WRITE(3,106) NTRIAL
      WRITE(3,95)(TITLE(I),I=1,20)
C
C     CALCULATE CHARGE DISTRIBUTIONS PARAMETER
C
      CALL CHARGE(KK)
      WRITE(3,106) NTRIAL
```

```
C
C    CALCULATE FORMATION RATES
C
     WRITE(3,95)(TITLE(I),I=1,20)
C
     CALL RATES(KK)
     WRITE(3,98)
     WRITE(3,95)(TITLE(I),I=1,20)
C
     CALL RESULTS(KK)
     GO TO 42
  94 FORMAT(2F10.0)
  95 FORMAT(10X,20A4)
  96 FORMAT(20A4)
  97 FORMAT(1H-,10X,'TIME OF BOMBARDMENT = ',E10.4,' MIN ',//,
    1 10X,'PROJECTILE Z-A',I5,'-',I3,5X,'Z/A = ',F7.3,/,
    2 14X,'TARGET Z-A',I5,'-',I3,11X,F7.3,/,
    3 10X,'COMPOUND Z-A',I5,'-',I3,11X,F7.3,//)
  98 FORMAT(1H1,45X,'PROGRAM ISOBAR',/)
  99 FORMAT (E10.4,4I5,F10.5)
 100 FORMAT(A2,I3,A1,I4,2I5,5E10.4,1X,F8.4)
 101 FORMAT(10X,A2,'-',I3,A1,3I5,4G11.4,' +/- ',2G11.4,10X,I5)
 102 FORMAT(1H0,' ERRONEOUS INPUT FOR THE LENGTH OF BBDT ',//,
    1 ' TOTAL LENGTH OF BBDT WAS STATED AS ',F10.4,' MIN ',//,
    2 ' SUM OF INPUT DELTA T-S WAS ',F10.4,' MIN ')
 104 FORMAT(7E10.4,2F5.2)
 106 FORMAT(1H1,9X,' CHARGE DISTRIBUTION INPUT DATA FOR TRIAL ',
    X I3)
 109 FORMAT(1X,/////)
 301 FORMAT(1H0,9X,'   A      ZD   ZP   ZG  T1/2 D   T1/2 P
    1      T1/2 GP     CROSS SECTIONS         SEPARATION TIME ',/,
    2 76X,'MB',18X,'MIN',/)
 132 CONTINUE
     STOP
     END
C*************************************************************
**
C    SUBROUTINE CORRECT                                    *
C                                          *
C*************************************************************
**
     SUBROUTINE CORRECT(NOB,NN,NN1,NN2)
     COMMON/BINPUT/NA(200),NZD(200),NZP(200),NZG(200),HLD(200),
    1 HLP(200),HLG(200),ST(200),SIG(200),ESIG(200),EL(200),
    2 ELM(200)
```

```
      COMMON/BTITLE/TITLE(20)
      COMMON/BCORECT/ C(5,200), BBDT(4,50), NBBDT(4)
      COMMON/BRACH/BRACH(200)
      REAL L0,L1,L2
      WRITE(3,881) NN,NN1,NN2
  881 FORMAT(1X,'NN=',I3,' NN1= ',I3,' NN2= ',I3)
      DO 882 K=1,NOB
  882 WRITE(3,883)K,(BBDT(I,K),I=1,4)
  883 FORMAT(1X,I3,3X,4F15.5)
      DO 10 J = 1, 5
      DO 10 I = 1, NN
   10 C(J,I)=0.0
CCCCCCCCCCCCCCCCCCCCCCCCCCCCCCCCCCCCCCCCCCCCCCCC
CCCCCCCCCCCCC
C                                      C
C     CORRECTIONS FOR NONUNIFORM BEAM, BASED ONCALCULATION
C
C     OF THE CORRECTION FACTORS FOR EACH PIECE OF THE BBDT    C
C     WEIGHTED BY THE FRACTION OF THE FLUENCE DELIVERED IN    C
C     THAT PERIOD OF TIME                           C
C                                      C
CCCCCCCCCCCCCCCCCCCCCCCCCCCCCCCCCCCCCCCCCCCCCCCC
CCCCCCCCCCCCC
      I=0
   20 I=I+1
      IF(I.EQ.NN+1) GO TO 30
      T2=HLD(I)
      T1=HLP(I)
      T0=HLG(I)
      NC=2
      IF(I.GT.NN2)NC=NC+1
      IF(I.GT.NN1)NC=NC+1
      DO 25 K=NBBDT(NC-1)+1,NBBDT(NC)
      CT=ST(I)
      DT=BBDT(3,K)
      TS = BBDT(3,K) + ST(I)
      TB = BBDT(1,K)
      FRAC = BBDT(4,K)
C
C    CORRECTION FOR DAUGHTER ATOMS FORMED DIRECTLY IN
C    NUCLEAR REACT.
C
      L2 = 0.693/T2
      RL2 = 1/L2
      PART1 = RL2*(1.0 - EN(T2,TB))*EN(T2,TS)
```

```
      C(1,I) = C(1,I) + (PART1*FRAC)
      IF(T1.EQ.0.0) GO TO 25
C
C     CORRECTION FOR DAUGHTER ATOMS FORMED BY DECAY OF
C     PARENT DURING BOMBARDMENT
C
      L1= 0.693/T1
      PART2 = ( ((1.0 - EN(T2,TB))/L2) + (EN(T1,TB) - EN(T2,TB))
     X / (L1 - L2)) * EN(T2,TS)
      C(2,I) = C(2,I) + (PART2 * FRAC)*BRACH(I)
C
C     CORRECTION FOR DAUGHTER ATOMS FORMED BY DECAY OF
PARENTS
C     DURING BOMBARDMENT
C
      PART3 = (1.0 - EN(T1,TB)) * (EN(T1,CT) - EN(T2,CT))/(L2-L1)
     X * EN(T1,DT)
C********THIS FORMULA HAVE BEEN CHANGED BY C.H. LEE NOV.
1984***
      C(3,I) = C(3,I) + (PART3 * FRAC)*BRACH(I)
   23 IF(T0.EQ.0.0) GO TO 25
C
C     CORRECTION FOR DAUGHTER ATOMS FORMED BY DECAY OF
C     GRANDPARENT DURING THE BOMBARDMENT
C
      L0=0.693/T0
      PA=1.0/L2
      PB=(L1*EN(T0,TB))/((L1-L0)*(L2-L0))
      PC=(L0*EN(T1,TB))/((L0-L1)*(L2-L1))
      PD=(L0*L1*EN(T2,TB))/(L2*(L0-L2)*(L1-L2))
      PART4 = (PA-PB-PC-PD)*EN(T2,TS)
      C(4,I) = C(4,I) + (PART4 * FRAC)*BRACH(I)
C
C     CORRECTION FOR DAUGHTER ATOMS FORMED BY DECAY OF
C     GRANDPARENT AFTER THE BOMBARDMENT
C
      IF(TS.EQ.0.0) GO TO 25
      PA=1.0-EN(T0,TB)
      PB=L1*EN(T0,CT)
      PC=(L1-L0)*(L2-L0)
      PD=L1*EN(T1,CT)
      PE=(L0-L1)*(L2-L1)
      PF=L1*EN(T2,CT)
      PG=(L0-L2)*(L1-L2)
      PART5= PA*(PB/PC + PD/PE + PF/PG)*EN(T0,DT)
```

```
C********THIS FORMULA HAVE BEEN MODIFIED BY C.H. LEE
NOV.1984***
     C(5,1) = C(5,1) + (PART5 * FRAC)*BRACH(I)
   25 CONTINUE
     GO TO 20
   30 WRITE(3,91)
     WRITE(3,92)(TITLE(I),I=1,20)
     WRITE(3,93)
     J = 1
     M = 45
   40 WRITE(3,102)
     WRITE(3,103)
     DO 50 I = J, M
     IF(I .EQ. NN+1) GO TO 60
   50 WRITE(3,104) EL(I),NA(I),ELM(I),NZD(I),SIG(I),ESIG(I),
    X (C(L,I),L=1,5)
     M = M + 44
     J = J + 44
     WRITE(3,109)
     GO TO 40
   60 RETURN
   91 FORMAT(1H1,45X,'PROGRAM MASSY',/)
   92 FORMAT(10X,20A4)
   93 FORMAT(1H0,9X,'CALCULATE GROWTH AND DECAY CORRECTION
FACTOR
    XS')
  102 FORMAT(1H0,10X,'   A     Z(I)     CROSS SECTION IN MB
    X                          CORRECTION FACTORS',/)
  103 FORMAT(66X,'    C(1,I)     C(2,I)     C(3,I)    C(4,I)
    X      C(5,I)')
  104 FORMAT(10X,A2,'-',I3,A1,I5,4X,E10.4,' +/- ',E10.4,15X,
    X 5G11.4)
 109  FORMAT(1X,/////)
     END
C*****************************************************************
*
C     SUBROUTINE CHARGE                                        *
C                                          *
C*****************************************************************
*
     SUBROUTINE CHARGE(NN)
     COMMON/BINPUT/NA(200),NZD(200),NZP(200),NZG(200),HLD(200),
    1 HLP(200),HLG(200),ST(200),SIG(200),ESIG(200),EL(200),
    2 ELM(200)
     COMMON/BTITLE/TITLE(20)
```

```
      COMMON/BCHARGE/ZMP(200),CC(200),ZMPP(200),ZMPG(200),
     X ZMZMP(200),CCB(200)
      COMMON/CHARGEa/WHAT(20),ZMPB(200),ZMZMPB(200),ZMPPB(200),
     X ZMPGB(200)
      COMMON/CPDSYS/KZP,KAP,KZT,KAT,KZCN,KACN
      DIMENSION RNA(200)
      IF(WHAT(1).EQ.3.0) GO TO 200
      DO 70 I=1, NN
      A = FLOAT( NA(I) )
   70  CC(I) = WHAT(5) + (WHAT(6)*A)
      IF(WHAT(1).EQ.2.0) GO TO 74
CCCCCCCCCCCCCCCCCCCCCCCCCCCCCCCCCCCCCCCCCCCCCCCCC
CCCCCCCCCCCCC
C                                              C
C              WHAT(1) = 1                             C
C                                              C
C    THIS DICTATES A CHARGE DIST. WITH                      C
C           CONSTANT Z/A          UCD RULE              C
C           WHAT(2) = 0  CN - UCD                       C
C           WHAT(2) = 1  TARGET - UCD                   C
C                         NEUTS OUT=WHAT(3)+WHAT(4)*A   C
C           SLOPING GAUSSIAN WIDTH   SIG=WHAT(5)+WHAT(6)*A   C
C                                              C
CCCCCCCCCCCCCCCCCCCCCCCCCCCCCCCCCCCCCCCCCCCCCCCCC
CCCCCCCCCCCCC
      WRITE(3,78)
      WRITE(3,79) WHAT(2),WHAT(3),WHAT(4),WHAT(5),WHAT(6)
C
C    TEST FOR ALFA DECAY OF PARENT AND OR GRANDPARENT
C
      DO 73 I=1, NN
      NTESTP=NZP(I)-NZD(I)
      NTESTP=IABS( NTESTP )
      NTESTG=NZG(I)-NZP(I)
      NTESTG=IABS( NTESTG )
      RU = WHAT(3) + ( WHAT(4)*FLOAT(NA(I)) )
      ZOA = FLOAT(KZCN) / (FLOAT(KACN)-RU)
      IF(WHAT(2).EQ. 0.) GO TO 72
      ZOA = FLOAT(KZT) / (FLOAT(KAT)-RU)
   72 ZMP(I) = ZOA*( FLOAT(NA(I)) )
      ZMZMP(I) = FLOAT(NZD(I))-ZMP(I)
      RNA(I) = FLOAT(NZD(I)) / FLOAT(NA(I))
      ZMPP(I) = ZMP(I)
      ZMPG(I) = ZMP(I)
      IF( NTESTP .GT. 1 ) ZMPP(I) = ZOA*(FLOAT(NA(I)) + 4.)
```

```
      IF( NTESTG .GT. 1 ) ZMPG(I) = ZOA*(FLOAT(NA(I)) + 8.)
   73 CONTINUE
      GO TO 570
CCCCCCCCCCCCCCCCCCCCCCCCCCCCCCCCCCCCCCCCCCCCCCCCCC
CCCCCCCCCCCCC
C                                          C
C              WHAT(1) = 2                         C
C                                          C
C     THIS DICTATES A CHARGE DIST. WITH                  C
C           SLOPING ZMP  ZMP=WHAT(2)+WHAT(3)*A+WHAT(4)*A*A   C
C                                          C
C           SLOPING GAUSSIAN WIDTH  SIG=WHAT(5)+WHAT(6)*A    C
C                                          C
CCCCCCCCCCCCCCCCCCCCCCCCCCCCCCCCCCCCCCCCCCCCCCCCCC
CCCCCCCCCCCCC
   74 WRITE(3,82)
      WRITE(3,83) WHAT(2), WHAT(3), WHAT(4)
      WRITE(3,84) WHAT(5), WHAT(6)
C
C    TEST FOR ALFA DECAY OF PARENT AND OR GRANDPARENT
C
      DO 75 I=1, NN
      NTESTP=NZP(I)-NZD(I)
      NTESTP=IABS(NTESTP)
      NTESTG=NZG(I)-NZP(I)
      NTESTG=IABS(NTESTG)
      A=FLOAT(NA(I))
      ZMP(I)=WHAT(2)+(WHAT(3)*A) + (WHAT(4)*A*A)
      ZMZMP(I)=FLOAT(NZD(I))-ZMP(I)
      RNA(I)=FLOAT(NZD(I))/A
      ZMPP(I)=ZMP(I)
      ZMPG(I)=ZMP(I)
      IF(NTESTP.GT.1) B=A+4.
      IF(NTESTP.GT.1) ZMPP(I)=WHAT(2)+(WHAT(3)*B)+(WHAT(4)*B*B)
      IF(NTESTG.GT.1) C=A+8.
      IF(NTESTG.GT.1) ZMPG(I)=WHAT(2)+(WHAT(3)*C)+(WHAT(4)*C*C)
   75 CONTINUE
  570 J = 1
      M = 45
  580 WRITE(3,81)
      DO 590 I = J, M
      IF(I .EQ. NN+1) GO TO 600
      AN = FLOAT(KAT)-( (FLOAT(KZT)*FLOAT(NA(I)))/FLOAT(NZD(I)) )
      RU = WHAT(3) + ( WHAT(4) * FLOAT(NA(I)) )
      IF(WHAT(1).EQ. 2.0) RU=0.0
```

```
      DELTA = RNA(I) - (FLOAT(KZCN) / ( FLOAT(KACN) - RU ) )
  590 WRITE(3,80)EL(I),NA(I),ELM(I),NZD(I),ZMP(I),RNA(I),DELTA,
     X ZMPP(I),ZMPG(I),ZMZMP(I),AN,SIG(I)
      M = M + 44
      J = J + 44
      WRITE(3,109)
      GO TO 580
  600 RETURN
CCCCCCCCCCCCCCCCCCCCCCCCCCCCCCCCCCCCCCCCCCCCCCCC
CCCCCCCCCCCCC
C                                          C
C              WHAT(1) = 3                          C
C                                          C
C    THIS DICTATES A CHARGE DIST. WITH TWO GAUSSIANS        C
C                                          C
C           CONSTANT GAUSSIAN WIDTH  SIG(A) = WHAT(2)       C
C           SLOPING ZMP  ZMPA = WHAT(3) + WHAT(4)*A         C
C           RELATIVE HEIGHT OF A  PA = WHAT(8)              C
C                                          C
C           CONSTANT GAUSSIAN WIDTH  SIG(B) = WHAT(5)       C
C           SLOPING ZMP  ZMPB = WHAT(6) + WHAT(7)*A         C
C           RELATIVE HEIGHT OF B  PB = WHAT(9)              C
C                                          C
CCCCCCCCCCCCCCCCCCCCCCCCCCCCCCCCCCCCCCCCCCCCCCCC
CCCCCCCCCCCCC
  200 WRITE(3,85) (WHAT(I),I=2,9)
      DO 250 I = 1, NN
      CC(I) = WHAT(2)
      CCB(I) = WHAT(5)
C
C    TEST FOR ALFA DECAY OF PARENT AND OR GRANDPARENT
C
      NTESTP = NZP(I) - NZD(I)
      NTESTP = IABS(NTESTP)
      NTESTG = NZG(I) - NZP(I)
      NTESTG = IABS(NTESTG)
      A = FLOAT(NA(I))
      ZMP(I) = WHAT(3) + WHAT(4)*A
      ZMPB(I) = WHAT(6) + WHAT(7)*A
      ZMZMP(I) = FLOAT(NZD(I)) - ZMP(I)
      ZMZMPB(I) = FLOAT(NZD(I)) - ZMPB(I)
      ZMPP(I) = ZMP(I)
      ZMPG(I) = ZMP(I)
      ZMPPB(I) = ZMPB(I)
      ZMPGB(I) = ZMPB(I)
```

```
      IF(NTESTP.LT.2) GO TO 220
      B = A + 4.
      ZMPP(I) = WHAT(3) + WHAT(4)*B
      ZMPPB(I) = WHAT(6) + WHAT(7)*B
  220 IF(NTESTG.LT.2) GO TO 250
      B = A + 8.
      ZMPG(I) = WHAT(3) + WHAT(4)*B
      ZMPGB(I) = WHAT(6) + WHAT(7)*B
  250 WRITE(3,86) EL(I),NA(I),ELM(I),NZD(I),ZMP(I),ZMZMP(I),
     X  ZMPB(I),ZMZMPB(I)
      RETURN
   78 FORMAT(1H0,20X,'UCD RULE',/)
   79 FORMAT(10X,' UCD RULE 0=CN,1=TGT...',1X,F2.0,/,10X,
     1 'NEUTS OUT = ',F5.2,' + ',F6.3,' X A ',20X,
     2 ' GAUSSIAN SIGMA = ',F5.3,' + ',F5.3,' X A ',//)
   80 FORMAT(10X,A2,'-',I3,A1,I5,5F10.4,5X,'Z-ZMP = ',F8.5,
     X 2X,F8.3,11X,E9.3)
   81 FORMAT(10X,' A(I)     Z(I)     ZP(A)     Z/A     TGTFZ/A
     X  ZMPP     ZMPG ',24X,'NEUTS TGT',10X,'SIGMA(MB)',/)
   82 FORMAT(1H0,9X,' EMPIRICAL Z/A ',//)
   83 FORMAT(10X, 'ZMP = (',E9.3,') + (',E9.3,') X A + (',E9.3,')
     X',' X A X A',/)
   84 FORMAT(10X,   'SIGMA=(',E9.3,') + (',E9.3,') A(I) ',/)
   85 FORMAT(1H0,9X,'TWO GAUSSIAN CHARGE DISTRIBUTION',//,10X,
     1 'GAUSSIAN A  WIDTH = ',F5.3,' ZMP = ',F7.3,' + ',F7.3,
     2 ' X A ',/,19X,' B  WIDTH = ',F5.3,' ZMP = ',F7.3,' + ',
     3 F7.3,' X A ',/,10X,' RELATIVE PROBABILITY OF A = ',F6.3,
     4 ' OF B = ',F6.3,//)
   86 FORMAT(10X,A2,'-',I3,A1,I5,F10.4,3X,'Z-ZMPA =',F8.5,5X,
     X F10.4,5X,'Z-ZMPB =',F8.5)
  109 FORMAT(1X,/////)
      END
C*************************************************************************
C     SUBROUTINE RATES                                          *
C                                                               *
C*************************************************************************
      SUBROUTINE RATES(NN)
      COMMON/BINPUT/NA(200),NZD(200),NZP(200),NZG(200),HLD(200),
     1 HLP(200),HLG(200),ST(200),SIG(200),ESIG(200),EL(200),
     2 ELM(200)
      COMMON/BTITLE/TITLE(20)
      COMMON/BRATES/RD(200),RP(200),RG(200),IYD(200),IYP(200),
     1 IYG(200),NTRIAL,RDB(200),RPB(200),RGB(200),FIYA(200),
```

```
     2 FIYB(200)
      COMMON/BCHARGE/ZMP(200),CC(200),ZMPP(200),ZMPG(200),
     X ZMZMP(200),CCB(200)
      COMMON/CHARGEa/WHAT(20),ZMPB(200),ZMZMPB(200),ZMPPB(200),
     X ZMPGB(200)
      COMMON/BRESULT/FIY(200),FC(200),SIGIY(200),SIGA(200),
     X ESIGIY(200)
C
C     ZERO THE BRATES COMMON BLOCK
C
      DO 10 I = 1, NN
      RD(I) = 0.
      RP(I) = 0.
      RG(I) = 0.
      RDB(I) = 0.
      RPB(I) = 0.
      RGB(I) = 0.
      FIYA(I) = 0.
      FIYB(I) =0.
      IYD(I) = 1
      IYP(I)=1
 10   IYG(I)=1
      I=0
 2    I=I+1
      PA=1.0
      PB=0.0
      IF(I.EQ.NN+1) GO TO 70
      KZTEST = NZP(I)-NZD(I)
      Z = FLOAT( NZD(I) )
      RD(I) = AGAUS(Z,ZMP(I),CC(I))
      FIYA(I)=RD(I)
C
C     TWO GAUSSIAN CALCULATION
C
      IF(WHAT(1).NE.3.0) GO TO 20
      PA = WHAT(8) / (WHAT(8)+WHAT(9))
      PB = WHAT(9) / (WHAT(8)+WHAT(9))
      RDB(I) = AGAUS(Z,ZMPB(I),CCB(I))
      FIYB(I)=RDB(I)
   20 FIY(I) = PA*FIYA(I) + PB*FIYB(I)
      IYD(I) = 2
C
C     CHECK FOR ALFA DECAY
C
      IF(KZTEST.EQ.-2) GO TO 60
```

```
C
C     TEST FOR INDEPENDANT YIELD
C
      IF(NZP(I).EQ.0.0) GO TO 2
      IYD(I) = 3
C
C     DOES THE DAUGHTER INTEGRATE THE CHAIN
C
      IF( HLP(I).EQ.0. ) GO TO 40
      Z = FLOAT( NZP(I) )
      RP(I) = AGAUS(Z,ZMP(I),CC(I))
      IF(WHAT(1).NE.3.0) GO TO 25
      RPB(I) = AGAUS(Z,ZMPB(I),CCB(I))
   25 IYP(I)=2
C
C     TEST FOR END OF CHAIN   PARENT SHIELDED
C
      IF(NZG(I).EQ.0) GO TO 2
      IYP(I) = 3
C
C     DOES THE PARENT INTEGRATE THE CHAIN
C
      IF( HLG(I).EQ.0.) GO TO 50
      KZDUM = NZG(I)+KZTEST
      RG(I) = GSUM(KZDUM,KZTEST,ZMP(I),CC(I))
      IF(WHAT(1).NE.3.0) GO TO 27
      RGB(I) = GSUM(KZDUM,KZTEST,ZMPB(I),CCB(I))
   27 IYG(I)=3
      GO TO 2
C
C     DAUGHTER INTEGRATES THE CHAIN
C
   40 RD(I) = RD(I) + GSUM(NZD(I),KZTEST,ZMP(I),CC(I))
      IF(WHAT(1).NE.3.0) GO TO 45
      RDB(I) = RDB(I) + GSUM(KZDUM,KZTEST,ZMPB(I),CCB(I))
   45 IYD(I) = 3
      GO TO 2
C
C     PARENT INTEGRATES THE CHAIN
C
   50 RP(I) = RP(I) + GSUM(NZP(I),KZTEST,ZMP(I),CC(I))
      IF(WHAT(1).NE.3.0) GO TO 55
      RPB(I) = RPB(I) + GSUM(NZP(I),KZTEST,ZMPB(I),CCB(I))
   55 IYP(I) = 0
      GO TO 2
```

```
C
C     CALCULATE FOR ALFA DECAY
C
   60 Z1 = FLOAT(NZP(I))
      RP(I) = AGAUS(Z1,ZMPP(I),CC(I))
      IF(WHAT(1).NE.3.0) GO TO 65
      RPB(I) = AGAUS(Z1,ZMPPB(I),CCB(I))
   65 IYD(I) = 4
      IYP(I) = 4
      Z0 = FLOAT(NZG(I))
C
C     TEST FOR END OF CHAIN  GRANDPARENT SHIELDED
C
      IF(Z0.EQ.0.) GO TO 2
      RG(I) = AGAUS(Z0,ZMPG(I),CC(I))
      IF(WHAT(1).NE.3.0) GO TO 67
      RGB(I) = AGAUS(Z0,ZMPGB(I),CCB(I))
   67 IYG(I) = 4
      GO TO 2
C
C     OUTPUT THE RESULTS OF THE CALCULATIONS
C
   70 J=1
      M = 45
      PA = 1.
      PB = 0.
      IF(WHAT(1).NE.3.) GO TO 570
      PA = WHAT(8) / (WHAT(8)+WHAT(9))
      PB = WHAT(9) / (WHAT(8)+WHAT(9))
  570 WRITE(3,101)
  580 WRITE(3,102)
      DO 590 I = J, M
      IF(I .EQ. NN+1) GO TO 600
      RD(I) = PA*RD(I) + PB*RDB(I)
      RP(I) = PA*RP(I) + PB*RPB(I)
      RG(I) = PA*RG(I) + PB*RGB(I)
  590 WRITE(3,103)IYD(I),RD(I),IYP(I),RP(I),IYG(I),RG(I),EL(I),
     X NA(I),ELM(I),NZD(I),FIY(I)
      M = M + 44
      J = J + 44
      WRITE(3,109)
      GO TO 580
  600 RETURN
  101 FORMAT(1H0,' CALCULATED RATES ')
  102 FORMAT(1H0,14X,'IYD    RATE D       IYP    RATE P',7X,
```

```
    1' IYG    RATE  G',17X,'Z      FIY',/)
  103 FORMAT(10X,I7,3X,G11.4,I7,3X,G11.4,I7,3X,G11.4,5X,A2,'-',
    X I3,A1,I5,2X,G11.4)
  109 FORMAT(1X,/////)
      END
C*******************************************************************
C     SUBROUTINE RESULTS                                   *
C                                                *
C ******************************************************************
      SUBROUTINE RESULTS(NN)
      COMMON/BINPUT/NA(200),NZD(200),NZP(200),NZG(200),HLD(200),
     1 HLP(200),HLG(200),ST(200),SIG(200),ESIG(200),EL(200),
     2 ELM(200)
      COMMON/BTITLE/TITLE(20)
      COMMON/BCORECT/ C(5,200), BBDT(4,50), NBBDT(4)
      COMMON/BCHARGE/ ZMP(200),CC(200),ZMPP(200),ZMPG(200),
     X ZMZMP(200),CCB(200)
      COMMON/CHARGEa/ WHAT(20),ZMPB(200),ZMZMPB(200),ZMPPB(200),
     X ZMPGB(200)
      COMMON/BRATES/RD(200),RP(200),RG(200),IYD(200),IYP(200),
     1 IYG(200),NTRIAL,RDB(200),RPB(200),RGB(200),FIYA(200),
     2 FIYB(200)
      COMMON/BRESULT/ FIY(200),FC(200),SIGIY(200),SIGA(200),
     X ESIGIY(200)
      COMMON/RESULTSa/ ESIGA(200),SIGC(200),ESIGC(200),
     X SIGIYA(200),SIGIYB(200),ESIGIYA(200),ESIGIYB(200)
      DIMENSION NTYP(8),FRC(200)
      DIMENSION X(400),Y(200)
      DIMENSION ZMZMPC(200)
      DATA NTYP/4H  ER,4HROR ,4H    ,4HIY  ,4HPCY-,4HBETA,
     X 4HPCY-,4HALFA/
CCCCCCCCCCCCCCCCCCCCCCCCCCCCCCCCCCCCCCCCCCCCCCCCCCCCCC
CCCCCCCCCCCCCC
C                                                C
C     RECALCULATE CROSS SECTIONS BASED ON GROWTH AND DECAY
C
C     CORRECTIONS AND THE FRACTIONAL INDEPENDENT YIELDS FROM
C
C     THE ASSUMED CHARGE DISTRIBUTIONS                   C
C                                                C
CCCCCCCCCCCCCCCCCCCCCCCCCCCCCCCCCCCCCCCCCCCCCCCCCCCCCC
CCCCCCCCCCCCC
      WRITE(3,204)NTRIAL
      J = 1
      M = 45
```

```
   10 WRITE(3,214)
      DO 15 I = J, M
      IF(I.EQ.NN+1) GO TO 20
      FC(I)=(C(1,I)*RD(I))/(C(1,I)*RD(I)+C(2,I)*RP(I)+
     X C(3,I)*RP(I)+C(4,I)*RG(I)+C(5,I)*RG(I))
      SIGC(I) = SIG(I)*FC(I)
      SIGA(I) = SIGC(I)/RD(I)
      SIGIY(I) = SIGA(I)*FIY(I)
      RE = ESIG(I)/SIG(I)
      IF(RE.LT.0.1) RE = 0.1
      ESIGIY(I) = RE*SIGIY(I)
      ESIGA(I) = RE*SIGA(I)
      ESIGC(I) = RE*SIGC(I)
      IF(WHAT(7).EQ.0.) WHAT(7) = 1.
      FACT = ( WHAT(6)*FLOAT( NA(I)) ) + WHAT(5)
      FRC(I) = SIGIY(I) / (FACT*RD(I)*WHAT(7)*2.50663)
      NK = IYD(I)*2-1
      NK1=NK+1
   15 WRITE(3,205)EL(I),NA(I),ELM(I),NZD(I),SIG(I),ESIG(I),
     X FC(I),SIGC(I),ESIGC(I),RD(I),SIGA(I),ESIGA(I),NTYP(NK)
     X ,NTYP(NK1)
      J = J + 44
      M = M + 44
      WRITE(3,109)
      GO TO 10
   20 WRITE(3,109)
      WRITE(3,216) (TITLE(I),I=1,20)
      J = 1
      M = 45
C
C     PREPARE DIFFERENT OUTPUT FOR TWO GAUSSIANS
C
   25 IF(WHAT(1).EQ.3.0) GO TO 250
      WRITE(3,217)
      DO 30 I = J, M
      IF(I.EQ.NN+1) GO TO 40
      DYNO = SIGA(I)/SIG(I)
      NK = IYD(I)*2-1
      NK1=NK+1
   30 WRITE(3,215) EL(I),NA(I),ELM(I),NZD(I),ZMZMP(I),SIGIY(I),
     X ESIGIY(I),DYNO,NTYP(NK),NTYP(NK1),RD(I),FRC(I)
      J = J + 44
      M = M + 44
      WRITE(3,109)
      GO TO 25
```

```
C
C     PLOT THE CHARGE DISPERSIONS
C
   40 WRITE(3,999)
  999 FORMAT(1H1)
      KK = 0
      DO 50 II = 1, NN
      DO 50 JJ = 1,3
      KK = KK + 1
   50 X(KK) = ZMZMP(II)
      KK = 0
      DO 60 II = 1, NN
      KK = KK + 1
      AA = SIGIY(II) + ESIGIY(II)
      Y(KK) = ALOG10(AA)
      KK = KK + 1
      AA = SIGIY(II) - ESIGIY(II)
      IF(AA .LE. 0.0) AA = 0.01
      Y(KK) = ALOG10(AA)
      KK = KK + 1
      AA = SIGIY(II)
   60 Y(KK) = ALOG10(AA)
      CALL PRNPLT(X,Y,4.0,0.08,2.0,0.06,0,0,KK)
      RETURN
CCCCCCCCCCCCCCCCCCCCCCCCCCCCCCCCCCCCCCCCCCCCCCCC
CCCCCCCCCCCCC
C                                                C
C     WHAT(1) = 3.0  IMPLIES TWO GAUSSIAN CHARGE DISPERTIONS   C
C                                                C
CCCCCCCCCCCCCCCCCCCCCCCCCCCCCCCCCCCCCCCCCCCCCCCC
CCCCCCCCCCCCC
  250 CONTINUE
      PA = WHAT(8) / (WHAT(8)+WHAT(9))
      PB = WHAT(9) / (WHAT(8)+WHAT(9))
      WRITE(3,254)
      DO 251 I = 1, NN
      FA = FIYA(I)
      FB = FIYB(I)
      RE = ESIG(I)/SIG(I)
      SIGIYA(I) = FA*PA*SIGA(I)
      SIGIYB(I) = FB*PB*SIGA(I)
      ESIGIYA(I) = RE*SIGIYA(I)
      ESIGIYB(I) = RE*SIGIYB(I)
      ZMZMPC(I) = (ZMZMP(I) + ZMZMPB(I)) / 2.0
      WRITE(3,252) EL(I),NA(I),ELM(I),NZD(I),ZMZMP(I),
```

```
     1 SIGIYA(I),ESIGIYA(I),ZMZMPB(I),SIGIYB(I),ESIGIYB(I),
     2 SIGIY(I),ESIGIY(I),ZMZMPC(I)
       ZMZMP(I) = ZMZMPC(I)
  251 CONTINUE
       GO TO 40
  109 FORMAT(1X,/////)
  204 FORMAT(1H0,' RESULTS OF TRIAL ',I3,//)
  205 FORMAT(5X,A2,'-',I3,A1,I5,2G11.4,5X,F7.4,2X,2G11.4,5X,
     X F7.4,2X,2G11.4,2X,A4,A4)
  214 FORMAT(1H0,25X,'MEASURED',25X,'CALC.     ',25X,
     1 'CALC. Y(A)',/,8X,' A     Z     SIG        ESIG',13X,
     2 'FC      SIGC      ESIGC',11X,'RD       SIGA       ESIGA
     3',/)
  215 FORMAT(10X,A2,'-',I3,A1,I5,5X,F8.5,5X,E10.4,' +/- ',E10.4,
     X 4X,F6.2,2X,A4,A4,4X,E10.4,6X,F10.5)
  216 FORMAT(10X,20A4)
  217 FORMAT(14X,'A',6X,'Z',7X,'Z-ZMP',8X,'SIGIY',9X,'ESIGIY',
     1 6X,'DYNOMITE',13X,'FRACTIONAL',/,69X,'FACTOR',13X,
     2 'CHAIN YIELD',7X,'CD-ERROR',/)
  252 FORMAT(2X,A2,'-',I3,A1,I5,2X,F6.2,3X,E10.4,2X,E10.4,5X,
     X F6.2,3X,E10.4,2X,E10.4,5X,E10.4,2X,E10.4,5X,F6.2)
  254 FORMAT(1H0,16X,'Z-ZMPA',4X,'SIGIYA',5X,'ESIGIYA',7X,
     1 'Z-ZMPB',4X,'SIGIYB',5X,'ESIGIYB',9X,'SIGIY',7X,'ESIGIY',
     2 7X,'Z-ZMPC',///)
       END
C*************************************************************************
C     FUNCTION AGAUS                                    *
C                                                       *
C*************************************************************************
      FUNCTION AGAUS(ZZ,ZMAX,W)
      DIMENSION PX(200)
C     CALCULATE AREA OF GAUSSIAN FROM ZZ-.5 TO ZZ+.5
      I = 1
      PX(I) = 0.0
      S = 2.0*(W**2)
      ZLOW = ZZ - 0.5
      PIE = 3.14159
      XN = PIE*S
      XN = 1.0/SQRT(XN)
      DO 999 I = 2, 101
      ZLOW = ZLOW + 0.01
      X = ZMAX - ZLOW
      XE = (X**2)/S
```

```
      PX(I) = PX(I-1) + XN*EXP(-XE)
  999 CONTINUE
      AGAUS = PX(101)*0.01
      RETURN
      END
C*****************************************************************
*
C     FUNCTION EN                                          *
C                                          *
C*****************************************************************
*
      FUNCTION EN(HALF,T)
      IF(T.EQ.0.0) GO TO 10
      EN = EXP(-0.693*T/HALF)
      RETURN
   10 EN = 1.0
      RETURN
      END
C*****************************************************************
*
C      FUNCTION GSUM                                       *
C                                          *
C*****************************************************************
*
      FUNCTION GSUM(KD,KT,ZMX,CD)
      K = KD
      RDUM = 0.
      RSUM = 0.
   60 K = K + KT
      ZW = FLOAT( K )
      RDUM = AGAUS(ZW,ZMX,CD)
      RSUM = RSUM + RDUM
      RTEST = RSUM - RDUM
      IF(RTEST-1.0E-7) 80,80,60
   80 GSUM = RSUM
      RETURN
      END
C*****************************************************************
C     SUBROUTINE PRNPLT                                    *
C                                       *
C*****************************************************************
      SUBROUTINE PRNPLT(X,Y,XMAX,XINCR,YMAX,YINCR,ISX,ISY,
     X NPTS)
C
C    PRINTER PLOT ROUTINE   M.S.ITZKOWITZ  MAY,1967
```

```
C    PLOTS THE #NPTS# POINTS GIVEN BY #X(I),Y(I) ON A 51 X 101
C    GRID USING A TOTAL OF 56 LINES ON THE PRINTER
C    IF #ISX# OR #ISY# ARE NON-ZERO, THE CORRESPONDING MAXIMUM
C    AND INCREMENTAL STEP SIZE ARE COMPUTED
C    IF EITHER INCREMENTAL STEP SIZE IS ZERO, THE PROGRAM EXITS
C    NEITHER OF THE INPUT ARRAYS ARE DESTROYED.
C    IF SCALING IS DONE THE CORRESPONDING NEW VALUES OF
MAXIMUM
C    AND STEP SIZE ARE RETURNED
C
     DIMENSION X(NPTS),Y(NPTS),GRID(105),XAXIS(9)
C
     DATA BLANK,DOT,STAR,PLUS,BAR/1H ,1H.,1H*,1H+,1H-/
C
  901 FORMAT(14X,105A1)
  902 FORMAT(1X,E10.3,2X,1H+,105A1,1H+)
  903 FORMAT(15X,103(1H.))
  904 FORMAT(2X,9(F13.0),2H (,I4,5H PTS))
  905 FORMAT(14X,9(1H+,12X))
 9800 FORMAT(46HISCALING ERROR IN PRNPLT, EXECUTION
TERMINATED)
C
     IF(ISX.NE.0) CALL PLSCAL(X,XMAX,XINCR,NPTS,100)
     IF(ISY.NE.0) CALL PLSCAL(Y,YMAX,YINCR,NPTS,50)
     IF(XINCR.EQ.0..OR.YINCR.EQ.0.) GO TO 800
     YAXMIN = 0.01*YINCR
     XAXMIN = 0.01*XINCR
     IZERO = YMAX / YINCR + 1.5
     JZERO = 103.5 - XMAX/XINCR
     IF(JZERO.GT.103.OR.JZERO.LT.4) JZERO=2
     WRITE(3,905)
     WRITE(3,903)
     DO 10 I = 1, 51
     IF(I.NE.IZERO) GO TO 16
     DO 14 J = 1, 105
   14 GRID(J) = PLUS
     GO TO 15
   16 DO 11 J = 1, 105
   11 GRID(J) = BLANK
   15 GRID(JZERO) = PLUS
     GRID(104) = DOT
     GRID(2) = DOT
     DO 12 K1 = 3, NPTS, 3
     DO 12 L = 1, 3
     K = K1 - 3 + L
```

```
      ITEST = (YMAX-Y(K)) / YINCR + 1.5
      IF(ITEST.NE.I) GO TO 12
      J = 103.5 - (XMAX-X(K))/XINCR
      IF(J.GT.103) J = 105
      IF(J.LT.3) J = 1
      GRID(J) = BAR
      IF(L.EQ.3) GRID(J) = STAR
   12 CONTINUE
      IF(MOD(I,10).EQ.1) GO TO 13
      WRITE(3,901) (GRID(J),J=1,105)
      GO TO 10
   13 YAXIS = YMAX - (I-1)*YINCR
      IF(ABS(YAXIS).LT.YAXMIN) YAXIS = 0.
      WRITE(3,902) YAXIS,(GRID(J),J=1,105)
   10 CONTINUE
      WRITE(3,903)
      WRITE(3,905)
      DO 20 M=1,9
      XAXIS(M) = XMAX - XINCR*(FLOAT(9-M))*12.5
      IF(ABS(XAXIS(M)) .LT. XAXMIN) XAXIS(M)=0.
   20 CONTINUE
      WRITE(3,904) XAXIS,NPTS
      RETURN
  800 WRITE(3,9800)
      CALL EXIT
      END
C*********************************************************************
C     SUBROUTINE PLSCAL                                    *
C                                          *
C*********************************************************************
      SUBROUTINE PLSCAL(V,VMAX,VINCR,NPTS,NDIVIS)
C
C     SCALING PROGRAM FOR USE WITH PRNPLT  M.S.ITZKOWITZ
MAY,1967
C     THIS VERSION ADJUSTS THE FULL SCALE TO 2.5, 5.0, OR 10.
C     TIMES 10**N AND ADJUSTS A MAXIMUM POINT TO AN INTEGER
C     MULTIPLE OF 5*VINCR
C
      DIMENSION V(NPTS)
      V(MIN) = V(1)
C
      V(MAX) = V(1)
      DO 10 I = 1, NPTS
      IF(V(I) .LT. VMIN) VMIN = V(I)
      IF(V(I) .GT. VMAX) VMAX = V(I)
```

```
      QRANGE = VMAX - VMIN
   10 CONTINUE
      IF(QRANGE .EQ. 0.) GO TO 8000
      QRANGE = 0.4342944*ALOG(QRANGE)
C
      IF(QRANGE) 20,20,30
   20 IRANGE = -QRANGE
      IRANGE = -IRANGE - 1
      IRANGE = -IRANGE - 1
      IRANGE = -IRANGE - 1
      QRANGE = QRANGE - FLOAT(IRANGE)
      RANGE = 10.**QRANGE
C
C     RANGE IS BETWEEN 1.0 AND 10.0
C
   30 IRANGE = QRANGE
   43 IF(RANGE .GT. 2.5) GO TO 41
      RANGE = 2.5
      GO TO 50
   41 IF(RANGE .GT. 5.0) GO TO 42
      RANGE = 5.0
      GO TO 50
   42 RANGE = 10.0
   50 TRANGE = RANGE*(10.**IRANGE)
C
C     TRANGE IS NOW 2.5, 5.0, OR 10.0 TIMES A POWER OF TEN
C
      VINCR = TRANGE/FLOAT(NDIVIS)
      IF(VMAX) 51,51,52
   52 IMAX = VMAX/(5.0*VINCR)
      XMAX = 5.0*VINCR*FLOAT(IMAX+1)
      GO TO 53
   51 IMAX = -VMAX/(5.0*VINCR)
      XMAX = 5.0*VINCR*FLOAT(-IMAX+1)
   53 IF(VMIN .GT. XMAX-TRANGE) GO TO 100
      RANGE = RANGE*2.0
      IF(RANGE-10.) 43,43,54
   54 RANGE = RANGE/10.
      IRANGE = IRANGE + 1
      GO TO 43
  100 VMAX = XMAX
      VMIN = XMAX - TRANGE
      RETURN
 8000 PRINT 9800
      WRITE(3,9800)
```

```
 9800 FORMAT(45H1PLSCAL CALLED TO SCALE ARRAY WITH ZERO
RANGE)
     CALL EXIT
     END
```

Sample input for massywalt.for

The first rows are similar to the input file for cross.for. The first column indicates the time on target for each beam on cycle in minutes. The second column contains the total number of beam particles during each cycle. No inputs are required for the beam off periods. After these rows there is a title row followed by a row giving the total beam time on target, the target A, Z, projectile A, and Z, respectively. Nuclides are grouped in small ranges of A listing the element symbol, nuclide A, meta or ground state, Z, and Z of the parent and Z of the grandparent nucleus (if applicable). The next numbers in each row contain the nuclide half-life (HL), the HL of the parent and the grandparent (if applicable), followed by the cumulative cross sections and the errors. After each grouping a set of parameters is given (called WHAT(I) in the code) that will be used to determine the charge distribution fits. The first number determines which equations will be used to determine the charge distributions, the second parameter determines the offset of the curve, the third gives the slope, and the fourth is the width parameter. The third and last parameters were set at zero for this analysis.

```
308.          5.38e13
379.          6.39e13
16.           5.89e12
1.            3.68e11
29.           1.07e13
6.            2.21e12
47.           1.76e13
170.          6.37e13
19.           7.12e12
41.           1.54e13
57.           2.13e13
382.          1.43e14
```

```
27.           1.01e13
3.            1.12e12
7.            2.45e12
451.          1.58e14
20.           6.99e12
39.           1.36e13
7.            2.45e12
10.           3.37e12
21.           7.34e12
849.          3.07e14
497.          1.74e14
1075.         3.76e14
29.           1.01e13
12.           4.19e12
250.          7.49e13
9.            3.15e12
0.0            0.0
Pb 1  Expt Mass Yield
4761.       208   82  136   54
BI204   83   84   850.6732E+030.2118E+030.9200E+010.1520E+010.4256E-01   0.0000
BI206   83   84   850.8986E+040.1267E+050.2940E+020.4690E+010.4398E+00   0.0000
PO206   84   85   860.1267E+050.2940E+020.5670E+010.1115E+010.1534E+00   0.0000
AT210   85   86   870.4860E+030.1440E+030.3180E+010.1065E+010.7177E-01   0.0000
RN211   86   87    00.8760E+030.3100E+010.0000E+000.2391E+000.3680E-01   0.0000

2.0       4.0       0.38      0.0       1.00       0.0
```

Sample output from massywalt.for

The output from this program includes the measured cumulative cross section, MEASURED SIG, the calculated independent cross section corrected for beta decay (if needed), CALC. SIGC or SIGIY, and an estimate of the isobaric cross section, σ(A) or SIGA. If the cross section is already an independent yield and no beta correction is needed, it is designated by "IY." Beta corrected cross sections are denoted by "PCY-BETA."

```
1                                        PROGRAM ISOBAR

  Pb 1  Expt Mass Yield
0 RESULTS OF TRIAL   1


0               MEASURED                        CALC.                          CALC. Y(A)
   A     Z     SIG        ESIG             FC      SIGC      ESIGC           RD       SIGA       ESIGA

BI-204    83  1.520     0.4256E-01      0.9099    1.383     0.1383          0.1387    9.971     0.9971    PCY-BETA
BI-206    83  4.690     0.4398          0.9921    4.653     0.4653          0.3007    15.48      1.548    PCY-BETA
PO-206    84  1.115     0.1534          0.8990    1.002     0.1379          0.0972    10.31      1.418    PCY-BETA
AT-210    85  1.065     0.7177E-01      0.8789   0.9361     0.9361E-01      0.1963    4.769     0.4769    PCY-BETA
RN-211    86 0.2391     0.3680E-01      0.8972   0.2145     0.3302E-01      0.0825    2.599     0.4000    PCY-BETA


   Pb 1  Expt Mass Yield
   A      Z       Z-ZMP        SIGIY         ESIGIY      DYNOMITE            FRACTIONAL
                                                          FACTOR             CHAIN YIELD       CD-ERROR

BI-204    83      1.48000     0.1383E+01 +/- 0.1383E+00      6.56  PCY-BETA    0.1387E+00         3.97767
BI-206    83      0.72000     0.4653E+01 +/- 0.4653E+00      3.30  PCY-BETA    0.3007E+00         6.17369
PO-206    84      1.72000     0.1002E+01 +/- 0.1379E+00      9.25  PCY-BETA    0.9723E-01         4.11269
AT-210    85      1.20000     0.9361E+00 +/- 0.9361E-01      4.48  PCY-BETA    0.1963E+00         1.90253
RN-211    86      1.82000     0.2145E+00 +/- 0.3302E-01     10.87  PCY-BETA    0.8254E-01         1.03688
```